Rat Model of Pre-Motor Parkinson's Disease: Behavioral and MRI Characterization.

A dissertation submitted in partial fulfillment of
the requirements for the degree of Doctor of Philosophy in
Biomedical Engineering
by

Pallavi Satish Rane

3/28/2011

Christopher H. Sotak, Ph.D.
Academic Advisor
Professor
Department of Biomedical Engineering
Worcester Polytechnic Institute

Jean A. King, Ph. D.
Research Advisor
Professor
Department of Psychiatry
University of Massachusetts Medical School, Worcester

George D. Pins, Ph.D.
Associate Professor
Department of Biomedical Engineering
Worcester Polytechnic Institute

Nanyin Zhang, Ph. D.
Assistant Professor
Department of Psychiatry
University of Massachusetts Medical School, Worcester

Gregory J. DiGirolamo, Ph. D.
Associate Professor
Department of Psychology
College of Holy Cross

Acknowledgements

As the “graduate student” part of my life draws to a close, I cannot help but look back and be grateful for the support of numerous friends, family members and members of the WPI and UMass community.

First and foremost, I have to mention my mentors Dr. Chris Sotak and Dr. Jean King. Dr. Sotak gave me a chance to start this journey and allowed me to start working in his lab even when I was just a first year student. Dr. Sotak, I cannot thank you enough for your support, encouragement, guidance, and most of all, for your patience with my “200 questions” attitude. You have always made me feel immensely welcome in this foreign country. You will always have a special place in my heart. Dr. Jean King has guided me through. Jean, CCNI has been a second family to me and I could not have made it through some really tough times without your support and kindness. You have been a role model to me, as one of the strongest women I have ever met in my life. I really admire your incessant working attitude.

I am grateful to Dr. George Pins from WPI, Dr. Nanyin Zhang from UMass, Worcester and Dr. Gregory DiGirolamo from Holy Cross for being on my committee and guiding me through the process. Dr. Pins, I appreciate you allowing me to use the microscope at the last minute to help me finish my work. Nanyin, I could not have finished my imaging studies and imaging analysis without your guidance. I really appreciate all the time you gave me to help me interpret my results. Gregg, I would really like to thank you for your guidance during the aversion behavior.

You really helped me nail that study and figure out the appropriate behavior. Thank you all for taking the time and effort to read my thesis.

I really appreciate my lab mates Wei Huang, Meghan Heffernan and Zhifeng Liang. Wei's support, Meg's wisdom and Zhifeng's immense knowledge regarding almost everything and most of all of your friendship, has made these years something I can remember as one of the most pleasant times in my life. I am really glad that I can call you all not just my lab mates but also my friends.

I thank Yvette Gonzales from CCNI and Jean Siequist from WPI for helping me through some crazy paperwork. I do not know how you guys deal with these things with the efficiency that you do. I appreciate Amanda Blackwood, Yin Guo and Dr. Schahram Akbarian who helped me during my immunohistochemistry studies.

I would like to take this opportunity to thank my friends Hemish, Jitish, Abhijit, Parul, Sarang, Kunal, Saurabh, Padmaja, Amit and Akanksha at WPI, my cousins Nirmala and Abhijeet Dalvi and my niece Natasha. You guys have been like a rock in my life and anchored me. Your love has helped me keep on going when everything seemed to fail.

Finally, I would like to thank my parents, Sheela and Satish Rane, my brother Charudatta and sister Poonam for being patient with my 'this is the year I am going to graduate' statement for the past 4 years. Aai and Baba, you are the best parents any one can have. I love you.

Table of Contents

Table of Figures

List of abbreviations

μ	Individual spin magnetic dipole moment
3WKPD	Parkinsonian rats as 3 weeks post toxin lesions
6-OHDA	6-hydroxydopamine (the toxin used to create the Parkinsonian model in this study)
ATP	Adenosine triphosphate
B0	External magnetic field
B1	Radio frequency pulse
BA	Butyric Acid
BOLD	Blood oxygenation level dependent
CD	Compound discrimination
CFB	Cerebral blood flow
CMRglu	Cerebral metabolic rate of glucose
CMR02	Cerebral metabolic rate of oxygen
CPu	Caudate Putamen
dOHb	deoxyhemoglobin
ED	Extra dimensional set shifting
ED/ID	Extra dimensional/ Intra dimensional set shifting

EPI	Echo-planar imaging
FID	Free induction decay
fMRI	functional MRI
ID	Intra dimensional shifting
IID	Initially irrelevant dimension
IP	Intra peritoneal
IRD	Initially relevant dimension
LRRK2	Leucine-rich repeat kinase 2
M	Net magnetization
MDM	Magnetic dipole moment
MPTP	1-methyl-4-phenyl-1,2,3,6-tetrahydropyridine
MRI	Magnetic resonance imaging
NaBu	Sodium butyrate
NR	Number of repetitions
OHb	Oxyhemoglobin
PD	Parkinson's disease
PINK1	Phosphatase and tensin homologue induced protein kinase 1
PRKN	parkin

RARE	Rapid acquisition relaxation enhancement MRI pulse sequence
RF	Radio frequency
ROI	Region of interest
ROS	Reactive oxygen species
RS	Resting state
SD	Simple discrimination
SN	Substantia Nigra
SNCA	α-synuclein
T1	Longitudinal relaxation time
T2	Transverse relaxation time
T2*	Transverse relaxation time due to inhomogeneities
TE	Time to echo
TH-staining	Tyrosine hydroxylase staining
TR	Repetition time
γ	Gyromagnetic (or magnetogyric) ratio

Abstract

Background

Parkinson's disease (PD) is a chronic, progressive, neurodegenerative disorder with currently no known cure. PD has a significant impact on quality of life of the patients, as well as, the caregivers and family members. It is the second most common cause of chronic neurological disability in US and Europe. According to National Parkinson's Foundation, there are almost 1 million patients in the Unites States and 50,000 to 60,000 new cases of PD are diagnosed each year. The total number of cases of PD is predicted to double by 2030. The annual cost associated with this disease is estimated to be $10.8 billion in the United States, including the cost of treatment and the cost of the disability.

Although it is primarily thought of as a movement-disorder and is clinically diagnosed based on motor symptoms, non-motor symptoms such as cognitive and emotional deficits are thought to precede the clinical diagnosis by almost 20 years. By the time of clinical diagnosis, there is 80% loss in the dopamine content in the striatum and 50% degeneration of the substantia nigra dopamine cells. The research presented in this thesis was an attempt to develop an animal model of PD in its pre-motor stages. Such a model would allow us to develop pre-clinical markers for PD, and facilitate the development and testing of potential treatment strategies for the non-motor symptoms of the disorder.

Specific Aims

There were five specific aims for this research:

- The first specific aim dealt with development of a rat model of PD with slow, progressive onset of motor deficits, determination of timeline for future studies, and quantification the dopamine depletion in this model at a pre-motor stage.
- The second and the third specific aims focused on testing for emotional (aversion) deficits and cognitive (executive functioning) deficits in this rat model at the 3 week timepoint determined during specific aim 1.
- The fourth specific aim was to determine the brain network changes associated with the behavioral changes observed our rat model using resting state connectivity as a measure.
- The fifth and the final specific aim was to test sodium butyrate, a drug from the histone deacetylase inhibitor family, as a potential treatment option for cognitive deficits in PD.

Results

The 6-hydroxy dopamine based stepwise striatal lesion model of pre-motor PD, developed during this research, exhibits delayed onset of Parkinsonian gait like symptoms by week 4 after the lesions. At 3 weeks post lesion (3WKPD), the rats exhibit 27% reduction in striatal dopamine and 23%reduction in substantia nigra dopamine cells, with lack of any apparent motor deficits. The 3WKPD rats also exhibited changes in aversion. The fMRI study with the aversive scent pointed towards possible amygdala dysfunction subserving the aversion deficits. The executive function deficits tested using a rat analog of the Wisconsin card sorting test, divulged an extra-dimensional set shifting deficit in the

3WKPD rats similar to those reported in PD patients. The resting state connectivity study indicated significant changes in the 3WKPD rats compared to age matched controls. We observed increased overall connectivity of the motor cortex and increased CPu connectivity with prefrontal cortex, cingulate cortex, and hypothalamus in the 3WKPD rats compared to the controls. These observations parallel the observations in unmedicated early-stage PD patients. We also observed negative correlation between amygdala and prefrontal cortex as reported in humans. This negative correlation was lost in 3WKPD rats.

Sodium butyrate treatment, tested in the cognitive deficit study, was able to ameliorate the extra-dimensional set shifting deficit observed in this model. This treatment also improved the attentional set formation.

Conclusion

Taken together, our observations indicate that, the model of pre-motor stage PD developed during this research is a very high face validity rat model of late Braak stage 2 or early Braak stage 3 PD. Sodium butyrate was able to alleviate the cognitive deficits observed in our rat model. Hence, along with the prior reports of anti-depressant and neuroprotective effects of this drug, our results point towards a possible treatment strategy for the non-motor deficits of PD.

Chapter 1. Introduction

Motivation

Parkinson's disease (PD) is a progressive neurodegenerative disorder that eventually leads to the patient being completely bed or chair bound and needing complete assistance. It affects 1-2% of the population over 65 years of age, making it the second most prevalent neurodegenerative disorder. There are almost 1 million patients in the Unites States alone; with 50,000 to 60,000 new cases of PD are diagnosed each year. The total number of cases of PD is predicted to double by the year 2030. The annual cost associated with this disease is estimated to be $10.8 billion in the United States (Chen, 2010; O'Brien et al., 2009). This cost includes, not just the cost of treatment of this disease, but also the cost of the disability that follows it. This is a chronic progressive disorder and has a significant impact on quality of life of the patients, as well as, the caregivers and family members (Chen, 2010).

Predominantly thought of as a motor disorder of the elderly, PD has also been known to have young and juvenile onsets starting at, as early as, 20 years of age. Exact causes of this disease are unknown. Most of the PD cases are thought to be idiopathic cases, but a combination of genetic mutations and exposure to environmental toxins are implicated in increasing an individual's risk. Currently known genes that are linked to PD, make up less than 20% of the total PD cases. In the 1980s, self administration of a contaminant of heroin, a drug of abuse, was linked to development of symptoms similar to motor symptoms in PD. This led to further research into environmental toxins as probable PD causes. Since

then, insecticides, pesticides, herbicides, wood preservatives, or metals like manganese and iron have been thought to play a major part in the PD etiology. PD has been shown to have increased prevalence in the rural, agricultural or farming regions, or areas with metal processing plants.

Ever since it was first identified by Dr. James Parkinson's in the 1817 as 'shaking palsy', PD is still clinically diagnosed based on presence of motor symptoms like tremors (trembling in hands, arms, legs, jaw, and face), rigidity (stiffness of the limbs and trunk), bradykinesia (slowness of movement) and postural instability (impaired balance and coordination). Even though it is thought of as a movement disorder, a variety of co-morbid non-motor symptoms are also reported in the PD patients including but not limited to depression, memory loss and executive function deficits, changes in sense of smell, deficits in recognition of various emotions and sleep disturbances. At the time of diagnosis of PD, there is generally irreversible damage the substantia nigra neurons (~50%) and reduction of the striatal dopamine (~80%). In fact, the predicted pre-diagnosis phase is thought to date back 5-20 years (Gaig and Tolosa, 2009; Hawkes et al., 2010). In the years prior to the onset of motor symptoms and clinical diagnosis, patients report a myriad of subtle non-motor deficits, which if quantified systematically, might provide us with the required markers for early detection. However, the problem is that these early signs either go unnoticed or are "written off" as a part of normal aging. Early detection may enable us to devise strategies to prevent further damage. Hence, the motivation behind this research was to develop an animal model of pre-motor stage PD, which would not have any significant motor deficits, but would exhibit slow

progressive onset of motor symptoms along with non-motor symptoms similar to those seen in PD. Such a model could then to be used to develop behavioral and functional MRI markers for the pre-clinical stage of PD. Pre-clinical markers, if developed, can lead to the early diagnosis of patients predisposed to this disease due to genealogy, proximity to toxic environments, or a combination of both. The advantage of animal models is that it allows us to more precisely control several aspects of a study, hence, enabling us to more precisely pin-point the mechanisms underlying the observed changes.

Another reason for development of this model was that, the currently available drugs and treatment methodologies focus on management of the motor symptoms of PD, and rarely treat the non-motor symptoms. In addition, the current drugs have also been shown to be ineffectual with the disease progression. In this research we also attempted to investigate novel treatment methodologies for alleviating the non-motor symptoms of PD.

Thesis outline

We begin with a discussion of Parkinson's disease, its scope of occurrence, and statistics within the population in Chapter 2. This chapter discusses history and etiology of Parkinson's disease, and its genetic and environmental causes. This discussion continues with clinical diagnostic methods and clinically recognized symptomology. The chapter ends with a discussion of pre-motor deficits observed in the disease and current treatment options available.

Chapter 3 provides an overview of magnetic resonance imaging. Spin physics, relaxation times, pulse sequences, and spatial encoding are discussed in this chapter. At the end of the chapter, the application of MRI in functional imaging of the brain is introduced.

Chapter 4 outlines the animal model devised for this study and its characterization with respect to motor deficits and immuno-histochemostry.

Chapter 5 describes our findings of aversion changes in this model of per-motor PD. This chapter also describes our results supporting possible deficits in response generation as observed in the functional MRI study.

Chapter 6 presents the executive functioning deficits observed in this rat model. Sodium butyrate treatment seems to mitigate the deleterious effects of 6-OHDA and may also have additional cognition enhancing effects.

Chapter 7 discusses resting state functional MRI as a technique to observe connectivity changes in the brain as a result of dopamine depletion and treatment. The results of this study agree with the findings reported in patients with PD.

Finally, Chapter 8 & Chapter 9 present the comprehensive summary and future directions for this research.

Chapter 2. Parkinson's disease

History

Written documentation of PD can be found in ancient literatures as old as the Ayrveda, an ancient Indian text thought to have been in existence since 5000 BC, where PD is referred to as 'Kamp Vata', translated literally as shaking palsy. There are additional references of this disorder in Chinese medical texts (500 B.C.), as well as, in ancient Roman and Greek writings. In the more recent times, a London based physician, James Parkinson, was the to first describe Parkinson's disease or 'shaking palsy', as it was then referred to as, in his publication called 'An essay on the Shaking Palsy' (Parkinson, 1817). He described the disorder as "Involuntary tremulous motion, with lessened muscular power, in parts not in action and even when supported; with a propensity to bend the trunk forwards, and to pass from a walking to a running pace: the senses and intellects being uninjured." (Parkinson, 1817) In this thesis, he goes on to describe the subtle onset of the motor deficits and their subsequent progression, based on his observations of different subjects on the streets of London. Identifying it as a disease separate from ordinary Palsy, Parkinson differentiated shaking palsy from paralysis of certain body parts which might be accompanied by tremors. In 1828, Wilhelm van Humboldt, a philosopher and diplomat, described in a letter, his own

Figure 1: Sir W. R. Grower's Parkinson's disease sketch

symptoms PD, which included micrographia, akinesia and changes in posture (Hindle, 2008). In 1861 and 1862, Jean-Martin Charcot and Alfred Vulpian added the mask face (characteristic expressionless face observed in PD patients), contractions of hands and feet, and rigidity to the list of symptoms. In addition to expanding the symptom list, Charcot finally renamed the shaking palsy as Parkinson's disease, in memory of Dr. James Parkinson (Hindle, 2008).

Demographics

PD is the second most common cause of chronic neurological disability in the US and Europe. 1-2% of people over 65 years of age have PD. According to the National Parkinson's Foundation, 50,000-60,000 new cases of PD are diagnosed each year in the United States and the demographic trends predict that the number of patients will double by the year 2030 (Chen, 2010; O'Brien et al., 2009). Dependent upon the age of the patient at disease onset, PD is classified as either juvenile-onset PD (<20years), early-onset PD (<50 years), or late-onset PD (>50 years).

Etiology of Parkinson's disease

The exact etiology of PD is not completely understood. The known causes of PD include genetics, environmental causes, or a combination of the two (Abou-Sleiman et al., 2006; Di Monte et al., 2002; Goldberg et al., 2003; Liu and Yang, 2005; Perez and Palmiter, 2005; Schapira, 2006; Steece-Collier et al., 2002; Vlajinac et al., 2010).

Genetics of PD

Recently, large scale genetic studies of families with a high prevalence of PD have led to discovery of a variety of genes linked to PD. Among those genes, mutations of SNCA (α-synuclein), PRKN (parkin), LRRK2 (Leucine-rich repeat kinase 2), PINK1 (phosphatase and tensin homologue induced protein kinase 1) and DJ-1 (also known as PARK7 or Parkinson's disease (autosomal recessive, early onset) 7) have been conclusively proven to cause PD (Bekris et al., 2010; Schapira, 2009; Steece-Collier et al., 2002).

SNCA is a protein expressed routinely throughout the mammalian brain. However, over-expression of this protein has been linked to loss of dopaminergic terminals in the striatum, mis-localization and accumulation of insoluble SNCA, and motor abnormalities (Fleming et al., 2004; Rockenstein et al., 2002). SNCA is also detected in the lewy bodies found in familial, as well as, idiopathic PD (Spillantini et al., 1997). However, it is not understood what the exact role of SNCA is and whether the wild type or certain mutations of SNCA lead to development of PD (Abou-Sleiman et al., 2006). Variations of SNCA mutation are found in early, as well as, late onset PD.

PRKN is an autosomal recessive gene that has been associated heavily with cases of young onset PD. In its normal form, PRKN is essential for mitochondrial function, possibly by protecting against deleterious effects of free radicals. Upon mutation, it is thought to cause mitochondrial damage and oxidative stress (Abou-Sleiman et al., 2006). However, studies of PRKN mutations in genetic mouse models failed to show the

classic dopamine changes observed in PD (Goldberg et al., 2003; Perez and Palmiter, 2005). Hence, it is thought that in PD patients with PRKN mutations, an additional environmental insult might be responsible for the reduction in dopamine, with the PRKN mutations increasing one's vulnerability to those factors.

Mutations of another autosomal dominant gene, LRRK2 are associated with less than 5-6% of familial PD cases. Hence, only a limited amount of post mortem data is available for this gene. Cases with LRRK2 mutation are typical of late onset PD. Lewy body pathology and nigrostriatal dysfunction, observed in cases with LRRK2 mutations, are indicative of idiopathic PD (Abou-Sleiman et al., 2006; Bekris et al., 2010). LRRK2's function in the body is not exactly understood. It is known to interact with other proteins, such as SNCA (Lin et al., 2009) and PRKN (Smith et al., 2005) which are also associated with PD.

PINK1 mutations have been reported in PD cases in diverse populations across the world including Europeans, Japanese, Chinese, Malay and Indians. Loss of PINK1 function adversely affects mitochondrial function and cell viability under stress. The most active domain in PINK1 is in its kinase domain. The same domain is also the site of many of the PINK1 mutations observed in PD. Hence, it is believed that disruption of the kinase activity is the disease mechanism in PINK1 mutation involved PD (Abou-Sleiman et al., 2006). Additionally, there are also observations of PINK1 mutation in the adenosine triphosphate (ATP) orientation site resulting in early onset PD (Bekris et al., 2010).

DJ-1 is a small ubiquitous protein present in neuronal, as well as, glial cells. Down regulation of DJ-1 has been linked to oxidative stress-induced cell death. DJ-1 deficient mice are hypersensitive to deleterious effects of MPTP (1-methyl-4-phenyl-1,2,3,6-tetrahydropyridine), a contaminant of a drug of abuse known to cause PD (Kim et al., 2005), suggesting DJ-1 might actively protects cells against apoptosis caused by exposure to oxidative stressors. However, DJ-1 mutations are quite rare and are found in only 1-2% of early onset PD cases (Abou-Sleiman et al., 2006). DJ-1 ,in its mutated form, interacts with PRKN, but in this case PRKN seems to be regulating the effects of DJ-1 mutations.

Hence, most of the genetic mutations related to PD seem to involve oxidative stress and mitochondrial dysfunction as the underlying mechanisms. There are several other genes that have been identified as precursors to PD. Figure 2 describes the pathways following mutation of various genes, that might ultimately be responsible for cell death in PD.

Together, all the known genetic cases make up only a small percentage (~20%) of the total PD cases, and even fewer can be attributed purely to genetic causes (Bekris et al., 2010; Schapira, 2006; Steece-Collier et al., 2002). It is also important to note that the majority of the PD cases, are the cases of late onset PD, and are thought to be caused by environmental insults, with genetic factors exacerbating the effect of those insults (Caudle and Zhang, 2009; Tanner, 2010).

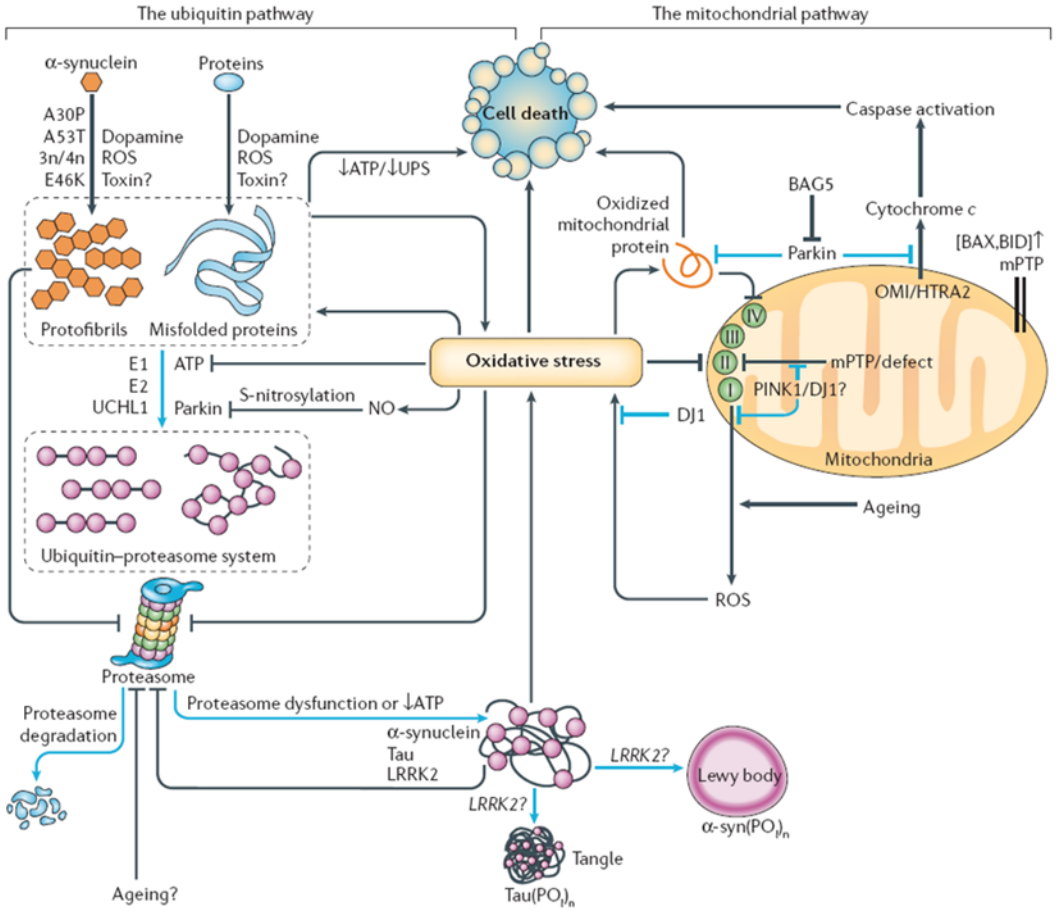

"The discovery of Mendelian inherited genes has enhanced our understanding of the pathways that mediate neurodegeneration in Parkinson's disease. One main pathway of cell toxicity arises through α-synuclein, protein misfolding and aggregation. These proteins are ubiquitinated and initially degraded by the ubiquitin–proteasome system (UPS), in which PRKN (parkin) has a crucial role. However, there is accumulation and failure of clearance by the UPS over time, which leads to the formation of fibrillar aggregates and Lewy bodies. α-Synuclein protofibrils can also be directly toxic, leading to the formation of oxidative stress that can further impair the UPS by reducing ATP levels, inhibiting the proteasome, and by oxidatively modifying PRKN. This leads to accelerated accumulation of aggregates. Phosphorylation of α-synuclein-containing or tau-containing aggregates might have a role in their pathogenicity and formation, but it is not known whether leucine-rich repeat kinase 2 (LRRK2) mediates this. Another main pathway is the mitochondrial pathway. There is accumulating evidence for impaired oxidative phosphorylation and decreased complex I activity in Parkinson's disease, which leads to reactive oxygen species (ROS) formation and oxidative stress. In parallel, there is loss of the mitochondrial membrane potential. This leads to opening of the mitochondrial permeability transition pore (mPTP), release of cytochrome *c* from the intermembrane space to the cytosol, and activation of mitochondrial-dependent apoptosis resulting in caspase activation and cell death. There is evidence that recessive-inherited genes, such as phosphatase and tensin homologue (PTEN)-induced kinase 1 (PINK1), Parkinson's disease (autosomal recessive, early onset) 7 (DJ1) and HtrA serine peptidase 2 (HTRA2, also known as OMI), might all have neuroprotective effects against the development of mitochondrial dysfunction, although the exact site of their action remains unknown. PRKN has also been shown to inhibit the release of cytochrome *c* following ceramide-induced stress, and is itself modified by the interacting protein BCL2-associated athanogene 5 (BAG5). Dysfunction of both pathways leads to oxidative stress, which causes further dysfunction of these pathways by feedback and feedforward mechanisms, ultimately leading to irreversible cellular damage and death. I–IV, mitochondial electron transport chain complexes I–IV; α-syn(PO4)n, phospho-α-synuclein; A30P, alanine to proline substitution at α-synuclein amino acid residue 30; A53T, alanine to threonine subsitution at α-synuclein residue 53; E1, ubiquitin activating enzyme; E2, ubiquitin conjugating enzyme; E46K, glutamic acid to lysine substitution at α-synuclein residue 46; NO, nitric oxide; 3n/4n, 3 or 4 copies of α-synuclein; Tau(POi)n, Tau (POi)n, phospho-Tau; UCHL1, ubiquitin carboxyl-terminal esterase L1." (Abou-Sleiman et al., 2006)

Figure 2: Pathways to parkinsonism (Abou-Sleiman et al., 2006). Reprinted with permission.

Environmental causes of PD

In the late 1970s and early 1980s, self administration of MPTP, a contaminant of drug of abuse, resulted in motor symptoms similar to those reported in PD, along with dopamine depletion in the brain (Langston and Palfreman, 1995). This observation led to further investigation of environmental causes such as toxin exposures as a contributing factor to PD. A 1996 study in Germany involving 380 PD patients and 379 controls, reported that exposures to wood preservatives, heavy metals including iron, zinc and manganese, or pesticides, had a significant correlation with PD development (Seidler et al., 1996).

Pesticide exposure has been shown to increase incidence of PD to almost 70% (Ascherio et al., 2006). An epidemiological study in Denmark farmers hospitalized between 1981 and 1993 revealed that workers at agricultural and horticultural farms were at significantly higher risk of developing PD (Tuchsen and Jensen, 2000). A cohort study in Hawaii plantations with a 30 year follow up indicated that duration of exposures to pesticides has a significant correlation to development of PD (Petrovitch et al., 2002). Severe short term exposures to pesticides, even in residential settings, has been shown to result in development of PD symptoms (Bhatt et al., 1999).

Additionally, drinking rural well water for over 5 years has shown to increase the risk of PD development by almost 90% in a California based study (Gatto et al., 2009). Researchers from that study believed that the observed prevalence was, in fact, a result of pesticide contamination of the well water. A study by Vlajinac et. at. links ingestion of well and

spring water to PD (Vlajinac et al., 2010) and adds insecticides to the list of contributing environmental factors. Another Korean study by Cho et. al. also reports similar findings linking well water to PD (Cho et al., 2008). Exposure to metals like manganese or iron have also been shown to produce symptoms similar to the clinical symptoms of PD (Willis et al., 2010). Manganese exposure in industry workers has been shown to mimic most of the symptoms of PD, including resting tremors, bradykinesia, rigidity, postural instability, changes in gait, dystonia and micrographia (Guilarte, 2010). A study of Alabama welders, routinely exposed to welding fumes, revealed a significantly high prevalence of PD among welders (Racette et al., 2005). A recent epidemiological study of 29 million Medicare beneficiaries by Dr. Willis and colleagues indicated that there was a significant correlation between metal emissions and urban incidences of PD (Wright Willis et al., 2010). (Figure 3)

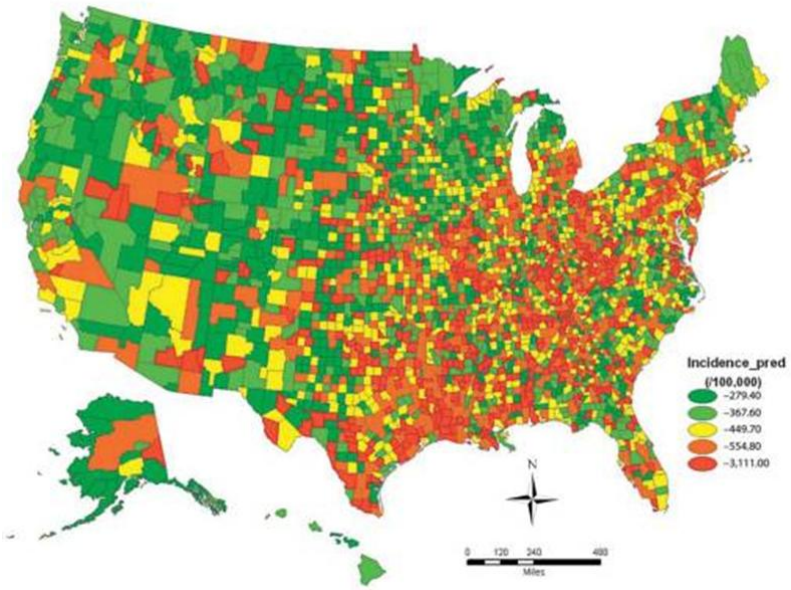

Figure 3: Prevalence of Parkinson's disease in the United States after country level age and race standardization (Wright Willis et al., 2010). The color scale indicates the number of Medicare recipients with Parkinson's disease for each 100,000. The scale runs from dark green, 1,175 per 100,000, to dark red, 13,800 per 100,000. Reproduced as per PubMed Central U.S. fair use guidelines.

All in all, environmental contribution to PD onset is quite significant. As mentioned in the previous section, it is possible that genetic factors increase one's vulnerability to the environmental insults, hence leading to development of PD. Similar to the observations in genetic PD, mitochondria dysfunction is thought to be central to toxin induced PD as well. Mitochondria functioning is essential for cell viability, but it is also a site of production of reactive oxygen species (ROS). ROS are chemically-reactive molecules containing oxygen capable of causing oxidative stress. Mitochondrial complex I and complex III are known to be responsible for keeping these ROS in control. Environmental toxins are known to inhibit functioning of these complexes, hence leading to mitochondria dysfunction and cell death by oxidative stress (Liu and Yang, 2005), leading to the pathology observed in PD.

PD neuropathology

The pathology in PD is known to affect the central, peripheral, and the entric nervous systems (Braak and Braak, 2000; Hawkes et al., 2010; Orimo et al., 2005). It has been shown to cause substantial cytoskeletal alterations in various brain regions in a slow but relentless manner (Kidd, 2000). In addition to being a disorder of the dopamine projection system, glutamatergic, cholinergic, tryptaminergic, GABAergic, noradrenergic, and adrenergic damage has also been reported in PD (Braak and Braak, 2000). Hence, the characterization of PD as solely a disorder of the dopamine projection system would not be a completely accurate statement.

Presence of lewy bodies, lewy neuritis, and dopaminergic degeneration are hallmarks of PD pathology, as was first demonstrated by F. Lewy in 1912 (Wakabayashi et al., 2006). Lewy bodies are protein aggregates that, among other proteins contain ubiquitin and α-synuclein. These can proteins be found in cell bodies and neurites of certain neuronal populations (Lotharius and Brundin, 2002), including hypothalamus, nucleus basalis, substantia nigra, locus ceruleus, dorsal raphe nucleus and dorsal vagal nucleus (Jager and Bethlem, 1960; Kakita et al., 1994; Ohama and Ikuta, 1976; Oyanagi et al., 1990; Wakabayashi and Takahashi, 1997). Lewy bodies have also been reported in the amygdala and the cerebral cortex (Braak et al., 1994; Hughes et al., 1992).

Dopamine pathology in PD is not homogeneous and not all dopaminergic neurons are affected by the pathology of PD. For example, severe loss of dopaminergic neurons is reported in the substantia nigra of PD patients (Halliday et al., 1990). The striatum, a part of the basal ganglia, which receives dopaminergic projections from the substantia nigra, is also significantly impacted by PD (Graybiel et al., 1990; Kish et al., 1988). The striatal damage is more severe in the putamen than in the caudate nucleus. The ventral tegmental area is affected to a lesser extent as compared to the substantia nigra (Gibb and Lees, 1991). The loss of dopamine in the nucleus accumbens is to a much lesser extent, and the dopaminergic neurons in the hypothalamus appear to be spared in PD (Matzuk and Saper, 1985).

The pattern of neuronal damage observed in PD is not random and shows specificity by region, neural cell type, and has a distinctive

bilateral symmetry, which has been noted consistently across postmortem studies in patients. Reasons for the selective degeneration are still unknown (Braak and Braak, 2000; Braak et al., 2003).

Diagnosis and clinical symptoms

James Parkinson originally erroneously asserted that sensory and intellectual abilities are unaffected in patients with the disease. Since then, the focus has primarily been on the motor aspect of PD symptomology.

Motor symptoms

According to the National Institute of Neurological Disorders and Stroke, the four primary symptoms of PD are (Weintraub et al., 2008):

1. Tremor (trembling in hands, arms, legs, jaw, and face)
2. Rigidity (stiffness of the limbs and trunk)
3. Bradykinesia (slowness of movement)
4. Postural instability (impaired balance and coordination).

Along with these there are secondary symptoms which also have been reported (Weintraub et al., 2008).

- Stooped posture, a tendency to lean forward
- Dystonia
- Fatigue
- Impaired fine motor dexterity and motor coordination
- Impaired gross motor coordination
- Poverty of movement (decreased arm swing)

- Akathisia (feeling of inner restlessness, leading to an inability to sit still or remain motionless)
- Speech problems, such as softness of voice or slurred speech, caused by lack of muscle control
- Loss of facial expression, or "masking"
- Micrographia (small, cramped handwriting)
- Difficulty swallowing
- Sexual dysfunction
- Cramping
- Drooling

Existence of one or more of the primary symptoms, along with medical history of the patient, is used to diagnose the disease. Responsiveness to Levodopa, one of the drugs used as a treatment for PD, is also considered a confirmation of PD diagnosis. According to the Hoehn and Yahr scale for PD stages (Hoehn and Yahr, 1967), PD patients go through five stages. (Figure 5)

Stage I: Very subtle, unilateral existence of one or more of the primary symptoms.

Stage II: Bilateral primary symptoms and additional secondary symptoms.

Stage III: Symptoms from stage two increase in severity, and problems with balance become prominent. At this stage, the person with Parkinson's is still independent.

Stage IV: Motor symptoms result in disability, leading to the patient needing assistance in most daily activities.

Stage V: Patient is bed or wheelchair bound and needs complete assistance.

Non-motor symptoms of Parkinson's disease

Recent reports in PD patients have confirmed the existence of a variety of non-motor symptoms (Bowers et al., 2006; Chen, 2010; Cools et al., 2001; Hawkes, 2008; Hawkes et al., 1997). These include:

- Hyposmia (reported in 80% of the patients at the time of diagnosis)
- Pain
- Cognitive deficits (about 50%; deficits in memory, attention, executive function and dementia are reported)
- Sleep disturbances (REM behavior change)
- Constipation and urinary problems
- Depression (10 – 40 %)
- Changes in aversion, fear and anxiety
- Compulsive behavior
- Lack of impulse control

These non-motor symptoms have been reported by PD patients years before the diagnosis. Currently, the research focus has shifted from the motor-symptoms to the non-motor symptoms as they may provide clues for pre-motor diagnosis of PD.

Pre-motor stages of Parkinson's disease

Although the nigrostriatal pathway remains a major focus, emerging information demonstrates the participation of both the mesocortical and cortico-limbic pathways in this disease process (Braak and Braak, 2000).

Post-mortem studies have shown existence of lewy bodies and lewy neurites, a marker of neurodegeneration, in the olfactory bulb, anterior olfactory nucleus, dorsal motor nucleaus complex, and pons pre-motor pathology in PD (Braak et al., 2003; Hawkes et al., 1997). PD patients report olfactory deficits years before the clinical diagnosis (Ponsen et al., 2009) and onset of PD symptoms have shown very strong correlation with reports of hyposmia four years before the onset(Ross et al., 2008). Excessive daytime sleepiness (Abbott et al., 2005), depression and anxiety (Arabia et al., 2007; Shiba et al., 2000) and constipation

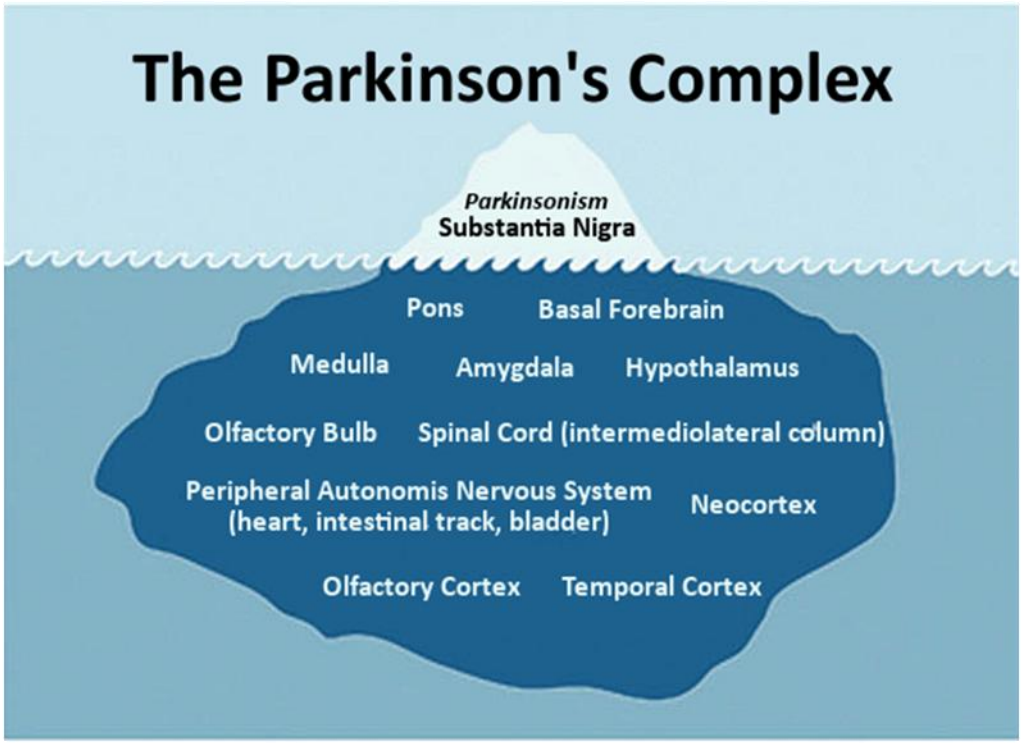

Figure 4: Tip of iceberg analogy of PD pathology. Reproduced with permission. (Langston, 2006)

(Langston, 2006) are also reported. Langstan refers to the substantia nigra symptoms as just the tip of the PD iceberg. (Figure 4)

Dopamine depletion is a very prominent marker of PD. However, by the time of onset of the motor symptoms in stage I (Hoehn and Yahr scale), more than 50% (Fearnley and Lees, 1991; Tang and Eidelberg, 2010) of the substantia nigra dopamine cells are degenerated and 80% of the striatal dopamine is depleted(Fearnley and Lees, 1991; Pahwa and Koller, 1995; Steece-Collier et al., 2002). Early PD patients show reduction in DA tracer uptake in the striatum in contralateral, as well as, ispilateral sides while a asymptotic twin study has indicated reduction in striatal DA uptake 2-21 years prior to motor symptoms (Gaig and Tolosa, 2009).

Thus, Braak et. al. proposed a new timeline (Hawkes et al., 2009) for PD, extending almost 20 years prior to the motor symptoms (Figure 5).

Braak Stage 1: Changes in bowel movement (<1 /day), bladder and erectile problems, and changes in olfaction (hyposmia or anosmia) might be some of the earliest signs of PD. These changes are accompanied by incidental lewy bodies in locus coeruleus, a nucleus in brain stem and olfactory pathology.

Braak Stage 2: PD patients in this stage exhibit one or more of the following symptoms: excess daytime sleepiness and REM sleep behavior disorder, depression (with serotonergic basis), and obesity. Pathology of coeruleus/subcoeruleus complex (CSC), magnocellular portions of the reticular formation, and posterior raphe nuclei are also observed. Since the raphe nucleus is also involved in memory and learning, cognitive deficits might be present.

Braak Stage 3: This stage is close to the Hoehn and Yahr stage I. The symptoms include unilateral motor deficits and depression (with dopaminergic basis). Lewy body pathology is observed in the substantia nigra and central nucleus of the amygdala. Even though Braak et. al. do not mention it, given the reports of striatal dopamine depletion observed almost 5 years before the onset of motor symptoms, dopamine depletion can be added to the pathology of late Braak stage 2 or early Braak stage 3.

Braak Stage 4: This stage is similar to the Hoehn and Yahr stage II with bilateral motor deficits and lewy body pathology in multiple sites, including interstitial nucleus of the stria terminalis, the accessory cortical and basolateral nuclei of the amygdala, the ventral claustrum, intralaminar nuclei of the thalamus (limbic circuit), the second sector of the Ammon's horn and the anteromedial temporal mesocortex. This pathology can also be accompanied by changes in impulse control,

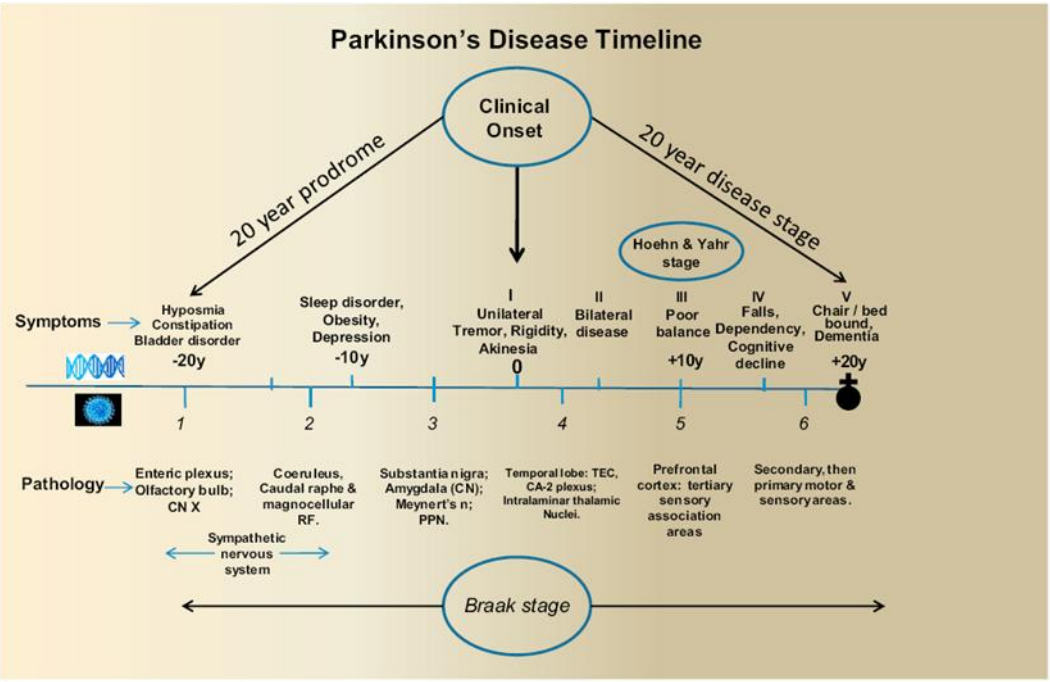

Figure 5: Progression of Parkinson's disease. Reproduced with permission. (Hawkes et al., 2009)

hypersexuality and pathological gambling, along with the coexisting emotional, cognitive and olfactory deficits.

Braak Stages 5 and 6: These stages are the late stages of PD with severe motor deficits, extensive cortical damage with additional lewy body pathology into the insular, subgenual mesocortex, anterior cingulate regions extending to pre-motor areas of neocortex, primary motor and sensory motor areas.

Treatment

Currently, there is no cure available for PD. The most commonly used drug is L-3, 4-dihydroxyphenylalanine (Levodopa or L-dopa) (Hauser, 2010). Unlike dopamine, L-dopa can cross the blood brain barrier when given systemically. Brain enzymes can convert L-dopa to dopamine; thus, making it a good dopamine-replacement therapy. This supplementation of dopamine with L-dopa is used to treat the motor symptoms of PD. Arvid Carlsson, a Swedish scientist, was the first to show reduction in PD symptoms in animals after treatment with L-dopa in the 1950s. He demonstrated that dopamine was indeed a neurotransmitter in the brain, and not just a precursor for norepinephrine. Initial trials of L-dopa treatment in humans included very low doses of the compound, which only produced transient effects. George Cotzias and his coworkers later extended this to the treatment of manganese poisoning and Parkinsonism by increasing the dose (Barbeau, 1969; Cotzias, 1968). Since then, it is a standard treatment for PD. Currently, it is also used in the diagnosis process that, a positive response to the L-dopa is considered a confirmation of PD. However, L-dopa treatment is known to stop working

suddenly for short durations from time to time (Hauser, 2010). It is prescribed in combination with dopamine deoxylase inhibitor. This combination prevents L-dopa's synthesis in the blood stream; hence, delivering more drug to the brain, reducing some of the side effects such as nausia. Even then, prolonged usage of L-dopa has shown to cause motor fluctuations and dyskinesia (spontaneous, involuntary movements). Hence, the start of treatment is delayed until the PD symptoms become severe enough that the benefits outweigh the side effects (Hauser, 2010).

Dopamine agonists can also be prescribed in combination with L-dopa. Severe side effects of this treatment have shown to cause problems such as heart valve damage, sleep disorder and impulse control disorders.

Anti-cholinergics, which decrease the activity of acetylcholine to balance out the production of dopamine and acetylcholine, can also be prescribed during mild PD. This combination has been shown to reduce some of the side effects of L-dopa. Adverse effects of these drugs include blurred vision, dry mouth and urinary retention, and confusion and hallucination in older patients.

MAO-B (monoamine oxydase-B) inhibitors and COMT (catechol-O-methyl transferase) inhibitors can be prescribed in conjunction with L-dopa in order to extend the effectiveness over longer periods of time. However, MAO-B inhibitors may interact with anti-depressants, narcotic pain killers and decongestants (Hauser, 2010; Parkinson'sDiseaseFoundation, Accessed 2011).

Thus, the available treatments primarily focus on supplementing the brain with dopamine, or stimulating the dopamine receptors with agonists in an effort to stimulate receptors in absence of dopamine. However, after a few years, most combinations of dopamine treatments tend to become less effective, and symptoms become more difficult to manage (Rascol et al., 2003). Another important point to note is that, none of these treatments effectively treat the non-motor symptoms of PD.

Summary

Parkinson's disease is a progressive neurodegenerative disorder which affects various parts of the nervous system in a highly selective and time dependent manner, eventually rendering the patient bed ridden and needing complete assistance over time. The exact causes of PD are still not completely understood, but genetic predisposal and impact of environmental toxins has been heavily linked to the development of the disease. The manifestation of motor deficits, currently used to diagnose PD, occurs relatively late during the progression of the disease. The current treatments neither reverse the morphological changes, nor arrest the progress of the disease. More research is needed to completely understand the pre-motor/pre-diagnosis stages of the disease and ultimately develop more effective treatment strategies.

Chapter 3. Magnetic Resonance Imaging

Nuclear Magnetic Resonance to Magnetic Resonance Imaging

Magnetic resonance imaging (MRI) is based on the principles of nuclear magnetic resonance (NMR), which was first described by Isidor Rabi during his study of atomic and molecular beam magnetic resonance method for observing atomic spectra. Later, Felix Bloch and Edward Mills Purcell independently applied principles of NMR to solids in 1946 (Henderson, 1983). In 1971, Raymond Damadian established the difference between the nuclear relaxation times of tissues and tumors (Henderson, 1983). Paul Lauterbur demonstrated imaging of small test tube samples using the principles of NMR in 1973, using the back projection method used in x-ray based computer tomography (Henderson, 1983; Lauterbur, 1973). MRI using phase and frequency encoding and the Fourier Transform NMR was first proposed by Richard Ernst in 1975 (Kumar et al., 1975). A few years later, in 1977, Raymond Damadian demonstrated a new MRI technique called field-focusing nuclear magnetic resonance, and Peter Mansfield developed the echo-planar imaging (EPI) technique (Henderson, 1983; Mansfield and Maudsley, 1977). In the late 70s, the word 'Nuclear' had serious negative connotations attached to it and it was there by dropped from the name and NMRI became MRI.

Nuclear spin and magnetic dipole moment

Nuclei of elements are made of positively charged protons and neutral neutrons with spins (Beall et al., 1984; Pykett et al., 1982). Individual protons and neutrons have ±½ spin. Two protons (or two neutrons) in

one nucleus cancel out the spins between them (Beall et al., 1984; Buxton, 2002). Elements with unpaired spins have an overall non-zero nuclear spin (I) and, thus, a magnetic dipole moment (MDM) associated with it (Jackson and Fox, 1999; Pykett et al., 1982) as represented by equation 3-1.

$$\mu = \gamma P \tag{3-1}$$

where $P = (h / 2\pi).[I(I+1)]^{1/2}$ (h = Planck's constant = 6.63 x 10-34 $kg.m.s^{-1}$) is the angular moment associated with the nucleus and γ is called the gyromagnetic (or magnetogyric) ratio (Jackson and Fox, 1999; James Jr et al., 1982; Pykett et al., 1982).

Nuclei with non-zero magnetic moment associated with them are exploited by MRI (Buxton, 2002; Rohlf and Collings, 1994). Table 1 shows the nuclei that are used commonly during MRI. The most commonly used amongst them is the hydrogen nucleus (^{1}H), also called the proton, because of its abundance in the human body (Beall et al., 1984; Henderson, 1983).

Nuclei	Unpaired Protons	Unpaired Neutrons	Net Spin	γ (MHz/T)	Biological Abundance (%)
^{1}H	1	0	1/2	42.58	0.63
^{2}H	1	1	1	6.54	
^{31}P	1	0	1/2	17.25	0.0024
^{23}Na	1	2	3/2	11.27	0.00041
^{14}N	1	1	1	3.08	0.015
^{13}C	0	1	1/2	10.71	0.094
^{19}F	1	0	1/2	40.08	-

Table 1: Nuclei commonly used for MRI

Under normal conditions, magnetic moments from multiple protons are randomly distributed. When placed in strong external static magnetic field (Bo) along the Z direction, these individual MDMs (μ, plural μs)

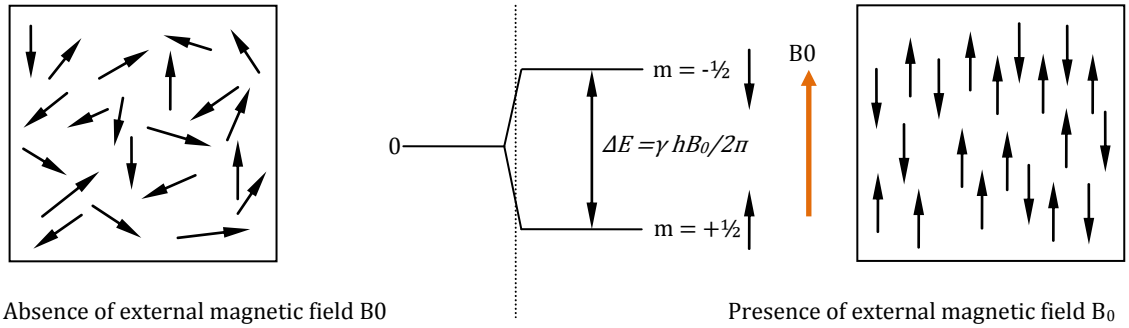

Figure 7: Random individual magnetic dipole moments, when exposed to strong external magnetic field B_0, realign themselves in either the high energy state, in the direction opposite to B_0, or in the low energy state in the direction parallel to B_0.

rearrange themselves either in a low energy state where their magnetic moments are parallel to the direction of the B0 or in a high energy state where their μs are in exact opposite direction as per Boltzmann's distribution (Figure 7). The two energy states are represented by equation 3-2.

m_i is ±½ for a proton (^1H isotope of hydrogen, found in abundance in-vivo) and h is Planck's constant (6.626 x 10^{-34} kg.m/s).

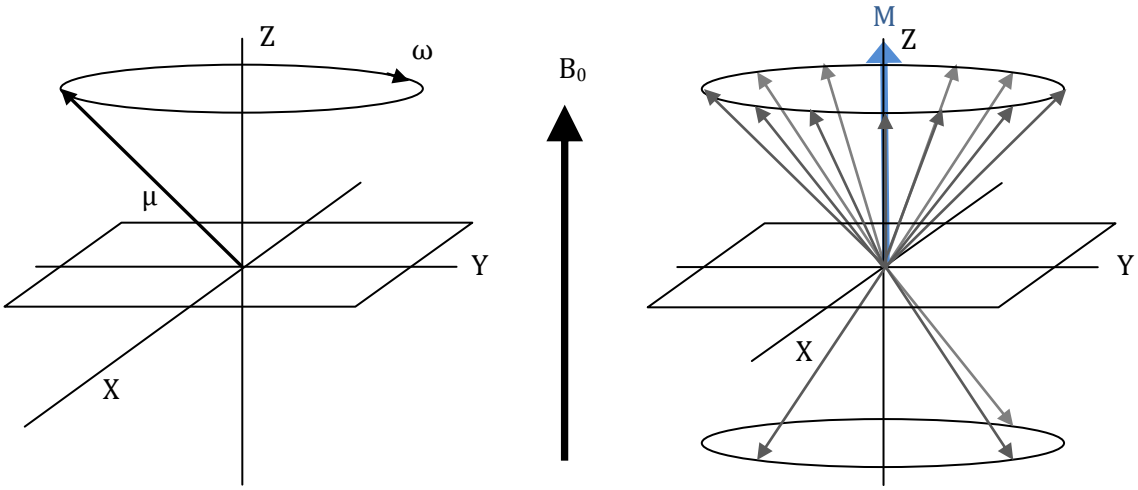

Figure 6: Individual magnetic dipole moment and net magnetization

$$E_i = -m_i\left(\frac{\gamma h B_0}{2\pi}\right)$$

3-2

The effective net magnetization (M) is the sum of all the μs. When the system is at Boltzmann's equilibrium, there are more μs in the lower energy state (i.e. in the same direction as Bo) than in the higher energy state (i.e. in the direction of −Bo). Thus, the effective net magnetization M is in the direction of Bo. The projections of the μs in the X-Y plane cancel themselves out (Figure 6). The net magnetization at Boltzmann's equilibrium is usually denoted by M_o. M_o depends purely on the Bo strength and the density of protons in the sample called the proton density (ρ) (Beall et al., 1984; James Jr et al., 1982; Liu et al., 1989).

While in these energy states, these protons continue to precess at frequency ω, Larmor frequency (Bargmann et al., 1959), given by the

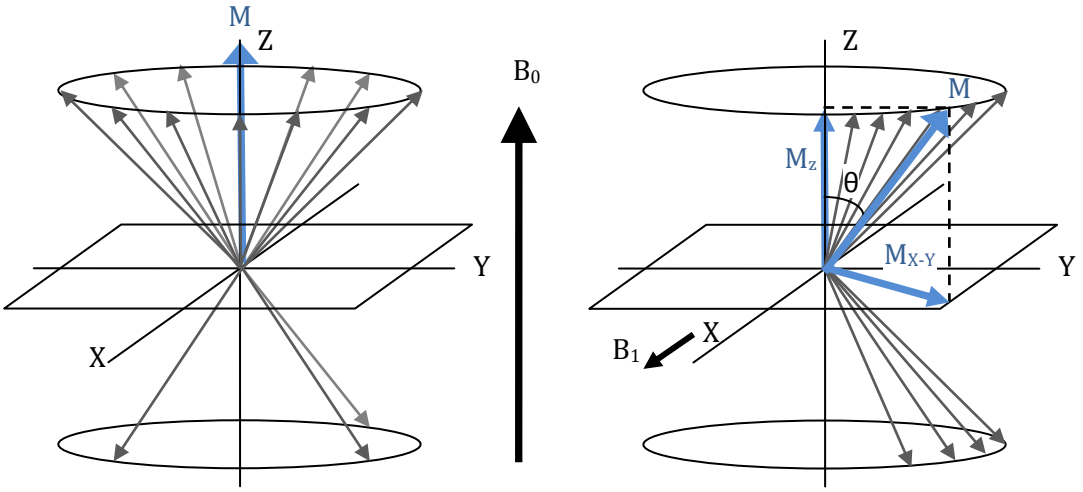

Effective total magnetization (M_z) at Boltzmann's equilibrium

Effective total magnetization (M) and its longitudinal component M_z and transverse component M_{X-Y} upon application of B_1

Figure 8: Upon application of RF pulse B_1, the net magnetization is rotated though a certain angle θ depending upon the energy provided by B_1.

Larmor equation 3-3

$$\omega = \gamma B_0 \quad \frac{rad}{s}$$

3-3

If enough energy is supplied, these μs can move to the higher energy states, effectively changing the direction of M (James Jr et al., 1982). (Figure 8)

This required energy is supplied in the form of a radio frequency (RF) pulse at the frequency ω/2π (Pykett et al., 1982), at right angle to B0 and is denoted by B1. Since B1 is at the same frequency as the μs, the protons at resonance start to absorb energy and start moving to the higher energy state. As more and more μs move to the higher energy state, the net magnetization is rotated towards the X-Y plane. The angle through which the net magnetization is rotated (θ, equation 3-4) is called the flip angle. θ depends upon the duration (t) and strength (B1) of the RF pulse, hence in turn, on the total energy supplied (James Jr et al., 1982; Pykett et al., 1982).

$$\theta = \gamma B_1 t$$

3-4

If B1 is applied such that θ = 90°, then the entire M_o is rotated to the X-Y plane. i. e. $M_{X-Y} = M_o$ and $M_z = 0$; and if θ = 180° then $M_{X-Y} = 0$ and $M_z = M_o$.

Longitudinal and Transverse relaxations

After the RF pulse B1 is removed, the net magnetization starts to return to the Boltzmann equilibrium (James Jr et al., 1982; Pykett et al., 1982).

This recovery happens due to two mechanisms. The first mechanism is called the transverse relaxation. During transverse relaxation, the X-Y component of the net magnetization, M_{X-Y}, disperses in what is called the transverse relaxation time or spin-spin relaxation time, T2 (James Jr et al., 1982; Pykett et al., 1982).

While under influence of B1, all the μs are in coherence and all the protons are spinning at the same frequency as B1, which is the Larmor frequency. The μs cannot stay aligned with each other after the B1 is removed. As they start to disperse and relax, every proton experiences not just the B_0, but also the magnetic field produced by the μs of the neighboring protons. This makes the net magnetic field experienced by each individual proton, slightly different from the one experienced by the other protons, causing them to start spinning at slightly different frequencies from each other. The result is an even larger difference between the external magnetization experienced by individual protons,

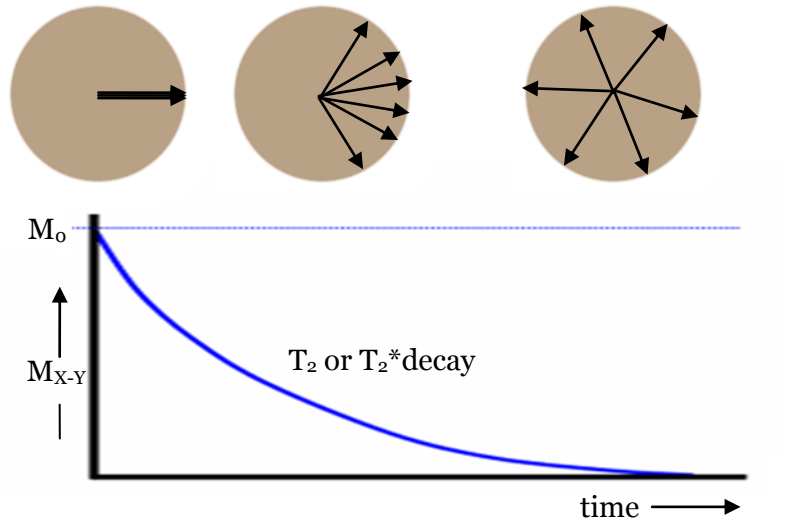

Figure 9: Transverse relaxation. After the B1 pulse is removed, the transverse component of the net magnetization disperses with T2 (or T2*) decay.

leading to loss of coherence between them. Hence, transverse relaxation is also called the spin-spin relaxation (Hinshaw and Lent, 1983; James Jr et al., 1982; Pykett et al., 1982). At any point of time t, the transverse magnetization M_{X-Y} is given by equation 3-5.

$$M_{X-Y} = M_0 \sin(\theta) e^{-t/T_2} \quad \text{3-5}$$

Where, θ is the flip angle. In practice, M_{X-Y} decays at a rate faster than T2 because of additional factors such as inhomogeneities in the magnetic field, susceptibility and diffusion. The resultant faster transverse decay time is called T2* (Buxton, 2002; Haacke et al., 1999; Pykett et al., 1982). M_{X-Y} at any point of time during T2* decay, can be computed simply by replacing T2 from the equations 3-5 with T2*value. As the size of the molecule that the protons are bound within increases, it increases the number of neighboring magnetic fields experienced by the proton. Hence,

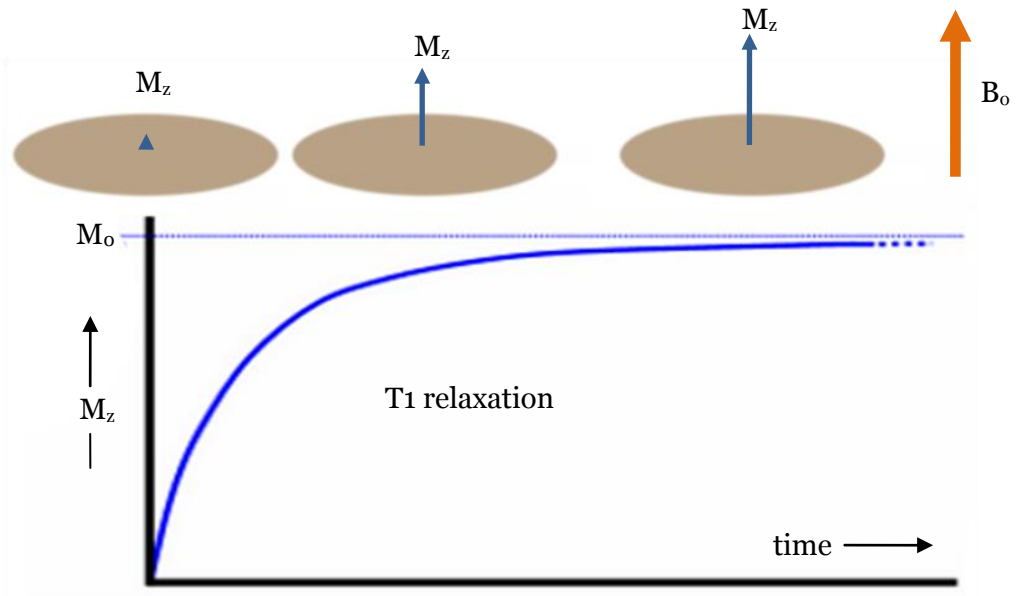

Figure 10: Longitudinal relaxation. After B1 is removed, Mz slowly relaxes to its Boltzmann equilibrium value.

the T2 time decreases as the molecular size increases (Figure 11).

In the second mechanism, the Z component of the magnetization recovers at a slower pace. The time for this recovery is called the longitudinal relaxation time or spin-lattice relaxation time, T1. T1 is dependent on how effectively the proton can transfer the excess energy to the surrounding lattice, in order to return to the ground/stable state (Hinshaw and Lent, 1983; James Jr et al., 1982; Pykett et al., 1982). Hence, the higher the resonance between the lattice and the proton, the shorter the T1. At any point of time (t) during the longitudinal relaxation, the value of M_z can be calculated as

$$M_z = M_0(1 - n\, e^{-\frac{t}{T1}}) \quad \text{3-6}$$

where n = 1-cosθ.

As the molecular size increases, the T1 relaxation time decreases and attains a minimum where the average rotational/translational frequency of the molecules matches the Larmor frequency. As the molecular size increases further, the T1 relaxation time also increases due to the increasing mismatch between the average molecular rotational/translational frequency and the Larmor frequency.

Thus, T1, T2, T2* and ρ depend on the biological sample and the magnitude of the main magnetic field (B_o). These are also the contributing factors to the contrast seen in most magnetic resonance images (Henderson, 1983; Liu et al., 1989; Pykett et al., 1982). The acquisition time at which the signal is acquired after the initial excitation decides the contrast achieved between neighboring tissues. (Figure 12)

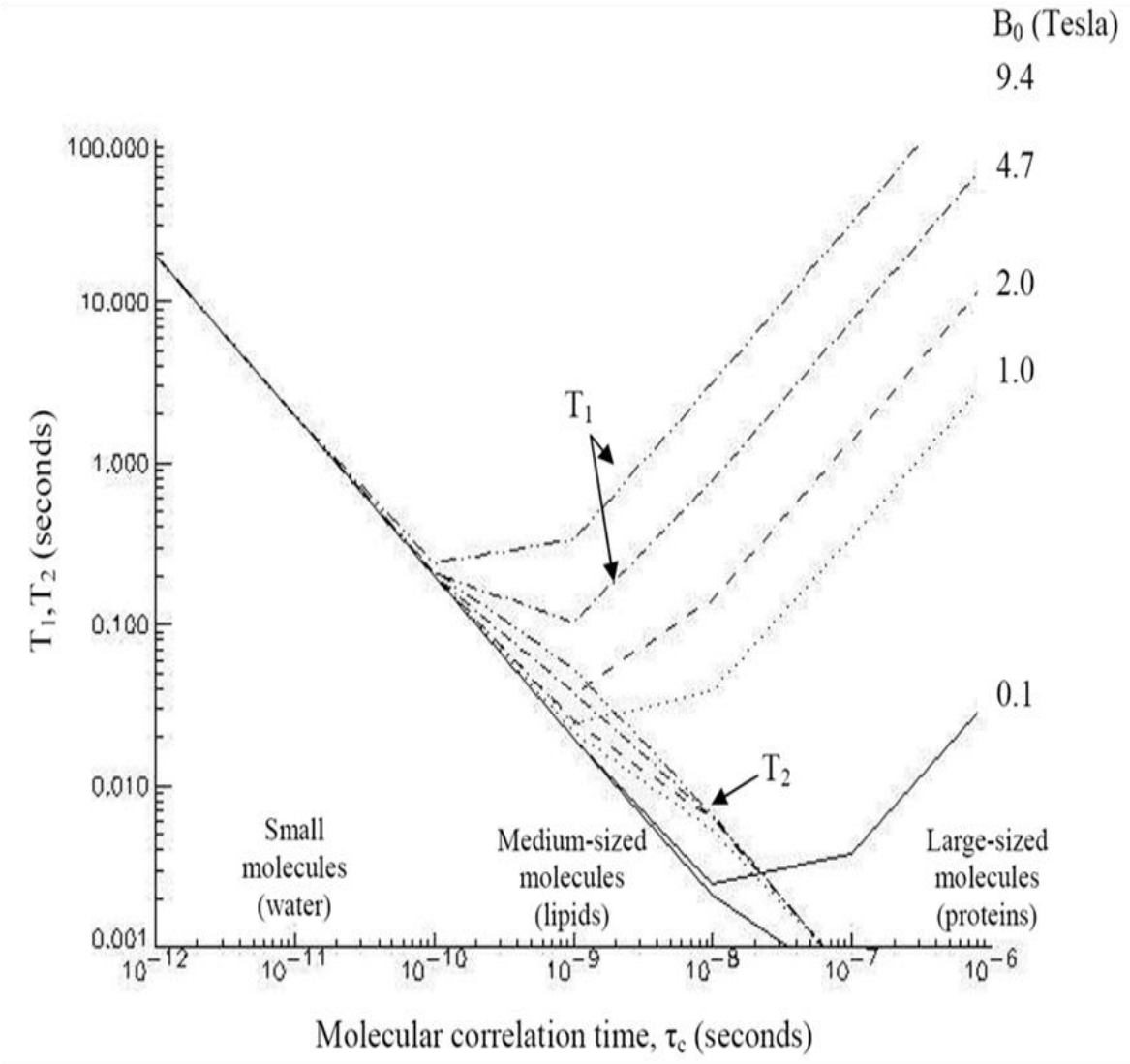

Figure 11: Plot of T1 and T2 relaxation times versus molecular correlation time (τc). For bulk water, T1 and T2 relaxation times are nearly identical (this is the so-called 'extreme narrowing' regime), while for larger molecules, such as lipids and proteins, T1 and T2 differ significantly. The dependency of T1 on the main magnetic field strength, Bo, is clearly demonstrated for medium-sized and large molecules. The minimum in the T1 curves is the point at which the rotational frequency of the molecules (i.e. 1/τc) equals the Larmor frequency.

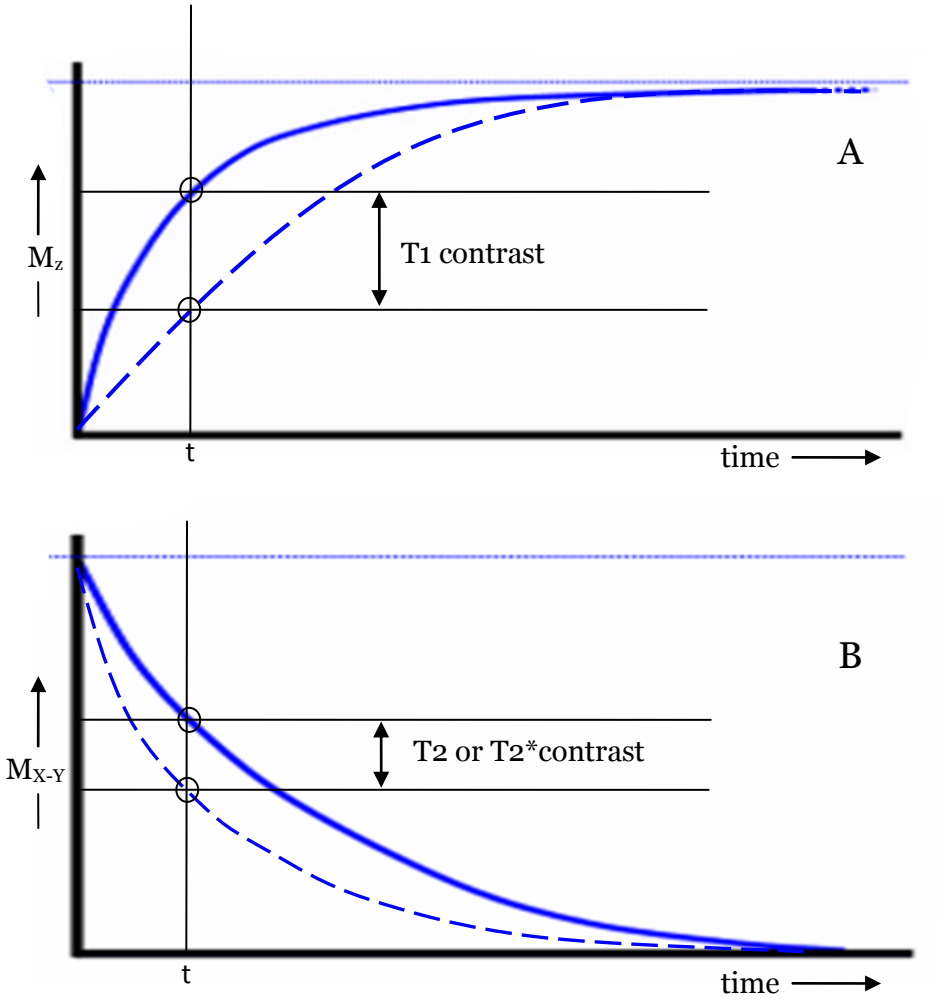

Figure 12: A. T1 contrast due to differences in T1 values of different tissues. The signal with a lower T1 (solid line) relaxes faster than signal with a higher T1 (dotted Line); B. T2 contrast due to different T2 vales of different tissues. Signal with lower T2 (dotted line) versus signal with longer T2 (solid line) have different M_{X-Y} values at the same time; hence result in different MRI intensities. In both cases, the contrast depends on the time (t) at which the signal is collected.

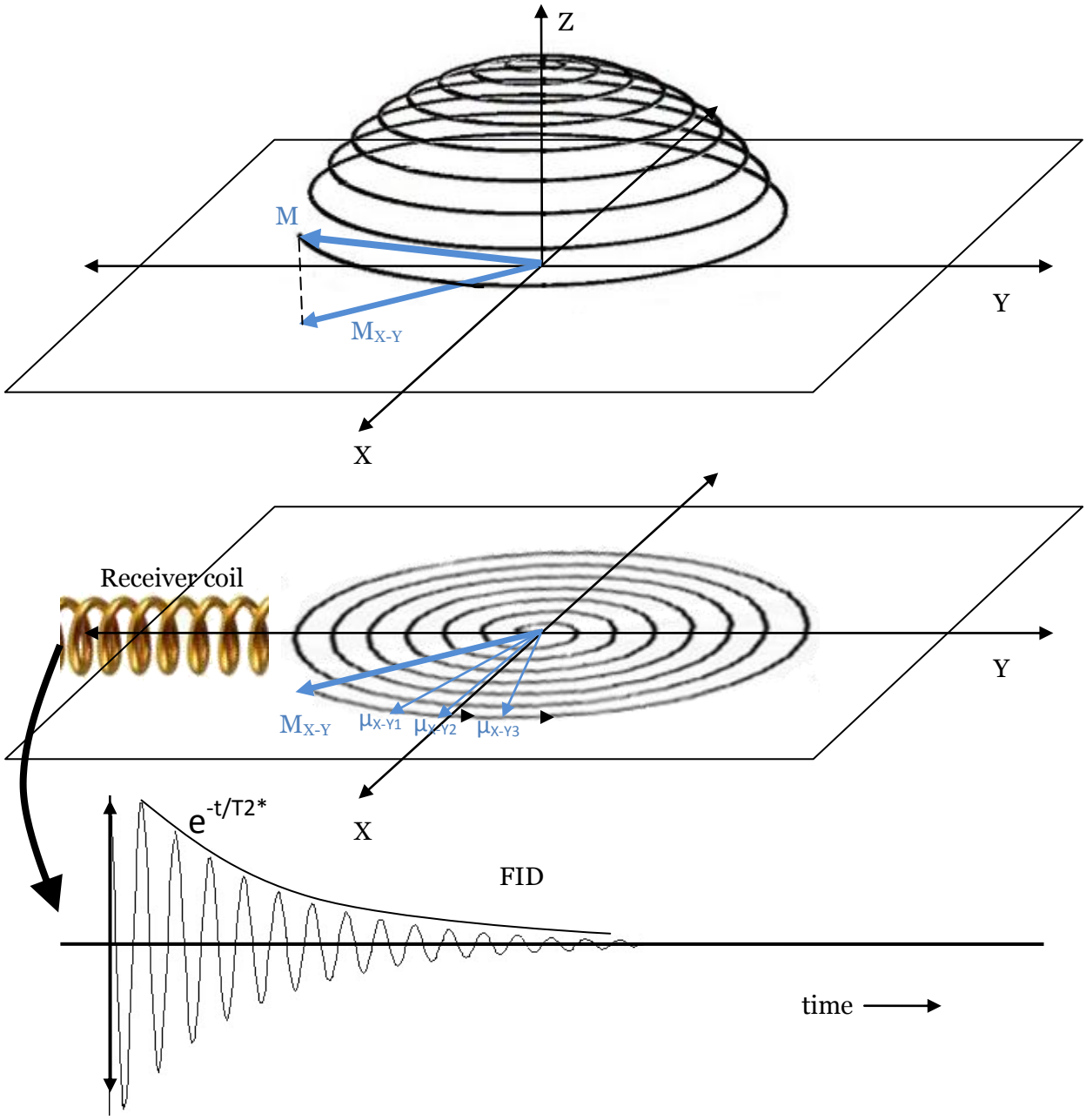

Figure 13: As the M spirals back to its Boltzmann equilibrium position in Z direction, its X-Y component (M_{X-Y}) induces an oscillating current into a receiver coil called the free induction decay (FID) before the individual proton MDMs (μ_{X-Y}s) dephase off. The rate of decay of FID is $e^{-t/T2^*}$.

Signal acquisition

M spirals back to its Boltzmann equilibrium position in Z direction after B1 is removed. During this time, its X-Y component, M_{X-Y}, is also changing. Before all the μ_{X-Y}s (X-Y components of μs)are completely dispersed off because of T2* decay, the oscillating magnetization induces an oscillating current into a receiver coil (Henderson, 1983; Hinshaw and Lent, 1983) according to the Faraday's law of induction. This oscillating signal is called the free induction decay (FID)(Kumar et al., 1975). (Figure 13) 'Free', because it is not under the influence of B1 anymore; and decay, because it decays to zero. The receiver coil is designed to measure the signal present in the X-Y plane. Hence, to collect either the transverse or the longitudinal component of M, it has to be moved to the X-Y plane. When X-Y components of the μs, μ_{X-Y}s, are dephased, they cancel each other out, hence, making the signal intensity zero. In order to induce sufficient signal into the receiver coil, it is important that all μ_{X-Y}s are in phase. The active rephasing and dephasing of the X-Y components is achieved by a sequence of RF pulses and/or a sequence of gradients called the pulse sequence. In order to understand how these pulse sequences work, it is important to understand an echo.

Echo

After removal of B1, each of the μs experiences a slightly different external magnetic field due to the surrounding μs. This makes the speed, at with these μ_{X-Y}s are dispersing off, different from each other. Some of them are fast while some are slow (Figure 15). They can be refocused by either flipping them through 180°, so that instead of going away from each other they start to move towards each other, or by exerting

additional external magnetic field, so that they are forced back together. When they finally come back in phase, the signal received is called an echo (Haacke et al., 1999; Hahn, 1950).

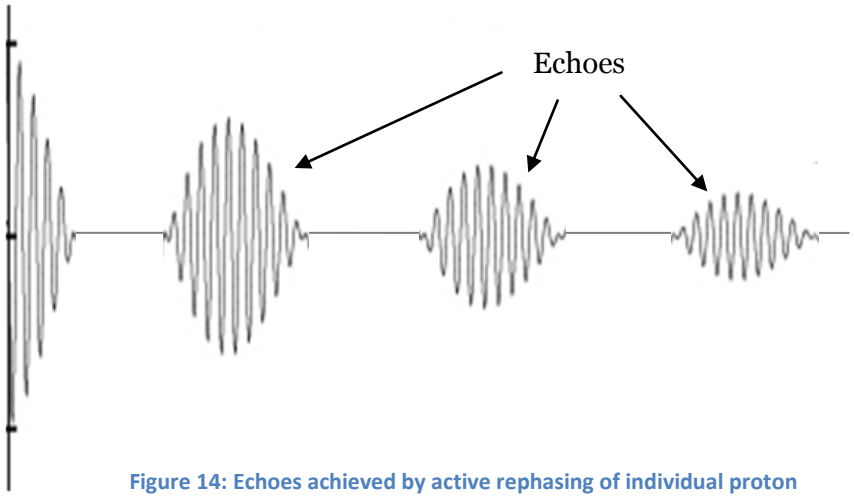

Figure 14: Echoes achieved by active rephasing of individual proton magnetic dipole moments.

Spin Echo RF pulse sequence

In a spin-echo pulse sequence, the rephasing of μ_{X-Y}s is achieved using a 180° RF pulse (James Jr et al., 1982; Liu et al., 1989). Initially we excite M by applying B1 pulse (the Figure 15 has θ = 90°). Right after the B1 pulse is removed, the μ_{X-Y}s start to dephase. After dephasing for some time, the fastest μ_{X-Y} is leading and the slowest one is trailing. At that time, an additional 180° B1 pulse is applied, such that now, the μ_{X-Y}s are flipped. The fastest μ_{X-Y} is now trailing, and the slowest one is in the lead. That way, the fast μ_{X-Y}s catch up to the slow ones in the same time that was given for dephasing in the first place. This gives rise to an echo (Pykett et al., 1982). This time to echo, from the application of the first 90° RF pulse, is denoted by TE, and hence, the 180° pulse is applied

exactly at TE/2 (Figure 16). The signal acquired using a spin echo sequence is T2 weighted and is unaffected by field inhomogeneity, and hence, T2* (Buxton, 2002; Haacke et al., 1999).

Gradient Echo RF pulse sequence

During a gradient echo pulse sequence, we do not apply the 180° refocusing pulse, as in the spin echo sequence (Buxton, 2002). Instead, an additional gradient is applied called the readout gradient in the frequency encoding direction. (Figure 17) Since this sequence forces the spins together and does not require an additional 180° pulse, it is much faster than the spin-echo sequences. Gradient echo signal intensity is weighted by T2*, which makes it a preferable for blood oxygenation level dependent functional MRI scanning. The signal acquired using a gradient echo pulse sequence is affected by susceptibility artifacts which occur at the interfaces of two materials of different magnetic susceptibilities like air and tissue interface near the sinus cavity (Buxton, 2002; Haacke et al., 1999).

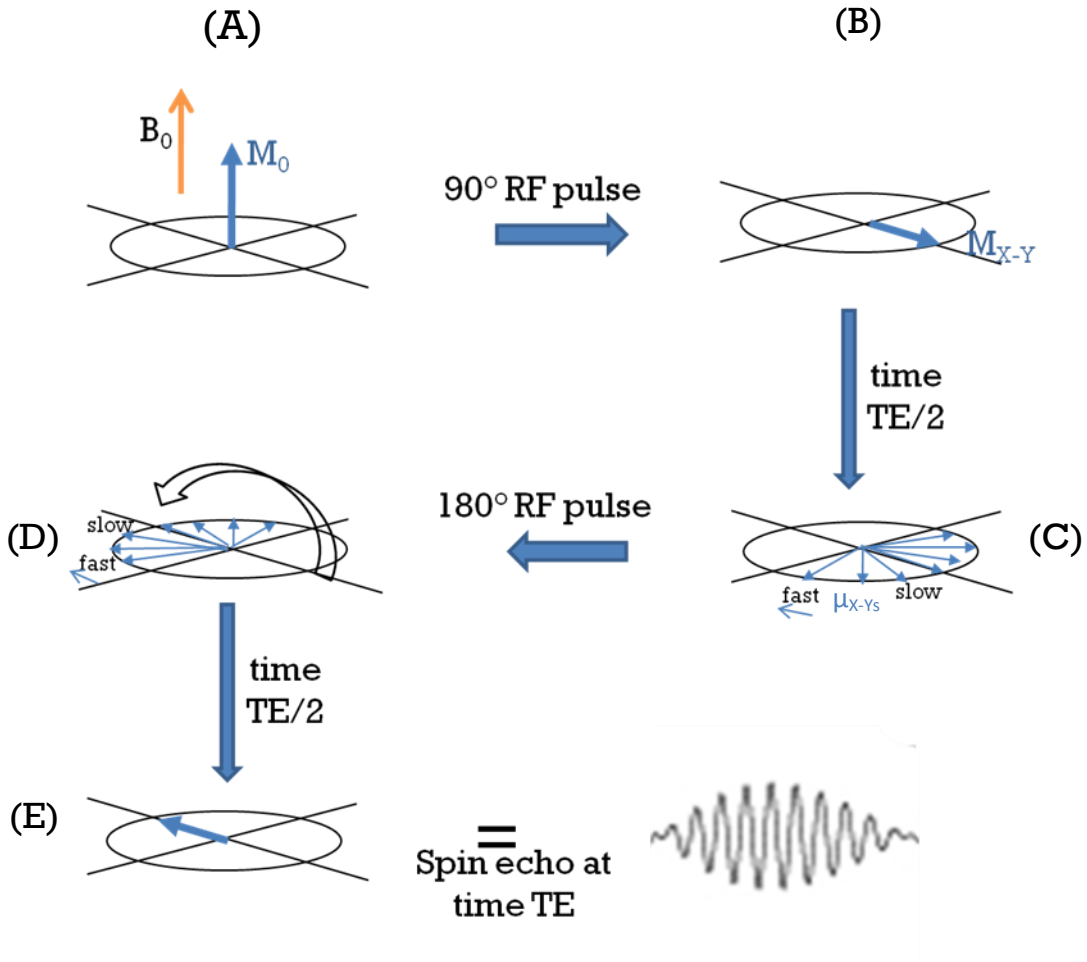

Figure 15: Formation of a spin in Spin Echo. Initially M_0 is aligned with B_0 (A). A 90° RF pulse knocks M_0 to the X-Y plane (B). After TE/2 time, the X-Y components of individual magnetic dipole moments (μ_{X-Y}) are dispersed with the fastest component leading and hence the farthest from the initial M_{X-Y} position (C). Another 180° RF pulse flips the μ_{X-Y}s such that the fastest component is now trailing (D) and after another TE/2 time, all the μ_{X-Y}s come back in focus resulting in an echo (E).

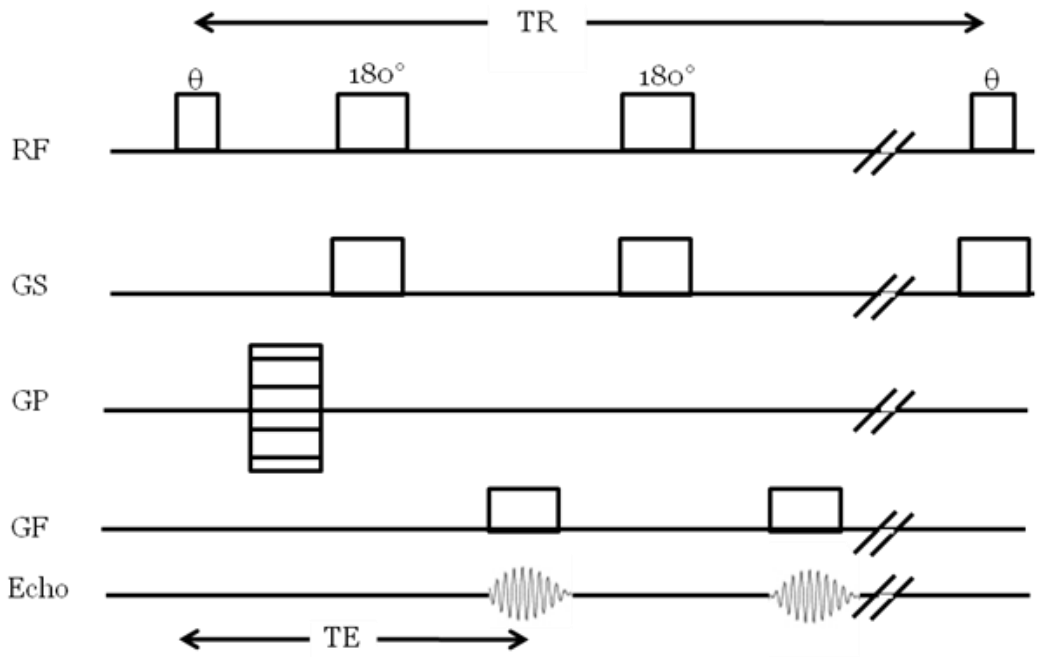

Figure 16: Spin Echo pulse sequence. GS, Slice selection gradient; GP, Phase encoding gradient; GF, Frequency encoding gradient; TR, Repetition time; TE, Time to echo.

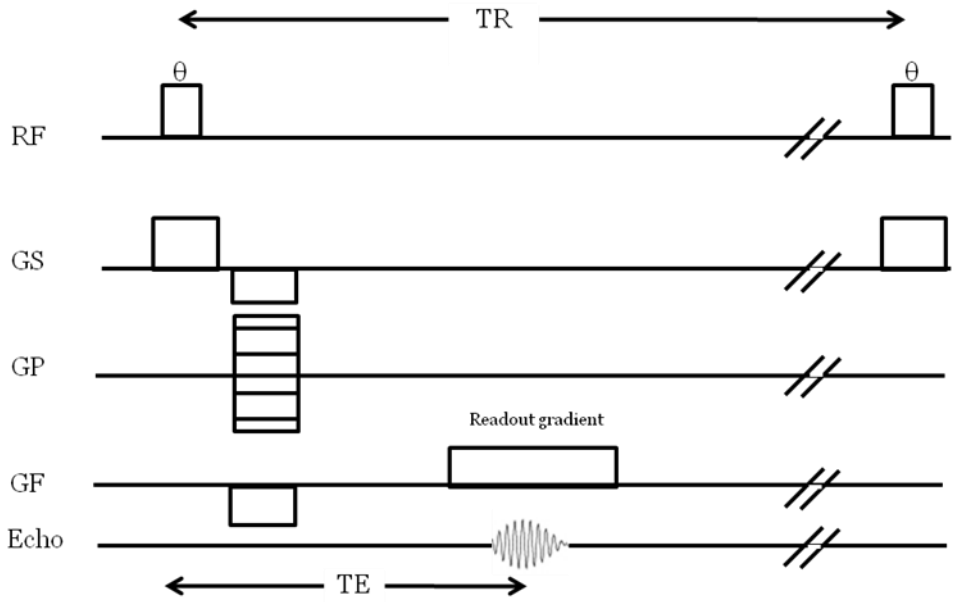

Figure 17: Gradient Echo pulse sequence. GS, Slice selection gradient; GP, Phase encoding gradient; GF, Frequency encoding gradient; TR, Repetition time; TE, Time to echo.

Spatial encoding

The collected signal is spatially encoded by additional magnetic gradients across X, Y and Z direction which change the B0 field from one point to the other, depending on the slope of the applied gradient (Haacke et al., 1999; Kumar et al., 1975). The Z gradient is applied along the B0 field and is applied during the application of the B1 RF pulse. This changes the Larmor frequency of the sample across the Z direction. This ensures that only one slice of the sample is in resonance with B1, and hence, it is the only one that is activated. Therefore, the Z gradient is also called the slice selection gradient. The smallest resolution in an MRI slice is a 3 dimensional volume called a voxel. The size of a voxel is determined by the slice thickness and in-slice resolution determined by the frequency and phase encoding gradients which will be discussed ahead. The X and the Y gradients, applied after the B1 pulse, are respectively called the frequency and phase encoding gradients. These gradients make protons each point within the selected slice experience a different magnetic field, making the protons to relax at different rates. This results in difference in the frequency and phase of the signal from each point within the selected slice. These parameters are used later to decide the position of the received signal.

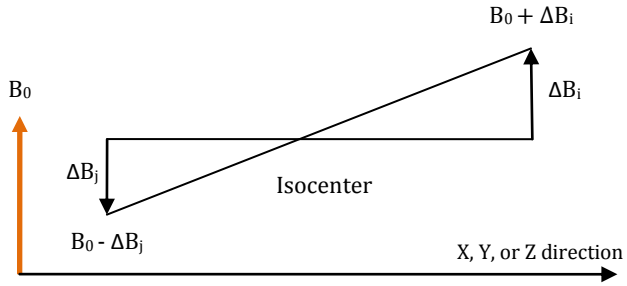

Figure 18: When a gradient of slope m is applied in one direction, the local magnetic field changes according to m and the distance from isocenter.

Slice selection

During MRI, slices are selected along the Z-direction, and hence, the slice selection grading is the Z-gradient. Z-gradient causes the Larmor frequencies along the Z axis to change e.g. ω1, ω2 as shown in Figure 19.

If we apply a B1 pulse with frequencies ω2±ωi, where ωi is a small value, it only excited spins in a thin slice around ω2 and the thickness of the slice is decided by the bandwidth ±ωi and the slope of slice selection gradient applied (Haacke et al., 1999; James Jr et al., 1982; Pykett et al.,

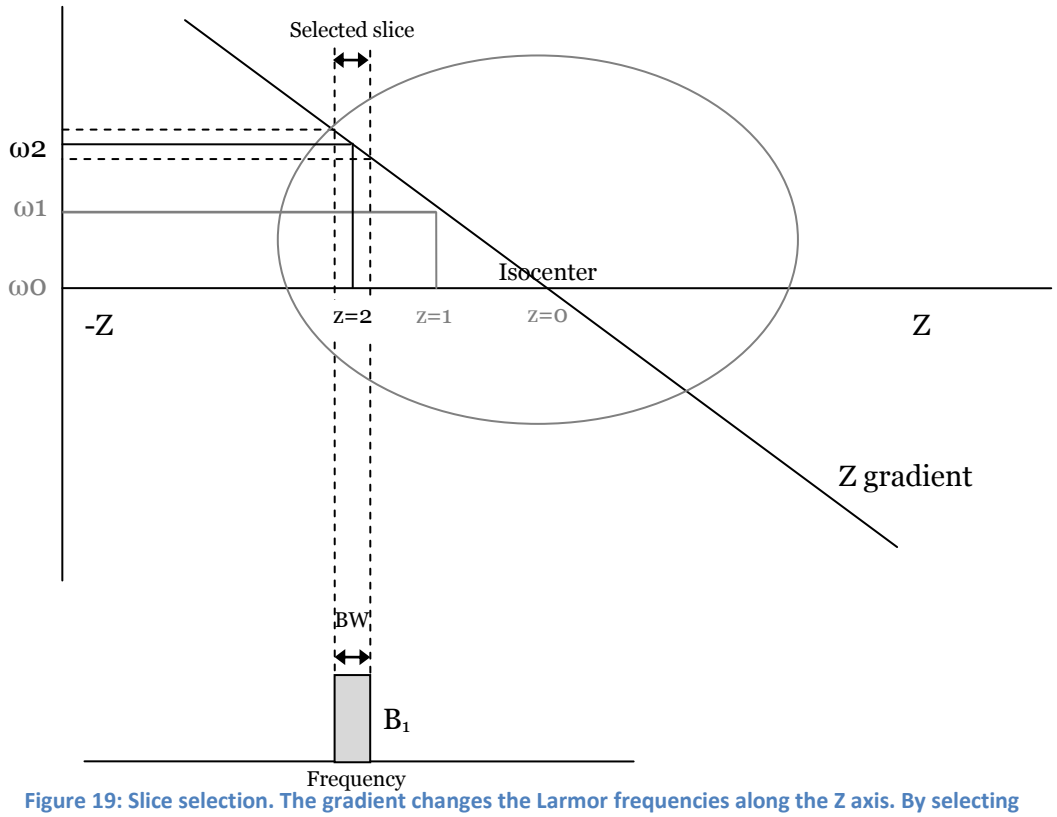

Figure 19: Slice selection. The gradient changes the Larmor frequencies along the Z axis. By selecting an excitation pulse of small bandwidth (BW), spins in only a thin slice can be activated.

1982).

Usually, the applied Z gradient is not completely homogenous and can induce additional inhomogeneity to the spins causing them to dephase quicker than desired. In order to compensate for that, right after removal

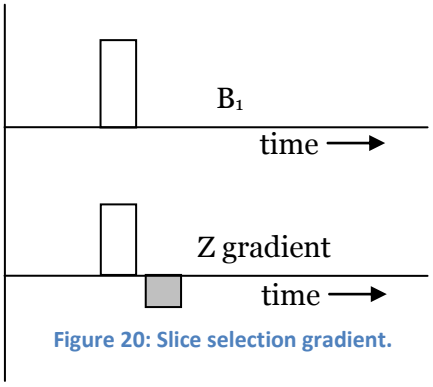

Figure 20: Slice selection gradient.

of the B1 pulse, a reverse Z-gradient is applied of the half the power (amplitude x time / 2) of the first Z-gradient. The timing diagram for the Z-gradient and B1 pulse is shown in Figure 20.

Phase encoding

After the slice selection RF pulse and the refocusing part of the Z-gradient are removed, all the spins in that slice are excited and are dephasing under the influence of B0. In order to delineate between point to point within the slice, a phase encoding gradient is applied along the Y axis. This causes the spins in different lines along the Y axis to dephase at different rates, while the Y-gradient is on. As soon as the Y gradient is off, the spins go back to their original frequency, but maintain the phase that was imparted upon them. In a single slice, only one of the phase-encoded lines is collected at one time. Hence, during the collection of a 64 x 64 voxel slice, the phase encoding gradient steps through 64 steps (Buxton, 2002; Haacke et al., 1999; Kumar et al., 1975).

Frequency encoding

Frequency encoding is usually the last step of spatial encoding. It is applied in a direction perpendicular to the phase encoding gradient, and it also changes the Larmor frequency of the spins. The difference is that, unlike the phase encoding gradient, the frequency encoding gradient is applied at the time the signal echo is being collected. This ensures that the signal acquired from different points in space has a different

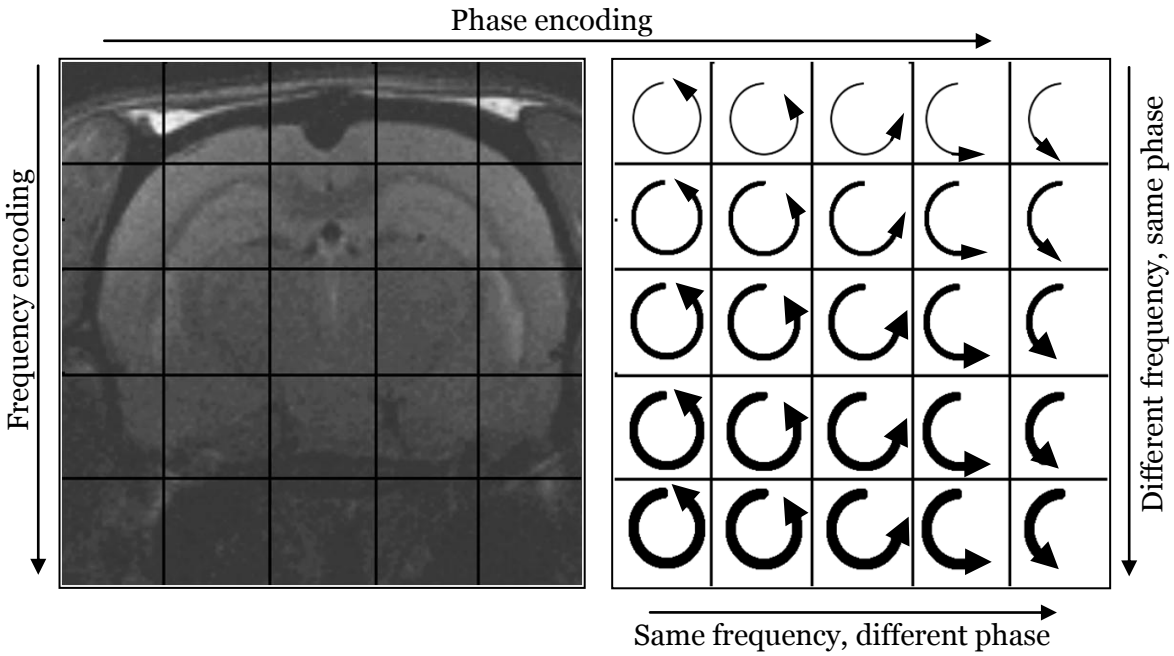

Figure 21: Signal from each point in the selected slice has a unique frequency and phase associated with it.

frequency associated with it. During each step of phase encoding gradient, one line of frequency encoded gradient is collected. Hence, for a 64 x 64 voxel slice, signal acquired during one phase encoding step, is a collection of 64 discrete frequencies (Buxton, 2002; Haacke et al., 1999; Kumar et al., 1975).

To summarize, one slice is acquired at a time, and each point in the selected slice has a unique frequency and unique phase associated with it as depicted in Figure 21. A single line of frequency encoded signal in the phase encoding direction is acquired during one TR period. Hence, 'n' TR periods are needed to acquire a slice with n x n voxels.

K-space

Frequency and phase encoded signal, received in the receiver coil, needs to be deciphered in order to re-establish the physical location of the signal in the image. The frequency and phase encoded form of the signal

is called the k-space of the image or raw data. The image reconstruction is achieved by applying the techniques of Fourier transform to the raw data (Pykett et al., 1982).

Fourier transform and MRI

Fourier transform (FT), is a mathematical technique that transforms a time-domain signal into its equivalent frequency-domain representation. A sine wave of frequency f and amplitude A in time domain, is represented by a single point on the frequency domain plot at (f,A) with frequency on the x axis and amplitude on the y axis as shown in Figure 22. Therefore, a signal that is a combination of various frequencies of different amplitudes, when Fourier transformed, can be represented by multiple points in the frequency domain. This enables the separation of the various frequencies (Haacke et al., 1999; Oppenheim et al., 1999). Conversely, inverse Fourier transform (IFT) can transform a frequency domain signal into its time domain representation.

Joseph Fourier (1768-1830) was the first one to use FT technique to

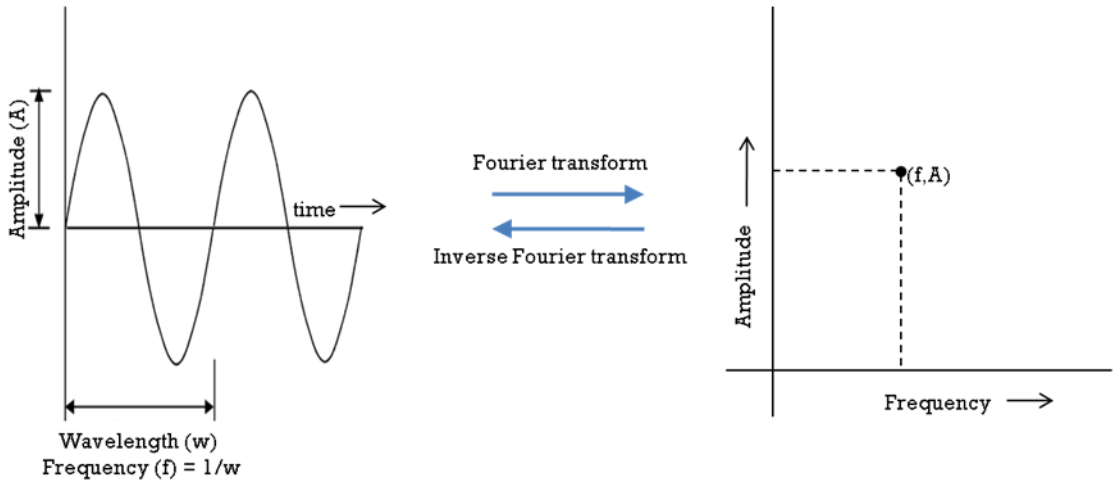

Figure 22: Traversing between time domain and frequency domain using Fourier transform and Inverse Fourier transform.

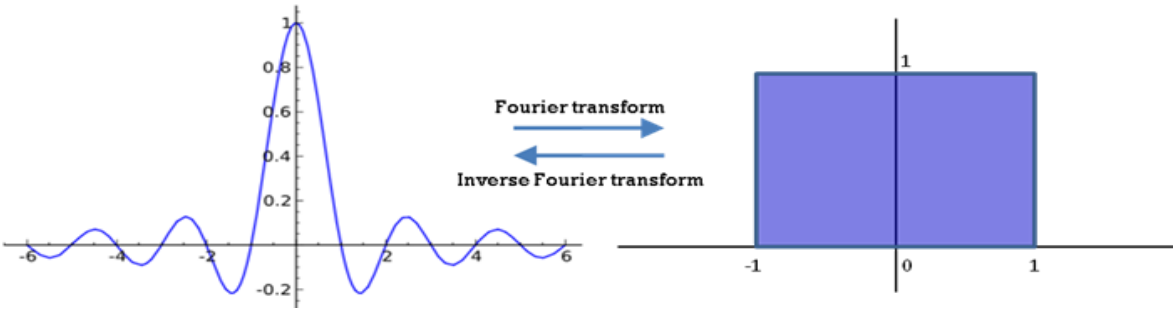

Figure 23: Fourier transform pair. SINC wave and a rectangular function are Fourier transform pairs of each other such that the Fourier transform or Inverse Fourier transform of either, results in the other.

look at heat dissipation. Richard Ernst proposed the use of FT in MRI in 1975 (Ernst, 2007; Kumar et al., 1975). In MRI, FT is applicable in excitation, as well as, in signal acquisition. The single slice excitation is achieved by application of RF B1 pulse of a small bandwidth. In order to achieve the rectangular frequency domain excitation pulse, as shown in Figure 19, its Fourier transform pair in time domain is applied. Figure 23 depicts the Fourier transform pair of a rectangular function called a continuous SINC function given by sin(x)/x. In practice, it is not possible to apply an infinitely continuous SINC wave and is approximated by applying a series of short rectangular pulses (Haacke et al., 1999).

The MRI signal acquired through the receiver coil, is a combination of multiple frequencies and different phases with their amplitudes representing the signal intensities. It is important to note that, the Fourier transform representation of a signal is a combination of real and imaginary parts, which together represent the amplitude, as well as, the phase of the signal. Therefore, the reconstruction of the image from the raw data in the frequency, phase and intensity format is achieved by applying two dimensional inverse Fourier transform to it (Kumar et al., 1975).

Functional MRI

Functional MRI (fMRI) is a leading technique for mapping the activity in different brain regions under various conditions. In 1990, Seji Ogawa demonstrated that, the presence of deoxyhemoglobin changes the T2* relaxation time of blood, hence, making it appear darker on echo-planner images (Ogawa et al., 1990b; Ogawa et al., 1990a). Ogawa suggested that blood deoxygenation can indeed be used as an endogenous contrast agent. John W. Belliveau and colleagues performed the first human functional MRI experiment using visual stimulus and demonstrated that the stimulation results in blood volume changes in the visual cortex (Belliveau et al., 1991). Almost immediately following Belliveau, additional work was done in humans demonstrating blood oxygenation level dependent changes in various cortical areas in a task dependent manner (Bandettini et al., 1992; Kwong et al., 1992; Menon et al., 1992).

Hemodynamic response, deoxyhemoglobin and MRI signal

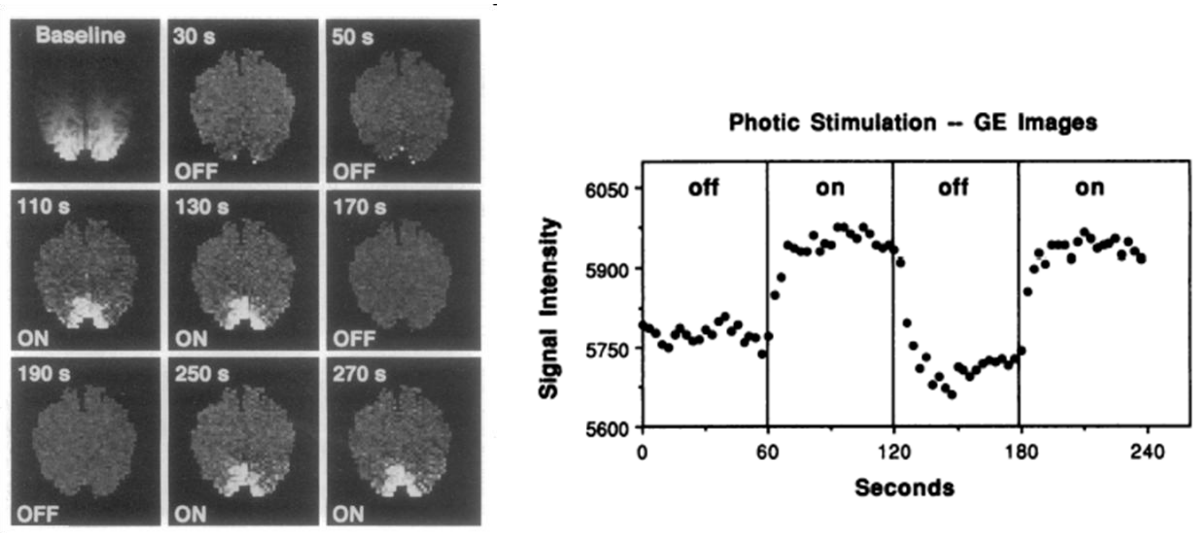

Figure 24: Signal intensity changes in the visual cortex following visual stimulation shown by Kwong and colleagues. (Kwong et al., 1992) Reproduced with permission from PNAS for non-profit and academic reproduction.

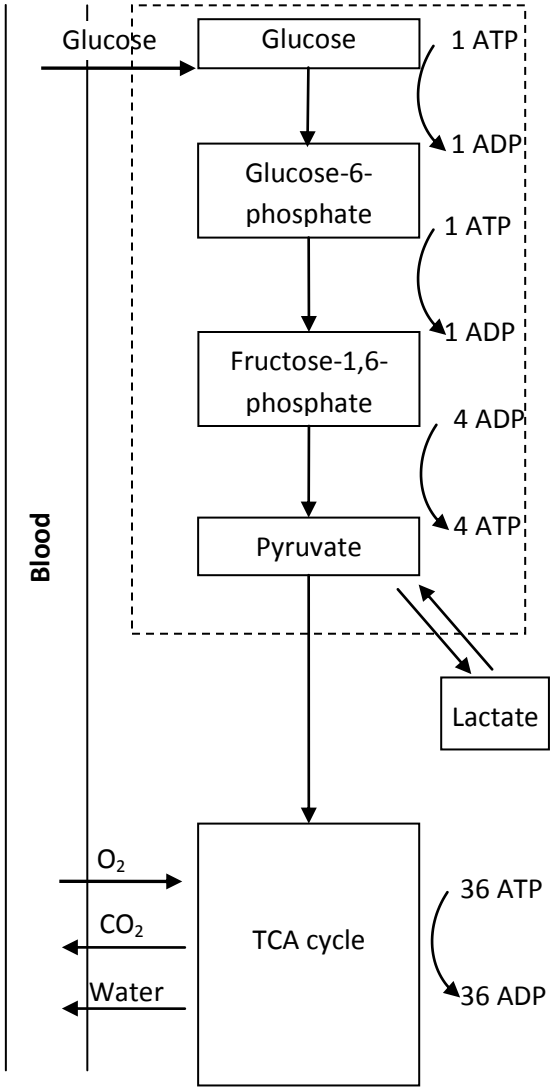

Figure 26: Glucose metabolism in tissue. Dashed line represents the glycolysis.

Normal Conditions

Steady levels of oxygenated and deoxygenated hemoglobin

Right after Stimulation

There is an increase in deoxyhemoglobin for a brief period of time

Hemodynamic response overcompensates for the demand of oxygen and glucose.

Increase in local blood volume and drop in deoxyhemoglobin below normal conditions

Figure 25: Hemodynamic response to neural activation.

"Local cerebral glucose metabolic rate (CMRglu) and cerebral blood flow (CBF) are greatly increased by focal increases in neural activity… Challenging the conventional formulation, we reported that a focal, physiological increase in neutral activity induced by peripheral tactile stimulation increased cerebral metabolic rate for O_2 ($CMRo_2$) minimally (5%), despite a large increase (29%) in local CBF." (Fox et al., 1988)

Under non-stimulated conditions, a brain region receives steady supply of blood flow and has basal levels of oxygenated and deoxygenated blood present in the capillaries around it (Buxton, 2002). As a brain region becomes

active during a neural response, there is an increase in the energy requirement and corresponding glucose metabolism (CMRglu). Activation also leads to an increase in the blood flow (CBF) to that region and resultant increase in the local blood volume (CBV) (Buxton, 2002). The initial belief was that, the increases in CBF and CBV are to compensate for increased energy demand and CMRglu. However, a 17% increase reported in the CMRglu does not explain the almost 30% rise in CBF measured using positron emission tomography (PET) (Fox et al., 1988). Hence, the extent of CBF increase is not well understood (Buxton, 2002).

In addition to a rise in CMRglu, increase in oxygen consumption (CMRo2) is also reported during brain activation. A significant correlation has been reported between the variations in CMRo2 and CBF along with changes in stimulation frequencies (Hoge et al., 1999a; Hoge et al., 1999b). However, the increase in CMRo2 is reported to be only 5% (Fox et al., 1988). This has resulted in a conclusion that, the increase in CMRglu is mostly due to glycolysis, unlike the slower oxidative metabolism of glucose. This has further been supported by an increase in lactate in the active brain regions as measured in magnetic resonance spectroscopy (Prichard et al., 1991; Sappey-Marinier et al., 1992; Singh, 1992). However, glycolysis is not as efficient in energy generation as the oxidative metabolism. In fact it can produce only as much as 1/16 of ATP (energy units in body) as the oxidative metabolism. This has led to the conclusion that the increase in energy consumption in the active state is of much smaller units than the increase in CMRglu and CBF.

Hence, the reason for overcompensation of CBF is still unclear. One speculation is that the overcompensation has evolved as a preemptive preventive measure against oxidative stress, causing ischemic damage to the brain cells (Squire, 2003).

Blood oxygenation level dependent fMRI

Blood oxygenation level dependent (BOLD) fMRI is based the fact that there is a change in the blood oxygen level in a brain region under stimulated conditions as compared to the baseline un-stimulated condition. Deoxyhemoglobin (dOHb) is paramagnetic in nature due to the unpaired electron within the heme- group (Reimer and Parizel, 2006) and gives rise to inhomogeneity in the surrounding magnetization (Ogawa et al., 1990b; Ogawa et al., 1990a). This inhomogeneity results in T2* shortening. Hence, more the dOHb in a region, the faster are the spins in that region dephased. This leads to reduction of the MRI signal induced into the receiver coil.

Under normal conditions, the basal levels of oxyhemoglobin (OHb) and dOHb result in a baseline of MRI signal. At the onset of the neural activity in a brain regon, there is a momentary increase in the dOHb in that region. This can be observed as an initial 'dip' in the fMRI signal. As the hemodynamic response increases the blood volume in that region, the OHb levels start to rise. The overcompensation of CBF leads to a drop in the dOHb/OHb ratio, even below the values at the baseline. OHb is diamagnetic, and hence, does not cause any inhomogeneities. This leads to a rise in the overall T2* allowing the spins to disperse at a slower rate; thus, resulting in an increase in the MRI signal intensity.

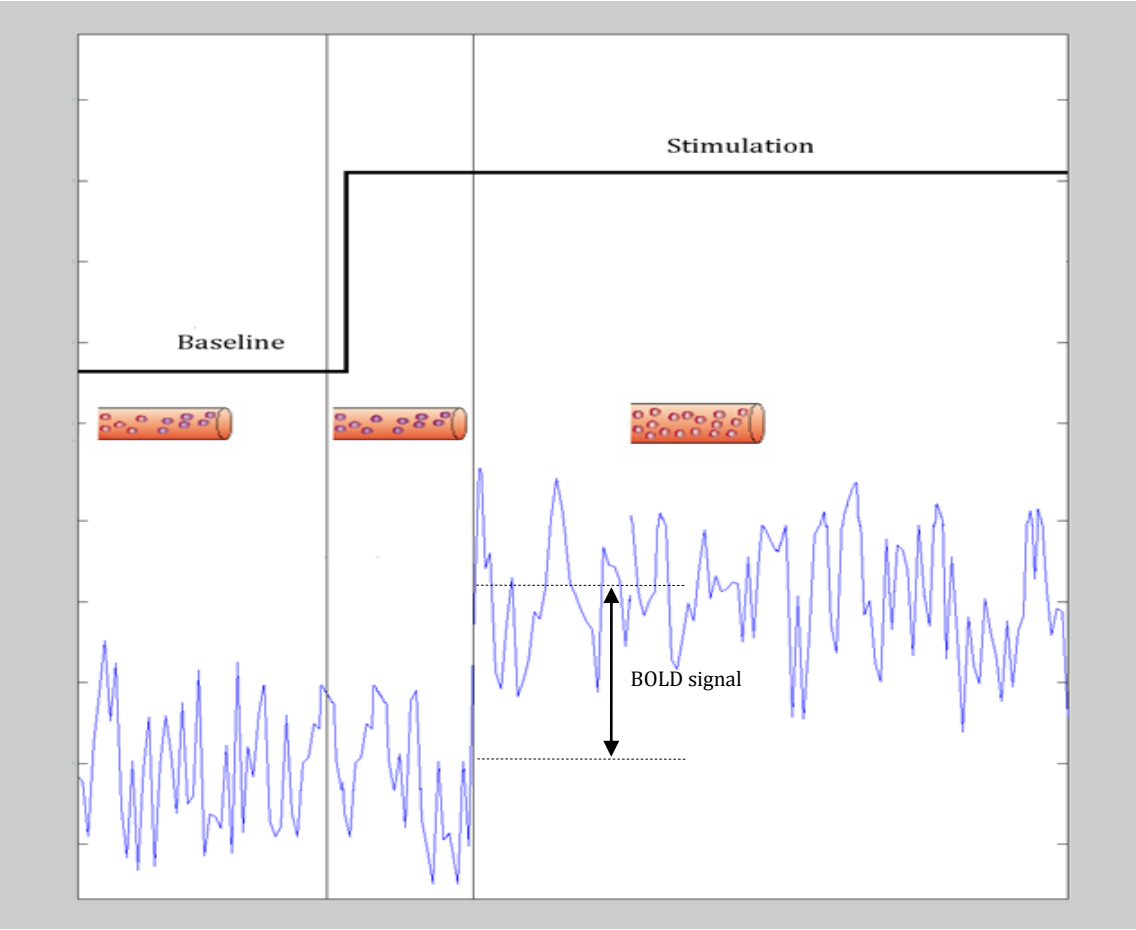

Figure 27: BOLD response. Right after the stimulus the amount of deoxyhemoglobin increases momentarily before it is overcompensated for by the hemodynamic response.

Most of the BOLD fMRI studies use block design, where the subject is imaged though periods of 'control' blocks interleaved with 'task' blocks. Multiple volumes of the fMRI images are collected through each of the blocks. Figure 27 represents a single block design, where the baseline is the control block and the stimulation is the task block. BOLD change is calculated as the change in signal intensity during the stimulation period, as a percentage of the baseline signal intensity.

Resting state MRI

Our brain is a highly wired network of connections. The level of functional connectivity of the brain is even higher than the mere

anatomical connectivity. BOLD activation based functional MRI focuses solely on changes in blood oxygenation of isolated brain regions under consideration, with respect to the applied stimuli. As described by Hebbian theory, 'Neuron's that fire together wire together', brain regions that have anatomical and/or functional connectivity should have significant temporal correlation between their activities.

Biswal's group was the first one to demonstrate existence of resting state connectivity. They performed two fMRI scans in each subject. In the first scan, they asked the subjects to rest without any cognitive, language, or motor tasks as much as possible, and the second scan was performed with a finger tapping task (Biswal et al., 1995). They found that the pixels activated during the task-related fMRI, also had significant correlation between them during the resting state (RS) scans. Shulman and colleagues observed decreased activity in various brain regions during cognitive tasks in their PET study (Shulman et al., 1997). The observed decreases were independent of the task. Raichle et. al. demonstrated steady oxygen extraction fraction in the brain during resting PET studies (Raichle et al., 2001). They proposed that brain has a default mode network, which is constantly active. This network is performing tasks, such as, information gathering with respect to possible predatory attack, without conscious attention to it (Gusnard et al., 2001; Raichle et al., 2001). Shulman group observed activity during stimulation in certain brain regions, which has been proposed as the turning off of the default mode network, while one needs to pay conscious attention to a particular task (Raichle et al., 2001; Shulman et al., 1997). Shmuel and Leopold recently demonstrated that BOLD signals have significant correlation

with local field potentials of neural activity in monkeys (Shmuel and Leopold, 2008). Hence, any correlation between the BOLD signals from two brain regions should indicate correlation between neural activities at the two regions. By this, temporal correlations in low frequency fluctuations (<0.1Hz) in BOLD signals recorded at different brain regions are considered a measure of functional connectivity between those regions (Biswal et al., 1997). The cardiac and respiratory signals in humans are in the rage of 0.6-1.1Hz and 0.1-0.5Hz, respectively (Cordes et al., 2001). In rats, the cardiac frequency is of the order of 4-5Hz and the respiratory frequency is of the range of ~1Hz (Majeed et al., 2009; Williams et al., 2006).

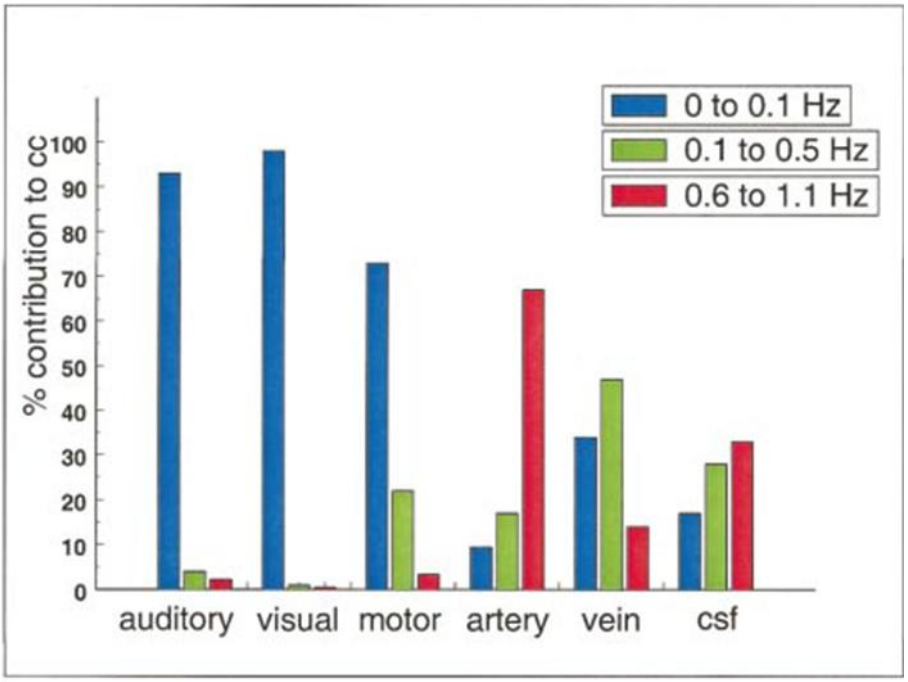

Figure 28: Contribution of various frequency ranges in the correlation coefficients for various seed regions (Cordes et al., 2001). Frequencies below 0.1Hz have higher contribution towards correlation coefficients for cortical areas. Reproduced with permission.

Temporal correlations between cortical BOLD signals have more than 90% contribution from signal frequencies below 0.1Hz, with less than 10% contribution from the respiratory and cardiac signals in humans as shown

by Cordes group in Figure 28 (Cordes et al., 2001); whereas, frequencies higher than 0.1Hz contribute towards the arterial and cerebral spinal fluid signal correlation with the rest of the brain. Williams groups has reported similar observations in rats, where the cortical correlations have higher specificity at frequencies below 0.1Hz (Williams et al., 2006). Technical instabilities, such as magnet drift have been shown to be

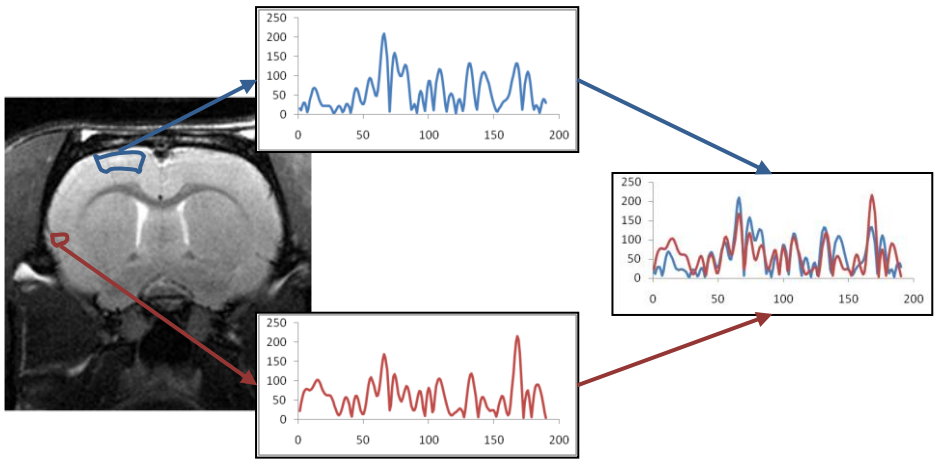

Figure 29: Temporal correlation between time series from two brain regions is an indicator of connectivity between the two regions. An average of low frequency BOLD signal fluctuations from all the voxels that lie within a chosen seed (blue) is generated. The correlation coefficient of this averaged timecourse, with that from every voxel within the brain (red), is used to generate the connectivity map for that seed region.

corrected by low pass filtering the data (Williams et al., 2006). Fox and colleagues has added to the understanding of the resting state network by showing that resting state connectivity can indeed be an indicative of performance (Fox et al., 2007).

As demonstrated in Figure 29, RS connectivity of any brain region can be computed by calculating the correlation coefficient of the average temporal fluctuations in that brain region (blue) with the temporal fluctuations of every voxel (red) in the brain.

RS connectivity has been observed in humans and animals, in conscious, as well as, in un-conscious state (Biswal and Kannurpatti, 2009; Greicius

et al., 2008; Pawela et al., 2008; Zhang et al., 2010). It is a very sensitive to brain network alterations, and has been shown to change under different affected states such as Alzheimer's Disease (AD) (Lustig et al., 2003; Rombouts and Scheltens, 2005), Depression (Anand et al., 2005), ADHD(Tian et al., 2006), Multiple Sclerosis (MS) (Lowe et al., 2008; Lowe et al., 2002) and even during normal aging (Andrews-Hanna et al., 2007).

Summary

Magnetic resonance imaging is a non-invasive imaging technique employing the property of magnetic dipole moment associated with unpaired nuclear spins existing in certain elements. These magnetic dipole moments, when subjected to a high external magnetic field, realign themselves in the direction of that field. If pushed out of that alignment by the presence of a second magnetic field, they follow a specific pattern while regaining their previous orientation after the secondary field is removed. This process of re-orientation gives rise to the MRI signal.

Functional MRI exploits the paramagnetic property of deoxyhemoglobin and the over-supply of oxygenated blood to an activated brain region as determined by the hemodynamic response, to indirectly map the neural activation in that region. This makes it a very useful technique in the study of neuroscience.

Chapter 4. Model development

Animal Models of Parkinson's disease

Animal models play an important role in medical research. They provide a researcher an opportunity to control various factors such as age, environment, diet and disease stages.

Currently, a variety of animal models are available for the study of PD, ranging from genetic based to toxin induced models. The genetic models in mice or flies have been rather informative regarding the etiology and pathogenesis of PD. However, generally these models either fail to show the distinctive neuropathology, such as loss of dopamine in the striatum, or have a complex breeding scheme, making them expensive to use (Bove et al., 2005; Terzioglu and Galter, 2008). In contrast to genetic determinants, the vast majority of PD cases are thought to be caused by environmental factors (Caudle and Zhang, 2009; Tanner, 2010). Therefore, the primary focus of this study has been on environmental approaches to PD symptoms and the neuropathology, as manifested in an animal model exposed to neurotoxins.

Toxins currently in use to develop Parkinsonian animal models include 6-hydroxy dopamine (6-OHDA), 1-methyl-4-phenyl-1,2,3,6-Tetrahydropyridine (MPTP), paraquat and rotenone(Terzioglu and Galter, 2008). Among these, MPTP is ineffective in causing neurotoxicity to dopaminergic cells in the rat for reasons which are not understood. Paraquat and rotenone's effects on the nigrostriatal pathway are inconsistent and unpredictable(Bove et al., 2005). Results by Terizioglu et. al. (Figure 30) summarize advantages and disadvantages of various

models (Terzioglu and Galter, 2008). Based on this knowledge, 6-OHDA was used to develop the model for our studies.

6-Hydroxy dopamine

The neurotoxin 6-OHDA is a dopamine analog, sharing some structural similarities with dopamine. It is easily taken up by dopamine transporters and known to cause oxidative stress, mitochondrial damage and neuro-inflamation (Na et al., 2010; Schober, 2004). Ungerstedt was the first to use 6-OHDA to produce dopaminergic lesions of the nigrostriatal system in the rat (Ungerstedt, 1968). This neurotoxin is not able to cross the blood brain barrier and if delivered systemically, it causes damage to the peripheral nervous system. Hence, the preferred route of administration for this toxin is intracranial delivery into specific brain regions. These injections produce localized dopamine depletion, making it possible to control the site and extent of lesion. In turn, this makes it possible to monitor and study the effects of dopamine lesions in different parts of the brain.

The exact pathways of 6-OHDA toxicity are not completely understood. An in-vitro study by Hanrott group showed that 6-OHDA is auto-oxidized to hydrogen peroxide within 5 minutes in extracellular space, which eventually causes oxidative stress leading to cell death (Hanrott et al., 2006). PC12 (rat pheochromocytoma cell line) cells exposed to 6-OHDA in the same study started to exhibit mitochondrial damage starting at 6 hours post treatment and loss of membrane integrity indicating cell death starting at 10 hours post treatment. Na et. al.'s study in rats with striatal lesions of 6-OHDA, points towards robust inflammatory response in both

the striatum and SN (Na et al., 2010). Another review paper by Andreas Schrober points out oxidative stress, mitochondrial damage and inflammatory response as results of various 6-OHDA lesion studies (Schober, 2004). These effects are very similar to the PD etiology in that similar observation have been made in postmortem studies in PD patients (Gaig and Tolosa, 2009).

Over the years, many different sites of 6-OHDA infusions have been studied, including substantia nigra (SN), medial forebrain bundle and the striatum. The most extensively studied SN and MFB lesions, consistently produce motor deficits and are thus utilized to model the motor deficits in PD (Deumens et al., 2002; Sakai and Gash, 1994). Usually, these lesions are severe and result in significant gait changes, such as shorter stride length, reduced limb swings while walking, reduction in paw contact and paw pressure, aphagia (problem in swallowing), akinesia, amphetamine induced rotations in the unilateral models and massive loss of dopamine cells in SN (Chuang et al., 2010; Deumens et al., 2002; Sakai and Gash, 1994). These models provide a practical way of testing treatment for motor deficits. However, severe motor deficits make it difficult to test any non-motor symptoms that are commonly observed in the pre-motor and early stages of PD.

When injected into the striatum, 6-OHDA causes local reduction of dopamine content in the striatum and retrograde degeneration of dopamine cells in the SN (Blandini et al., 2007; Fleming et al., 2005; Yuan et al., 2005). These lesions are progressive in nature and result in lower levels of dopamine cell loss over a period of many weeks after the

insult (Sauer and Oertel, 1994). This allows the testing of potentially neuroprotective treatments in a time dependent manner, which is much more relevant to clinical treatment regimens (Lindholm et al., 2007). Double bilateral lesions of the striatum with 6-OHDA have shown to produce long lasting dopamine loss without compensatory effects weeks after the infusion (Ben et al., 1999). As discussed in Chapter 2, striatal dopamine depletion has been observed in early-stage PD patients and is projected to date back many years before the onset of the clinical symptoms. As discussed in Chapter 2, striatal dopamine has reduced by almost 80% and the there is almost 50% loss of substantia nigra cells by the time onset of motor symptoms in PD. Hence, the striatal 6-OHDA lesion model is a viable option for modeling pre-motor stage PD.

Model	PD symptoms	PD pathology	Advantages	Disadvantages
6-OHDA	Motor impairments after bilateral lesion Easily quantifiable turning behavior after unilateral lesion	Reduced DA levels in the striatum Massive loss of dopamine neurons No intracellular aggregates	Works in mice, rats, and monkeys Well characterized Used in dyskinesia models	Does not pass the blood–brain- barrier (needs intracerebral injection, which increases variability) Fast, massive neurodegeneration Poor construct validity
MPTP	Motor impairments	Reduced DA levels in the striatum Massive loss of dopamine neurons With chronic administration, formation of aggregates with little LB resemblance	Lipophilic Systemic administration Works mainly in mice Well characterized Good construct validity	Highly toxic to humans (dangerous to administer) Reduced reliability
Paraquat	Motor impairments	Reduced DA levels in the striatum Loss of dopamine neurons in the SN No aggregate formation	Systemic administration	Toxic for the whole organism Not well characterized Low construct validity
Rotenone	Motor impairments	Reduced DA levels in the striatum Massive loss of dopamine neurons No aggregate formation	Systemic administration Works only in rats	Toxic for the whole organism Low construct validity
Dj-1 KO, Pink1 KO, Parkin KO	Little motor impairment	Only slight DA pathology	Good construct validity	Slight DA pathology
α-Synuclein wild-type and A53T, A30P overexpression	Little motor impairment	Little DA pathology Intracellular aggregates with little LB resemblance	Good construct validity	Slight DA pathology
$En1^{+/-}$, En2 KO	Some motor impairment	Reduced DA levels in the striatum Massive loss of dopamine neurons only in the SN during the first 3 months No aggregate formation	Slow neurodegeneration	Poor construct validity Other cell groups affected in the central nervous system No progression of degeneration after 3 months
Pitx3-aphakia	Motor impairment	Reduced DA levels in the striatum Massive loss of dopamine neurons in the SN only	Slow neurodegeneration	Poor construct validity Other cell groups affected in the central nervous system
MitoPark (DAT-cre, Tfam lox/lox)	Motor impairment	Reduced DA levels in the striatum Massive loss of dopamine neurons, predominantly in the SN Intracellular aggregates with little LB resemblance	Adult onset of symptoms Slow symptom development Good construct validity	Complex breeding scheme

Scoring of dopamine neuron: slight loss (< 30%); loss (30–70%); massive loss (> 70%). The construct validity of a model refers to the degree to which the rodent model reproduces known PD etiology (low = no findings in PD patients indicate a role in PD etiology for the toxin or genetic modification that the model is based on; poor = some findings point to a role in PD etiology; good = findings in PD patients indicate a causative role for genetic modifications reproduced in the model); KO, knock out.

Figure 30: Summary and advantages and disadvantages of selected rodent models of PD. (Terzioglu and Galter, 2008) Reproduced with permission.

Experimental procedures

Animals

Adult male Long Evans rats (300-350g, N= 48) were obtained from Harlan Sprague–Dawley Laboratories (Indianapolis, IN). The animals were group-housed (2 per cage) in Plexiglas cages and maintained in ambient temperature (22–24°C) on a 12/12 h light/dark cycle. Food and water was provided ad libitum. All procedures were approved and monitored by the University of Massachusetts Medical School Institutional Animal Care and Use Committee. Animals were randomly assigned to various studies as stated in Table 2. The animals from all the groups were age matched.

Study	Group	Number of rats per group
Spontaneous locomotion	Control	5
	3WKPD (3weeks post 6-OHDA lesion)	5
Elevated beam test	Control	5
	3WKPD	5
Gait analysis	Control	4
	2WK (2weeks post 6-OHDA lesion)	4
	3WK (3weeks post 6-OHDA lesion)	4
	4WK(4weeks post 6-OHDA lesion)	4
Immunohistochemistry	Sham (Sham lesioned rats)	6
	3WKPD	6

Table 2: Rat assignment per motor and Immunohistochemistry studies.

Surgery

Rats from the 6-OHDA lesion group and sham lesion group were anesthetized with 3-5% Isoflurane and set up in a stereotactic system (myNeuroLabs, Leica Microsystems, Richmand, IL). They were maintained at 1.5-2.5% Isoflurane during the surgery. The 6-OHDA lesion

rats received a total of 12 µg of 6-OHDA in the CPu (caudate putamen; 0.7mm rostral to bregma, ±3mm lateral to midline, 5mm ventral to skull surface). The infusion was achieved in two separate steps of 10 µg and 2 µg in 1 µl of vehicle (0.1% Ascorbic acid in 0.9%NaCl) two days apart, using PE50 tubing attached to Hamilton micro-syringes. The sham lesioned group went through the same procedure as the 6-OHDA lesion group with the exception of receiving 6-OHDA.

Figure 31: Site of 6-OHDA lesions

Spontaneous locomotion test

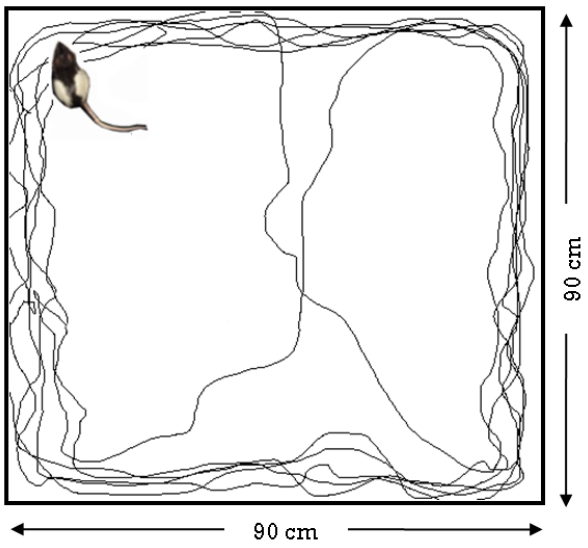

Figure 32: Spontaneous locomotion test apparatus consisted of a 90 cm x 90 cm black Plexiglas arena. The rat was allowed to walk freely in it for 5 minutes. An overhead camera along with the Ethovision software (Noldus Information Technology, Leesburg, VA) recorded and analyzed the rat's movement.

At the three week time point, control and 3WKPD rats were allowed to freely move in a black Plexiglas arena (90cm x 90 cm) for five minutes. Their behavior was recorded using an overhead camera.

Elevated beam test

The test apparatus consisted of a 1.5 inch wide and 36 inch long wooden beam. One end of the beam had a black enclosed platform that the rats could rest on at the end of the test. The entire assembly was 3.5 feet above the ground. Each rat was placed on the end away from the

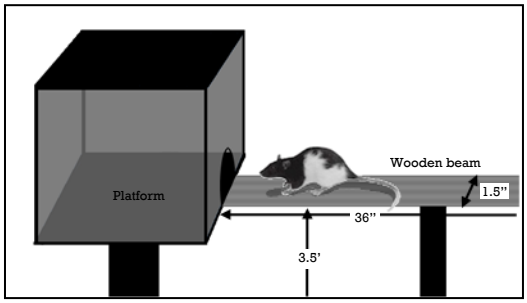

Figure 33: Elevated beam walk. Rat was placed at one end of the 1.5 inch x 36 inch wooden beam at 3.5 feet above the ground, and allowed to walk to a platform on the other end.

platform, and allowed to walk to the platform. Each rat performed 3 trials and the first trial was ignored as the acclimation trial. The second and third trials were scored for time to cross the beam and number of slips during that time period. Time to cross the beam as scored starting a timer/stop watch as soon as the rat was placed on the far end of the beam and stopping as soon as his fore paws reach the platform. A slip was defined as slip (movement off of the beam) of any of

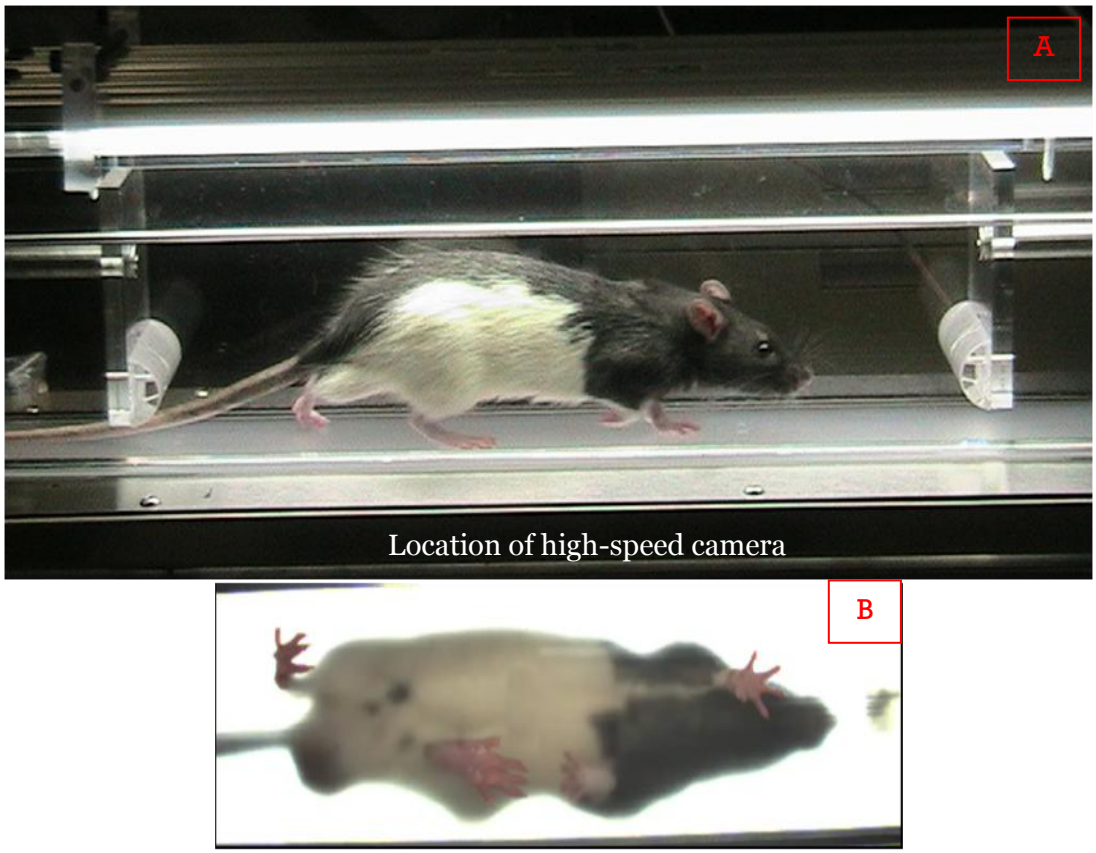

Figure 34: DigiGait gait analysis system by Mouse specifics. A. Setup included a translucent treadmill. Rats were allowed to talk on the treadmill while a high-speed camera situated underneath recorded its movement. B. image taken by the high-speed camera situated underneath the treadmill.

the limbs off of the beam during the process of placing that limb on the beam. Number of slips was recorded at the end of each trial.

Gait Analysis

Controls, and 2, 3 and 4 weeks post 6-OHDA lesion rats were tested for motor deficits using DigiGait Imaging system (Mouse Specifics, Inc., Quincy, MA). The system uses a transparent treadmill with a high speed camera situated below it. After the gait videos were recorded, they were scored for 26 different parameters concerning the stride, breaking and paw placement using DigiGait analysis and imaging software (Mouse Specifics, Inc., Quincy, MA).

Immunohistochemistry

Tyrosine hydroxylase (TH) staining was performed on rat brain slices to determine dopamine loss in the striatum and the SN. TH is an enzyme responsible for the first step in synthesis of dopamine from tyrosine in-vivo, and hence serves as an indirect measure of dopamine content in cells (Nagatsu et al., 1964). TH-staining is a commonly used technique to quantify dopamine.

Sham and 3WKPD rats were anesthetized with 200mg/kg of IP pentobarbital and perfused intra-cardially with 120 ml of 4% paraformaldehyde solution in 0.1M phosphate buffer (PFA). The rats were decapitated, the brains were quickly removed and post fixed for 2 hours in PFA, followed by another 48 hours in 30% saline solution in 0.1M phosphate buffer at 4°C. The brains were frozen on dry ice and sliced into 25um thick slices on a microtome (SM2000R, Leica Microsystems, Buffalo Grove, IL). Four slices each were collected through the striatum

and through the SN. The slices were incubated in 1:500 Monoclonal anti-TH mouse primary antibody (T2928, Sigma-Aldrich, St. Louis, MO) in 1M PBS/0.3%Triton X-100 (TRX) overnight at 4°C. The next day, slices were washed in 1M PBS three times and incubated in 1:200 mouse IgG secondary antibody in TRX (Vectastain Elite ABC kit, Vector Labs, Burlingame, CA) for 1 hour followed by H_2O_2 incubation for 1 hour at room temperature. The slices were washed three times in PBS after each step. Finally, the staining procedure was completed using 1:50 DAB in TRX (D9015, Sigma-Aldrich, St. Louis, MO) and the slices were mounted on slides for further analysis. The concentrations used during the staining procedure were empirically determined by Akbarian lab at UMass Medical school after trying out various concentrations recommended by Sigma-Aldrich in their product sheet for optimum staining contrast.

Data Analysis

Spontaneous locomotion test

The open field behavior was analyzed using Ethovision software (Noldus Information Technology, Leesburg, VA) for total distance moved in the five minutes. No statistics was performed because of lack of any difference between the group means.

Elevated beam walk test

The last two trials of each rat were averaged to calculate the average time to cross the beam and average number of slips per rats. These values were compared between groups to test for any difference between the

groups. No statistics was performed because of lack of any difference between the group means.

Gait Analysis

DigiGait analysis and imaging software by Mouse Specifics analyzed the gait videos for 26 different parameters. Multivariate ANOVA with bonferroni correction for multiple comparisons was used to compare groups. Among the 27 parameters stride frequency, stride length and stride duration were selected based on the significant difference observed in them between controls and 4 weeks post 6-OHDA rats. These parameters are relevant to PD, since gait changes such as shorter and quicker steps are observed during Parkinsonian gait.

TH-staining

Images of the slices were collected using an Olympus BX51 microscope attached to QICAM FAST1394 digital camera with 1.25x zoom on the striatum and 10x zoom on the substantia nigra. ImageJ software (http://rsb.info.nih.gov/ij/) was used to calculate TH-staining intensity in the CPu and the TH-stained cells in the substantia nigra, as described by Abramoff group (Abramoff et al., 2004). To measure the CPu dopamine content, the CPu TH-staining intensity was measured using ImageJ. The

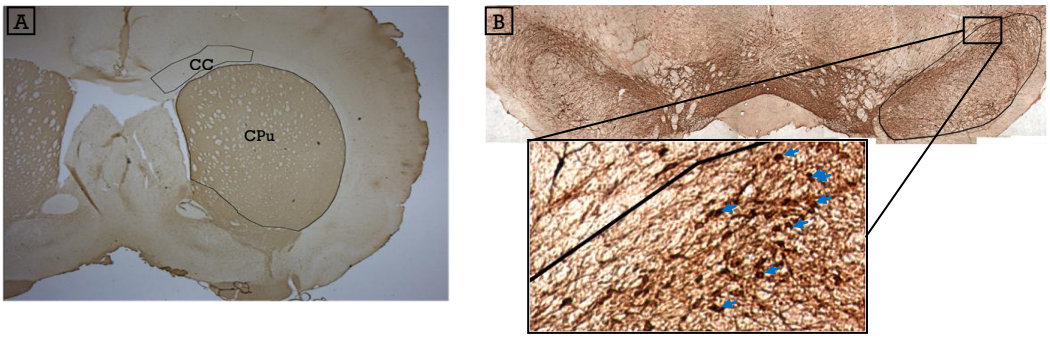

Figure 35: Analysis of dopamine content in striatum and dopamine cell density in substantia nigra.
A. For analyzing dopamine content in striatum (CPu), the average tyrosine hydroxylase staining intensity of the average CPu staining intensity was measured. The average corpus callosum (CC) staining intensity was subtracted from it as a backgroud measure. B. To measure the substantia nigra staining intensity, the substantia nigra was marked as shown and the area was measured. The dopamine cell bodies in the zoomed in version are marked with arrows. All the dopamine cells were counted using the 'cell counter' plugin in ImageJ.

corpus callosum staining intensity served as an internal control for background staining intensity (Figure 35A). Difference between CPu staining intensity and corpus callosum staining intensity was recorded for each brain slice. Figure 35B represents the measurement of dopamine cell density in substantia nigra. The substantia nigra area was marked and measured using ImageJ. All the dopamine cells within the marked area were counted using 'cell counter' plugin in ImageJ. Dopamine cells are marked with arrows in zoomed in section of Figure 35B. Dopamine cell density per slice was calculated as number of cells per square μm^2 of substantia nigra area. Between group comparisons were done using univariate ANOVA.

Results

There was no difference between the total distances walked by the control versus the 3WKPD groups in the open field arena (Figure 36). The 3WKPD rats were able to cross the elevated beam in almost the same duration and with no additional slips in the elevated beam walk test (Figure 37). During the gait analysis test, multivariate ANOVA with bonferroni correction for multiple comparisons, revealed significant main group effect in stride duration ($F_{(3,12)} = 6.135$, $p<0.004$), stride length ($F_{(3,12)} = 5.838$, $p<0.005$), and stride duration ($F_{(3,12)} = 5.448$, $p<0.006$). The rats at 4 week post lesion had significantly smaller stride duration ($t_{(7)} = 3.85$, $p<0.03$), higher stride frequency ($t_{(7)} = 3.15$, $p<0.03$) and shorter stride length ($t_{(7)} = 3.19$, $p<0.03$) as compared to controls in the post hoc analysis. Both, the 2 and the 3 week post lesion groups, did not demonstrate any significant deficits in any of the 26 parameters examined

during the gait analysis experiment. However, the 3 week post lesion rats exhibited a trend in the direction of developing deficits in stride frequency, stride length and stride duration (Figure 39). The smaller stride duration, higher stride frequency and shorter stride length are very analogous to the shuffling gait observed in human PD patients.

The univariate ANOVA of the TH-staining results revealed a significant difference between the two groups in the CPu staining intensity ($F_{(1,10)}$=15.9, $p<0.05$) and the substantia nigra cell density ($F_{(1,10)}$=13.454, $p<0.05$). The CPu had 27% reduction in the average TH-staining intensity (Figure 38A) while there was a 23% loss of the TH-stained cells in the substantia nigra in the 6-OHDA lesioned rats as compared to the sham lesioned rats at the three week time point (Figure 38B).

Conclusion

The dopamine loss in CPu and SN of the 6-OHDA lesioned rats, at 3 weeks post lesion, was lower than the reports of 80% striatal loss of dopamine and 50% dopamine cell loss in the SN in PD patients, at the time of onset of motor symptoms. The 6-OHDA lesioned rats neither exhibited any motor deficits in spontaneous locomotion, nor did they exhibit any changes in gait during the extensive gait analysis at the three week time point. As previously put forth in the Braak stages of PD, at the beginning of Braak stage 3, the motor symptoms are not yet apparent, but the SN pathology has started. That timeline also matches with the reported pre-motor striatal dopamine depletions. Hence, we believe that this model might in fact mimic the symptomology of early Braak stage 3 or late Braak stage 2. Based on the dopamine depletion and lack of motor

deficits, three weeks was chosen as the time-point for the studies performed throughout the rest of this research.

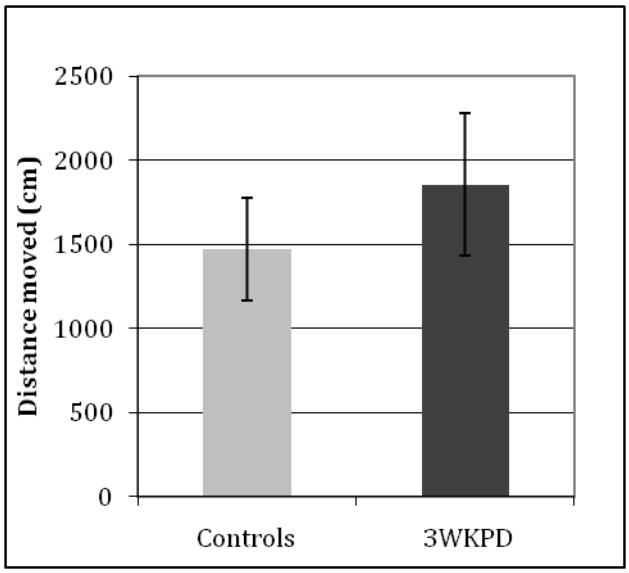

Figure 36: Rats did not exhibit any deficits during spontaneous locomotion test.

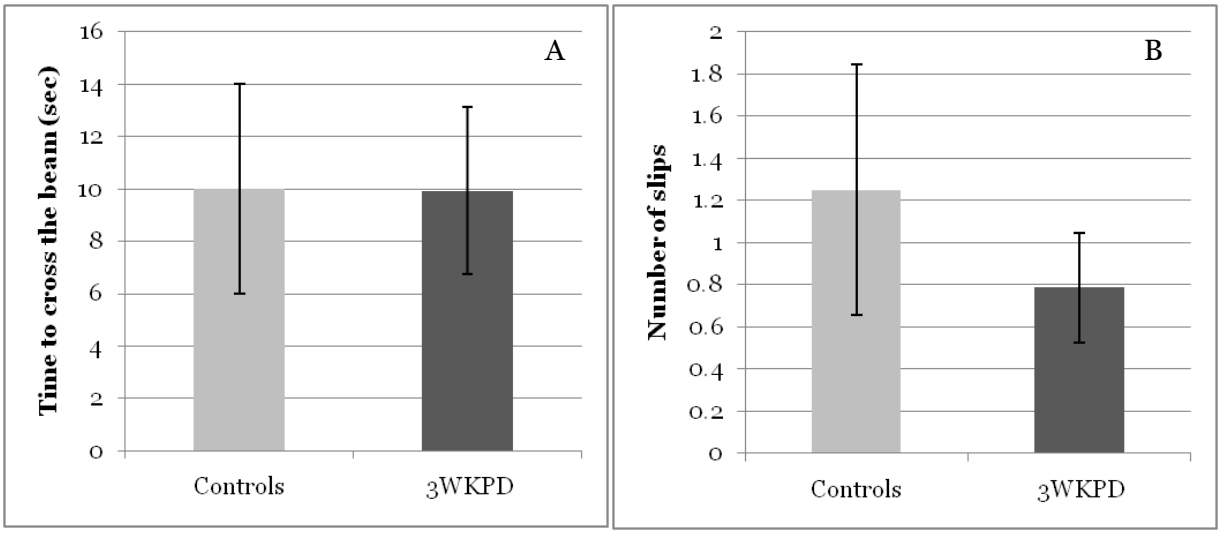

Figure 37: 3WKPD rats did not exhibit any deficits in the elavated beam walk test in terms of the time to corss the beam (A) and number of slips (B).

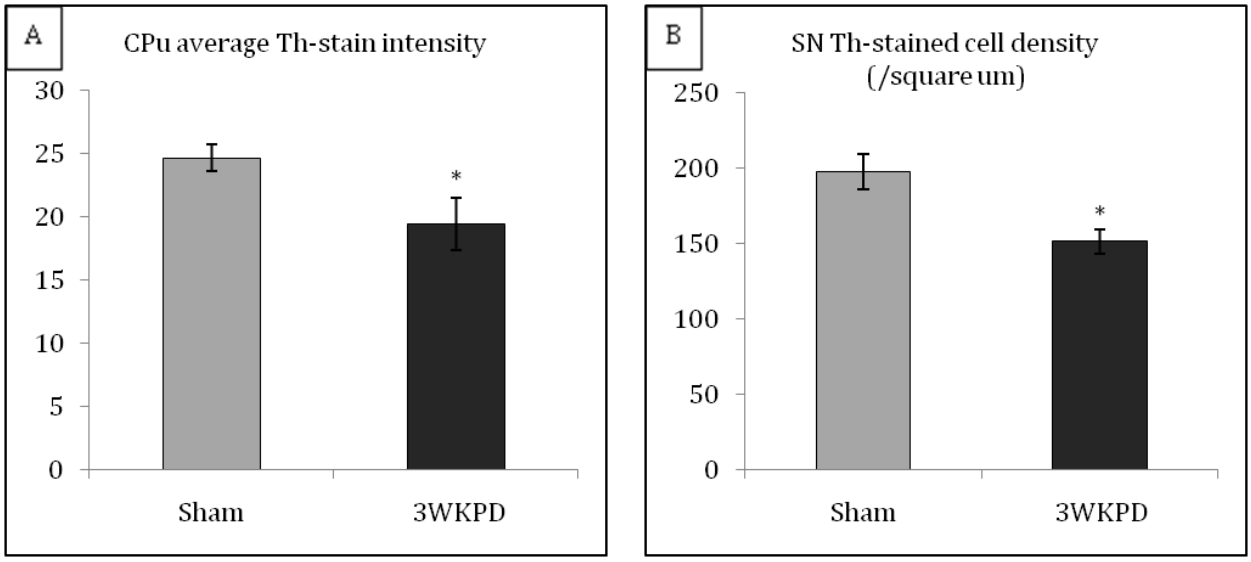

Figure 38: Immunohistochemistry results. (A) Average TH-staining intensity in the CPu; (B) Number of TH-stained cells in the substantia nigra. (*p<0.05)

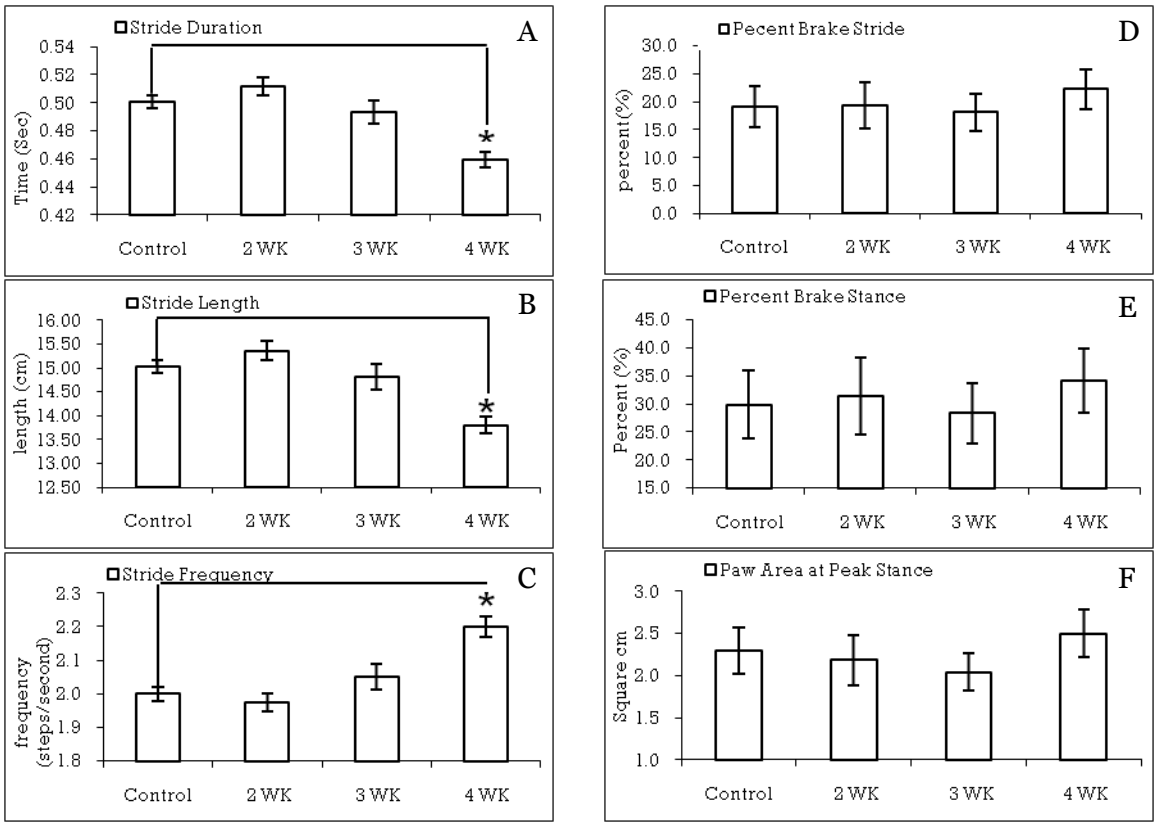

Figure 39: Gait analysis results in unlesioned controls and rats at 2, 3 and 4 weeks post 6-OHDA lesions. Significant gait changes are observed in the 4 weeks post 6-OHDA lesion group compared to unlesioned control group in Stride duration (A), stride length (B), stride frequency (C) (*p<0.005 maximum). Other gait parameters including percentage of the stride duration spent in breaking position (D), percentage of the stance in breaking position (E), and paw area at peak stance (F) did not have any significant differences between the groups.

Chapter 5. Aversion changes in PD[1]

Rational

Emotional alterations appear to be among the more critical features of the non-motor deficits in PD. Deficits in recognition of facial expressions of various emotions like anger (Clark et al., 2008; Kan et al., 2002; Sprengelmeyer et al., 2003), surprise (Clark et al., 2008), happiness (Clark et al., 2008), fear (Clark et al., 2008; Sprengelmeyer et al., 2003), sadness (Ariatti et al., 2008; Clark et al., 2008; Sprengelmeyer et al., 2003) and disgust (Kan et al., 2002; Sprengelmeyer et al., 2003; Suzuki et al., 2006), have been reported in Parkinson's disease (PD). In a model of facial expressions of different emotions, Suzuki and others (Suzuki et al., 2006) have shown that PD patients have significantly lower sensitivity scores to disgust, but retain their sensitivity to other emotions. Results by Bowers and colleagues (Bowers et al., 2006) also demonstrated reduced startle reactivity and lower self reported arousal during exposure to aversive pictures in early to middle stages of PD, compared to age matched controls. These reports suggest lower sensitivity to disgust and aversion in clinical PD patients. Sprengelmeyer and colleagues have reported significant deficit in disgust recognition in un-medicated PD patients, but not in medicated PD patients, leading researchers to speculate that disgust recognition deficit could be a result of lower levels of dopamine (Sprengelmeyer et al., 2003). In addition, converging evidence links basal ganglia pathologies with alterations in aversion (Hayes et al., 2007; Mitchell et al., 2005; Montagne et al., 2006;

[1] Results of this study have been published in Rane P, King JA. Exploring aversion in an animal model of pre-motor stage PD. Neuroscience 2011..

Paulmann et al., 2009). Basal ganglia pathology, as well as, reduced dopamine levels are reported in PD years before the onset of clinical motor symptoms (Burn et al., 1992; Gaig and Tolosa, 2009). This has led to the hypothesis that the aversion deficits may indeed precede the motor deficits of PD.

The main brain regions implicated in disgust processing and aversion response generation include insular cortex, basal ganglia and amygdala. In general, the insular cortex has been thought of as the main processing region of the aversive stimuli, including olfactory (Heining et al., 2003; Royet et al., 2003; von dem Hagen et al., 2009) and gustatory (Small et al., 2003) stimuli, pictures of facial expressions of disgust (Sprengelmeyer et al., 1998), pictures of contamination (Wright et al., 2004), as well as, experience and imagination of disgust (Jabbi et al., 2008) in healthy human population. Also, inhibition of insular cortex has been shown to block taste aversion memory in rats (Desgranges et al., 2009). Similarly, right ventral striatum, a part of the basal ganglia, is another region that has been shown to have significant differential BOLD activation in response to disgusting odors in healthy human populations (Heining et al., 2003), implying involvement of ventral striatum not just in recognition, but in the processing of disgust stimuli. The third brain region, the amygdala, has been known to be involved in processing aversive stimuli and also in generating an appropriate behavioral response (Davern and Head, 2011; Reilly and Bornovalova, 2005). Damage to the amygdala has shown to block aversion (De Martino et al., ; Ghods-Sharifi et al., 2009). Since pathologies of all three regions have been observed in PD at different stages of the disease(Alvarez-Erviti et

al., ; Burn et al., 1992; Kikuchi et al., 2001), the observed behavioral deficits could be a result of dysfunction of either the aversion processing brain regions, the response generating brain regions, or both.

In this study we examined whether aversion deficits exist in the pre-motor stages of PD by exploring the behavioral response of our rat model to the aversive odor of butyric acid (BA) (Endres and Fendt, 2009; Fendt and Endres, 2008). As discussed in Chapter 4, this model demonstrates significant depletion of TH-positive neurons in the striatum and substantia-nigra, but lacks any significant motor deficit. Hence, any observed aversion changes would support the notion of these changes preceding the motor deficits.

The current study employed grooming behavior as a measure of arousal (Denmark et al., 2010; Homberg et al., 2002). Self-grooming behavior is part of the process that may decrease arousal to restore the homeostatic status disturbed by anxiogenic and/or stressful stimuli (Gispen and Isaacson, 1981; Jolles et al., 1979; Kalueff and Tuohimaa, 2005; Kametani, 1988). We also tested for any changes in avoidance of the aversive odor that might be a result of the 6-OHDA lesions. Additionally, BOLD fMRI was performed to look at corresponding changes in neural activation.

We hypothesized that the rats from the PD model group would exhibit lower aversion behavior. In addition, we proposed lower BOLD activation in response to aversive stimulus would be seen in several brain regions associated with disgust processing and response generation in PD animals as compared to the controls.

Experimental Procedures

Animals

Adult male Long Evans rats (300-350g, N = 108) were obtained from Harlan Sprague–Dawley Laboratories (Indianapolis, IN). Animals were randomly assigned to various studies as stated in Table 3. The animals were group-housed (2 per cage) in Plexiglas cages and maintained in ambient temperature (22–24°C) on a 12/12 h light/dark cycle. Food and water was provided ad libitum. All procedures were approved and monitored by the University of Massachusetts Medical School Institutional Animal Care and Use Committee. Surgeries on sham and 3WKPD group were performed as described in Chapter 4. All tests were performed at 3 weeks past the last surgery.

Study	Group	Number of rats per group
Arousal Behavior test	Control	16
	Sham	16
	3WKPD	16
Avoidance behavior test	Control	10
	Sham	10
	3WKPD	10
fMRI	Control	10
	Sham	10
	3WKPD	10

Table 3: Rat assignment per different tests in aversion study.

Arousal Behavior Test

For avoidance behavior, rats were acclimated to an empty test cage, similar to a home cage without the bedding material, for 5 minutes each, on two days prior to the test day. On test day, rats had three additional 5-minute acclimation trials with a setup similar to the one on the two previous days. However, during these sessions, there was an addition of

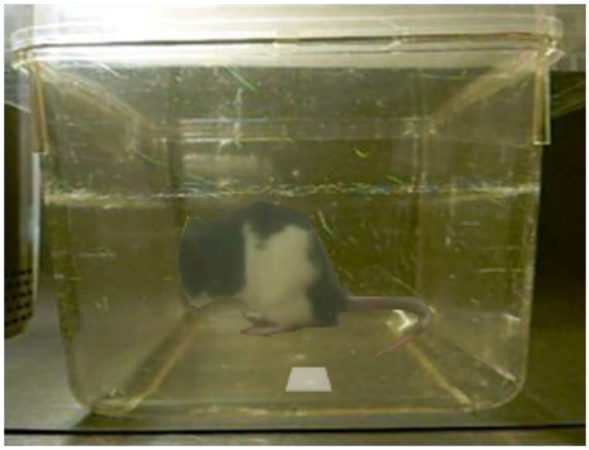

Figure 40: Arousal behavior test. 10µl of butyric odor was presented on a 2 cm x 2 cm filter paper pad. The rat's behavior is recorded for 5 minutes. The videos were scored later for time spent grooming and time spent exploring the filter paper pad.

an unscented filter paper pad (2 cm x 2 cm) in the cage (Figure 40). Rats were allowed a one minute inter-trial break, during which the filter paper pad was removed from the cage. During the actual test, the rat behavior was recorded for 5 minutes in the test cage with 10ul of butyric acid (99+%, Sigma-Aldrich) on a filter paper pad in one corner of the cage lid. The videos were later scored for grooming time and duration of approach behavior to the scented pad.

Avoidance Behavior Test

The avoidance behavior test was based on a test by Endres and Fendt (Endres and Fendt, 2009). The test arena was a 90cm x 90cm black Plexiglas arena. An overhead camera with Ethovision software (Noldus Information Technology, Leesburg, VA) was used to score the behaviors. Four corner zones of 30cm x 30cm each were virtually marked using the software. Each of the four corners contained one 2cm x 2cm filter paper pad. Rats were acclimated for 5 minutes one day prior to the test day. On the test day, each rat was taken out of the home cage and placed in a holding cage for 2 minutes. They were acclimated to the arena again for 2 minutes and brought back to the holding cage. The rats then performed 4 trials of 5 minutes each in the arena. During each trial, they were allowed to explore the arena freely, while 10ul of BA was added to one of the four zones while the other 3 were left unscented. The odor zone was chosen

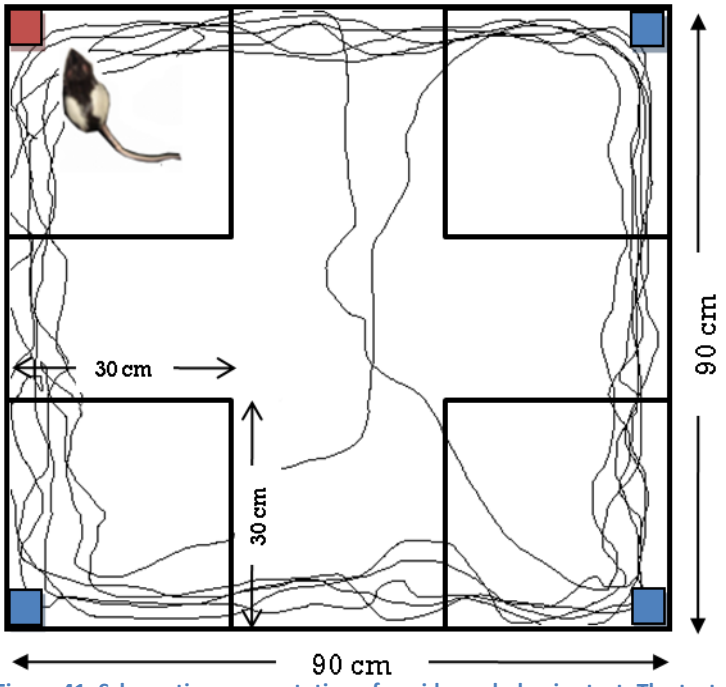

Figure 41: Schematic representation of avoidance behavior test. The test was conducted in a 90cm x 90cm black Plexiglas arena, virtually divided into four 30cm x 30 cm corner zones. At the four corners, four 2cm x 2cm filter paper pads were attached to the bottom of the area using a double sided adhesive tape. Each rat performed four 5 minute trials. During each of the trials, 10ul of Butyric acid was added to one of the corners chosen at random. The red square represents presence of scent in one of the corners. The blue squares represent the corners with blank filter paper pads. The rat's behavior was recorded using an overhead camera and behavior was analyzed using Ethovision software (Noldus Information Technology, Leesburg, VA)

randomly, but included one trial each per corner as the odor corner to eliminate the effect of corner preference. Rats performed two sessions of two consecutive trials each, with a 2 minute rest period between the trials in a holding cage. Between the two sessions, the rats spent 20 minutes in the home cage to eliminate any stress related to long test periods. The track from each trial was analyzed for approach frequency and time spent in each of the four zones.

Functional MRI

Functional MRI was performed on awake rats as described by King et. al. (King et al., 2005). The setup consisted of a head holder body tube combination in order to secure the rat with a surface coil – volume coil combination for Imaging. Rats were anesthetized with isoflurane and restrained in the head holder and body tube set up. Effects of isoflurane wore off before the imaging session. EMLA cream, a local anesthetic, was used to relieve any discomfort associated with the head holder. Rats were

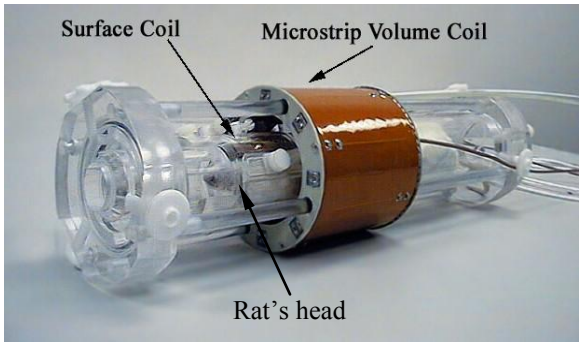

Figure 42: MRI imaging setup. Rat is secured at the teeth with a bite bar and a pair of ear plugs at the ears in the head holder. His body is restrained in a body tube. The head holder-Body tube combination is placed inside a surface coil – Volume coil MR imaging setup. Local anesthetic was applied to the rat's ears to relieve any discomfort of this set up and rats were acclimated to this setup for nine days before the test day.

acclimated to this setup for 9 days prior to the imaging session. A previous study in our lab has shown that repeated acclimation reduces the stress of imaging.(King et al., 2005) Functional MRI was performed on 4.7T/40cm horizontal bore magnet (Oxford, UK) with 20 G/cm magnetic field gradients and Bruker Biospec console (Bruker, Germany). A ^{1}H dual coil system (Figure 42,Insight NeuroImaging Systems, Worcester, MA) with a transmitting volume coil and a surface receiving coil was used for imaging.(Ludwig et al., 2004) All of the images were acquired over a 32 mm x 32 mm FOV and included 18 1mm slices. The scanning session included one anatomical and one single functional scan. The anatomical scan was acquired using multi-slice spin echo (RARE) sequence with matrix size of 256 x 256, RARE factor = 8, repetition time (TR)=2125 ms, effective echo time (TE) = 50 ms and 4 averages . The functional scan was acquired using Gradient-Echo Echo Planar Imaging sequence with matrix size = 64×64 (0.5 x 0.5 mm resolution), TR=1 s, TE = 30ms, flip angle = 60◦. The functional scan included 180 repetitions (NR) within the scan, with a total scan length of 180 seconds. Rats were exposed to air during the first 60 seconds and to 10ul of BA during the remaining 120 seconds.

Data Analysis

Arousal Behavior

The videos from the arousal behavior test were scored for the total time spent grooming and approaching (rat's nose within half of an inch from the pad) the filter paper pad containing the odor. Any values falling 2 standard deviations away from the group means were eliminated from the final mean calculation. Univariate ANOVA with general linear model was used to compare grooming times and approach times between groups.

Avoidance Behavior

The aversion behavior tracks were analyzed for frequency into different zones, total time spent in the zone, and time during each visit to the different zones for each of the 4 trials per rat. Tracks with values falling 2 standard deviations away from the overall group means were eliminated from the final mean calculation. The 4 trials were averaged per rat to obtain one set of values per rat. The results were compared between the control, sham and 3WKPD groups using Repeated measures ANOVA with bonferroni correction for multiple comparisons. Two separate comparisons were done for zone frequencies and zone times. The 3WKPD group was then compared with the sham group to test the effects of 6-OHDA lesions on the avoidance behavior.

Imaging Study

Each fMRI scan was motion corrected using SPM8 software (Functional Imaging Laboratory, London, UK). A region of interest (ROI) map was generated for each subject by registering their anatomical scan to a built-

in, fully segmented rat brain atlas in Medical Image Visualization and Analysis (MIVA, http://ccni.*wpi*.edu/*miva*.html). A code written in MATLAB (Mathworks Inc., Natick, MA, USA) generated percent blood oxygen level dependent (BOLD) maps with $p<0.001$ for every voxel in the 64 x 64 x 18 volume. For each ROI, the average BOLD value was calculated per subject by averaging all the voxels in the BOLD map that fell within the particular ROI. BOLD fMRI activation values for olfactory bulb (OFB), anterior olfactory nuclus (AON), piriform cortex (PirC), nucleus accumbens (NAcc), Insular cortex (InsC), basal nucleus of amygdala (BNA), lateral nucleus of amygdala (LNA), central nucleus of amygdala (CNA) and medial nucleus of amygdala (MNA) were fed into SPSS for statistical analysis. These ROIs were chosen a priori, based on their involvement in olfactory and aversion processing. Repeated measures ANOVA with bonferroni correction was used to compare the three groups. Additional univariate ANOVA with bonferroni correction for multiple comparisons for was used to do pair-wise comparisons between groups for the percent BOLD signals within different ROIs.

Results

During the 5 minute arousal behavior test, all of the control, sham and 3WKPD groups spent equal time exploring the scent. The univariate ANOVA revealed no difference between the approach time ($F_{(2,45)}=0.193$, $p=0.825$), but there was a significant main group effect in the grooming behavior ($F_{(2,45)}=4.343$, $p<0.02$). Post-hoc tests with bonferroni correction revealed significantly lower grooming in the 3WKPD group as

compared to sham ($t_{(31)}$=2.52, p<0.05) and control ($t_{(31)}$=2.64, p<0.04) groups (Figure 43).

Repeated measures ANOVA with bonferroni correction for multiple comparisons for zone frequencies in the avoidance behavior test revealed a significant main effect of scents ($F_{(1,23)}$=26.858, p<0.001), but no group effect ($F_{(2,23)}$=0.266, p=0.769) and no scent x group interaction ($F_{(2,23)}$=0.666, p=0.524). However, there was a significant main effect of scent ($F_{(1,23)}$=4.458, p<0.05), significant main effect of group effect ($F_{(2,23)}$=4.615, p<0.03), qualified by significant scent x group interaction ($F_{(2,23)}$=4.918, p<0.02). The repeated measures ANOVA between control and sham grouups indicate that, there were no significant differences between the two groups (Figure 45). There was a significant main effect of scents ($F_{(1,13)}$=22.309, p<0.001) in the relative frequencies to the BA zone versus the no-scent zones (Figure 45A), confirming that both, the

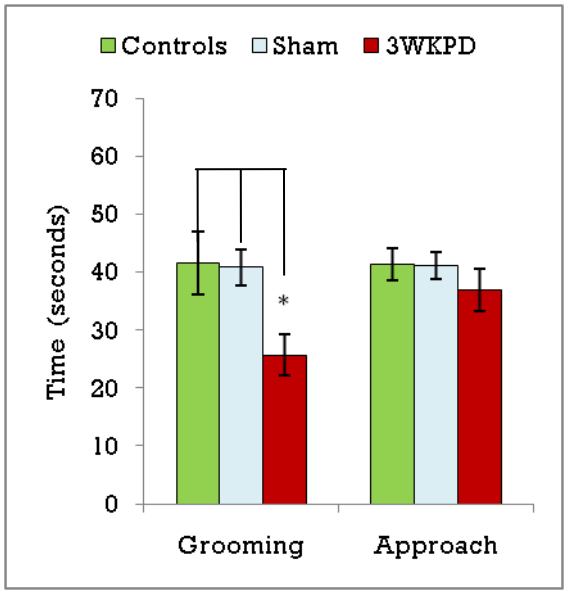

Figure 43: Arousal behavior test results. Significantly lower grooming in the 3WKPD group as compared to sham (*$t_{(30)}$=2.52, p<0.05) and control (*$t_{(31)}$=2.64, p<0.04)

controls and the shams, treated the BA zone differently than the no-scent zones, and there was an overall increase in frequency to the BA zone. There was no significant group effect or scent x group interaction ($F_{(1,13)}$=0.009, p=0.927). The total time spent by the rats in the different zones (Figure 45B) had a main effect of scent ($F_{(1,13)}$=81.407, p<0.001) and no significant scent x group interaction ($F_{(1,13)}$=0.481, p=0.499) among the control and sham groups.

The hypothesis that the 3WKPD rats would have deficits in avoidance was tested by comparing their performance with the sham lesioned rats, using repeated measures ANOVA (Figure 46). The 3WKPD rats did not have any significant main group effect ($F_{(1,17)}$=0.308, p=0.586) in the zone frequencies as compared to shams (Figure 45A), but there was a significant main effect of scents ($F_{(1,17)}$=19.53, p<0.001). This implied that, irrespective of the group that they belonged to, rats treated the BA zone differently from the no-scent zone. Both groups had relatively higher frequencies to the BA zone compared to the no-scent zones (Figure 46A). The repeated measured ANOVA of the total zone times in the BA versus no-scent zones between the sham and 3WKPD groups (Figure 46B) revealed a significant overall group effect ($F_{(1,17)}$=4.92, p<0.05), qualified by significant scent x group interaction ($F_{(1,17)}$=6.026, p<0.03). There was a lack of significant effect of scent ($F_{(1,17)}$=0.872, p=0.363). Additional univariate analysis of BA zone time revealed that the time spent in the BA zone was significantly higher in the 3WKPD group as compared to the sham group ($t_{(17)}$ = 2.395, p<0.03).

Analysis of BOLD activation in ROIs based on a priori hypothesis revealed a significant group x ROI interaction ($F_{(16,144)}$=4.97, p<0.001). Lack of significant group effect ($F_{(2,18)}$=3.109, p=0.069) indicated that there were no significant difference between the overall BOLD activation between the groups. Additional univariate analysis with bonferroni correction revealed that all the groups had similar activation of the olfactory system ($F_{(2,22)}$=0.601, p=0.557 for OFB; $F_{(2,22)}$=0.9, p=0.42 for AON; and $F_{(2,22)}$=0.068, p=0.935 for PirC; Figure 47A). Among the post processing areas, NAcc ($F_{(2,22)}$=2.374, p=0.118) and InsC ($F_{(2,22)}$=1.018, p=0.377) did not reach significance either (Figure 47B). But the 3WKPD group had significantly lower positive BOLD activation in the sub-regions of the amygdala such as CNA($F_{(2,22)}$=8.418, p<0.002), BNA ($F_{(2,22)}$=8.629, p<0.002) and LNA ($F_{(2,22)}$=8.672, p<0.002) (Figure 47B) compared to controls and sham lesioned rats, while the MNA did not reach significance ($F_{(2,22)}$=0.84, p=0.446).

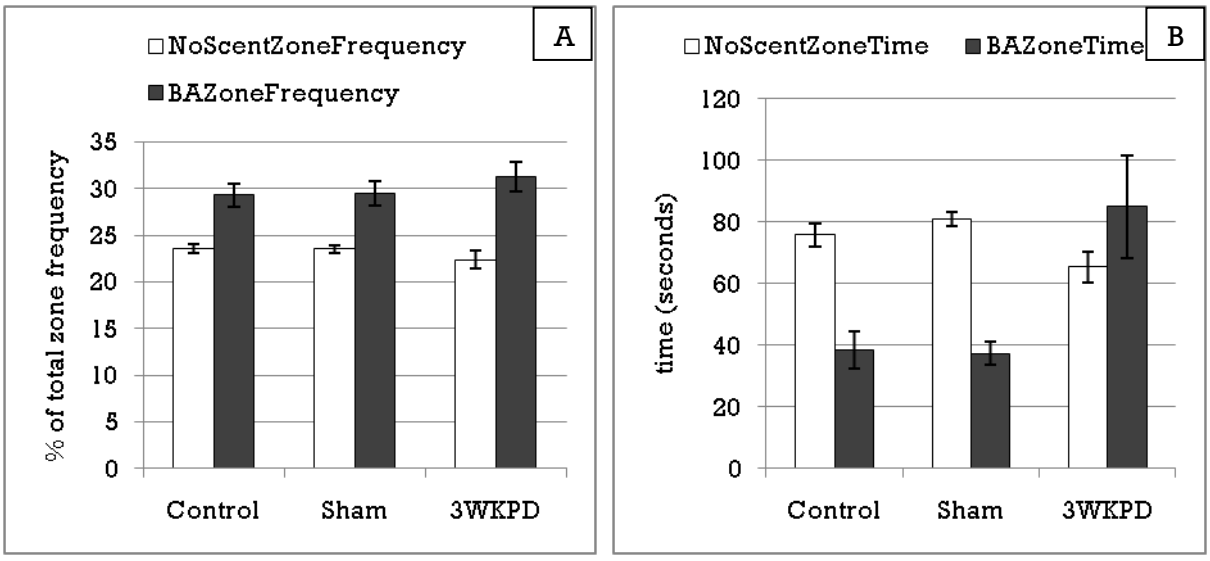

Figure 44: Comparison of all three groups. Frequencies to BA zone versus no scent zones (A) had a significant main effect of scent ($F_{(1,23)}$=26.858, p<0.001) but no effect of group; Zone times (B) had a significant main effect of scent ($F_{(1,23)}$=4.458, p<0.05), as well as, a significant main effect of group effect ($F_{(2,23)}$=4.615, p<0.03), qualified by significant scent x group interaction ($F_{(2,23)}$=4.918, p<0.02)

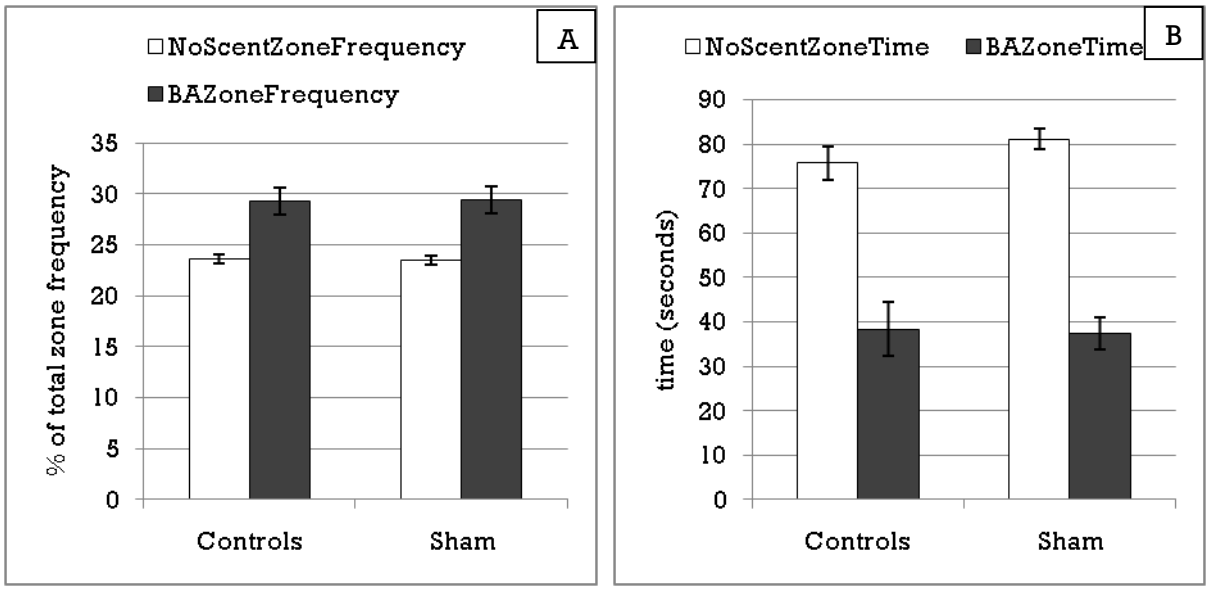

Figure 45: Avoidance behavior: Control versus Sham comparisons. Shams and controls responses had no significant differences as indicated by ANOVA for repeated measures using general linear model with respect to frequencies to butyric acid (BA) zone versus no-scent zones (A), and Total time spent in BA zone versus no-scent zones (B). There was a significant main effect of scent in both the comparisons ($F_{(1,13)}$ = 22.309, p<0.001 for zone frequencies; $F_{(1,13)}$ = 81.407, p<0.001 for total zone times).

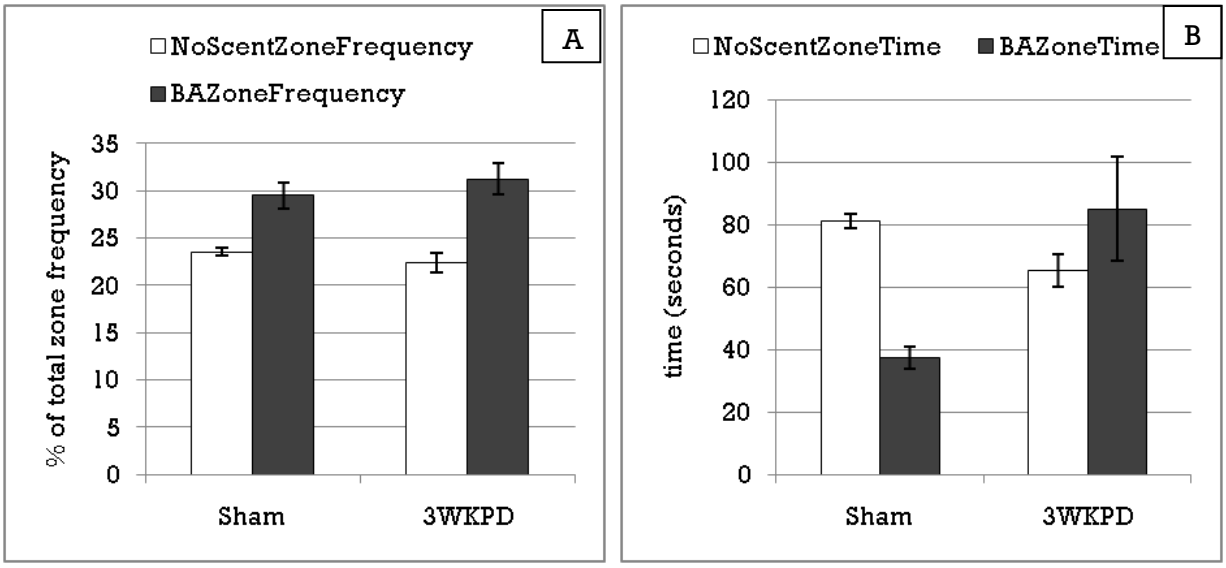

Figure 46: Avoidance behavior: Sham versus 3WKPD comparisons. Shams and 3WKPD responses were compared using ANOVA for repeated measures using general linear model. For the zone frequencies (A), there was a significant main effect of scent ($F_{(1,17)}$ = 22.309, p<0.001) but no significant group effect ($F_{(1,17)}$= 0.758, p=0.396) implying similar recognition of presence of the butyric acid (BA) odor in one of the scents. There was a significant main effect of group ($F_{(1,17)}$= 4.92, p<0.05) as well significant scent to group interaction ($F_{(1,17)}$= 6.026, p<0.03) for total zone times (B). Further investigation of the time spent in butyric acid zones indicated a significant difference between the two groups ($t_{(17)}$= 1.77, p< 0.03).

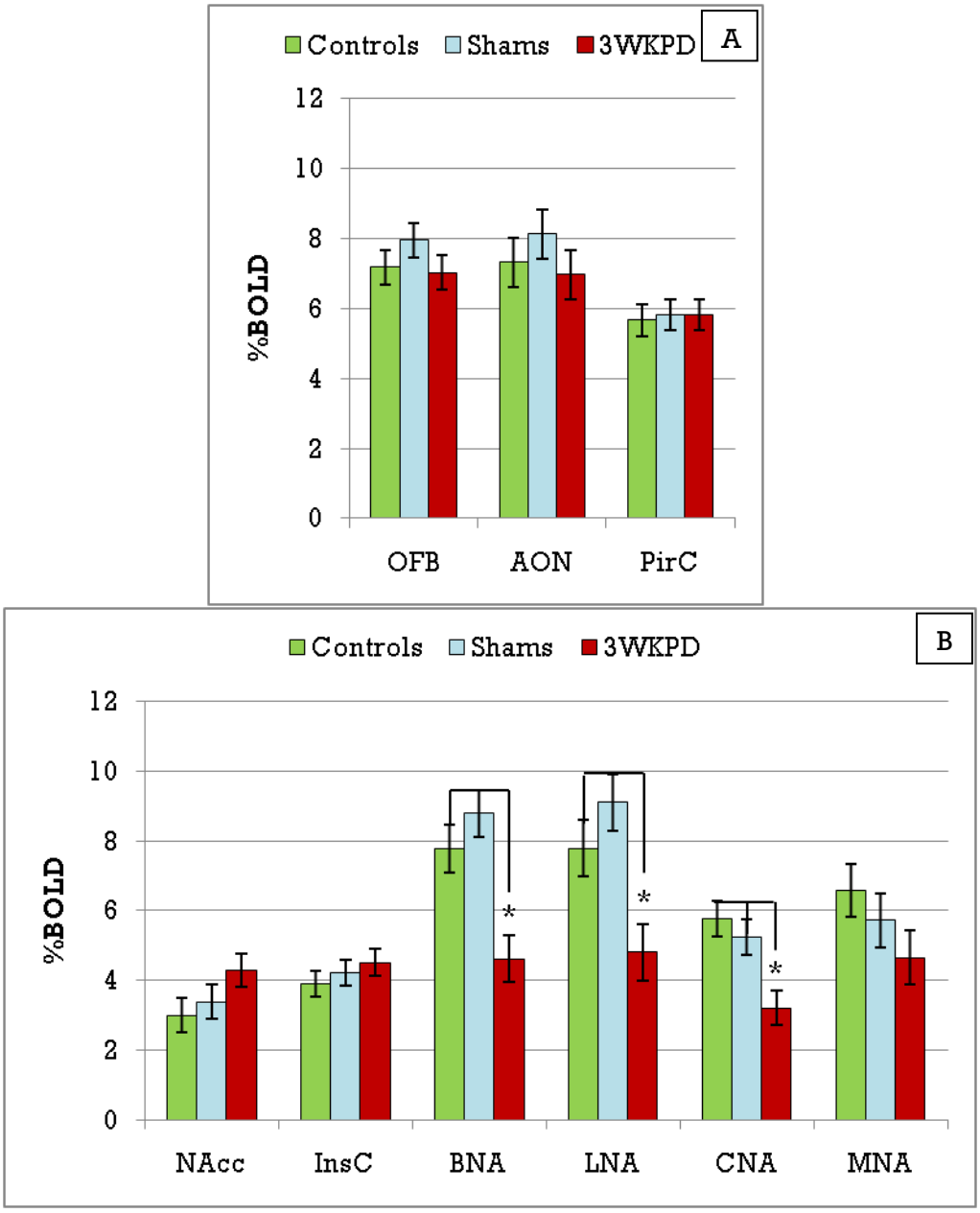

Figure 47: Functional MRI results upon exposure to butyric acid. (A) Percentage BOLD activation in the olfactory system. (OFB, olfactory bulb; AON, anterior olfactory nucleus and PirC, piriform cortex); (B) Percentage BOLD activation in the post-processing areas. (NACC, nucleus accumbens; BNA, baso-nucleus of amygdala; LNA, lateral nucleus of amygdala; CNA, central nucleus of amygdala; MNA, medial nucleus of amygdala). (*CNA($F_{(2,22)}$=8.418, p<0.002), *BNA ($F_{(2,22)}$=8.629, p<0.002) and *LNA ($F_{(2,22)}$=8.672, p<0.002))

Discussion

These studies showed that, in a rat model of pre-motor PD, produced through the utilization of stepwise 6-OHDA lesions of the CPu, there was significantly lower arousal to the aversive BA odor. However, there was no significant difference in the arousal response by the sham group compared to controls. Additionally, the sham and control rats exhibited equivalent avoidance of the butyric acid smell as exhibited by lower time spent in the corner with the BA odor in the avoidance behavior test. A comparison of the 3WKPD rats with the sham lesioned rats accounted for the effects of the surgical procedure, and indicated a group dependent response, that is, the rats' reactions to the BA zone versus no-scent zones were dependent on whether they belonged to the sham group or the 3WKPD group. Higher time spent with the aversive odor by the 3WKPD group implied a diminished avoidance of aversive odor compared to the sham group. These results parallel the observations noted in early stages of human PD, where PD patients exposed to aversive pictures exhibit blunted reactivity and report less arousal as compared to controls, in spite of recognizing the negative/aversive nature of those pictures (Bowers et al., 2006; Sprengelmeyer et al., 2003).

One of the possible explanations of lower grooming and lower avoidance is that PD rats failed to smell the aversive odor, as olfactory deficits are common in pre-motor PD. However, the lack of difference in the exploratory behavior between the groups in the arousal and avoidance behavior tests, along with equivalent BOLD activation of the olfactory system in the fMRI study, do not support this premise. Furthermore, it is important to note that, hyposmia in the pre-motor phase of PD in human

studies has been reported to be selective of odors and concentrations. Therefore, it is not a uniform loss of olfaction across all scents (Berendse and Ponsen, 2009; Ponsen et al., 2004).

Another possible consideration to address the behavioral deficits in aversive behavior in the PD rat model is the role of brain regions that process aversive stimuli including Insular cortex, Nucleus Accumbens and Amygdala complex. Involvement of Insular cortex has been reported during aversion processing in human (Jabbi et al., 2008; Small et al., 2003; Sprengelmeyer et al., 1998), as well as, in rat studies (Desgranges et al., 2009). Our results did not indicate any differences in the insular cortex activation between groups, which might have been a contributing factor to the observed deficits in the behavioral responses. This result is in accordance with the disease stage-dependent hypoperfusion of insular cortex observed in human PD patients where there is no significant difference between the controls and early PD patients. (Kikuchi et al., 2001)

The NAcc is also associated with aversion processing and plays a critical role in integrating excitatory (D1) and inhibitory (D2) inputs from Ventral Tegmental Area (VTA) (Carlezon and Thomas, 2009). While the VTA itself has a uniform response to both rewarding and aversive stimuli, the NAcc neurons respond selectively, with either an inhibitory response to rewarding stimuli or an excitatory response to aversive stimuli. (Roitman et al., 2005) Hence, NAcc neurons are believed to be involved in attaching valance to a stimulus by either selective activation or inhibition of neurons.(Carlezon and Thomas, 2009; Roitman et al., 2005;

Schoenbaum and Setlow, 2003) We observed positive BOLD activation in NAcc in controls, shams and 3WKPD rats, without any significant group effect.

The current results point towards a probable dysfunction in the link between processing the aversive stimuli and generating the appropriate response in PD rats. The amygdala region, which is known to process emotions and generate the response cascade to stressful/aversive stimuli, had an overall lower positive BOLD activation in PD. When selective nuclei in the amygdala, medial (MNA), basal (BNA), lateral (LNA) and central (CNA) nuclei, were examined individually, significantly lower BOLD activation was observed in the BNA, LNA and CNA of PD rats compared to both sham lesioned and control rats.

The amygdala complex comprises of a multi-level system that orchestrates both sensory input and output. In regards to olfaction, the MNA is thought to receive inputs from accessory olfactory bulb (Davern and Head, 2011); inhibition of baso-lateral amygdala has been shown to result in impairment of conditioned olfactory aversion (Desgranges et al., 2008); and CNA thought to mediate behavioral response to aversive stimuli (Finn et al., 2003). Given the results of our studies, we speculate that the MNA, which serves as the input to the amygdala complex, is functional in the PD rats while the BNA, LNA and CNA, which orchestrate the response, might be impacted. Hence, it appears that the behavioral deficit shown by PD rats in our study is mainly a result of deficit in generation of an appropriate response to the aversive stimulus and not due to the inability to process the stimulus. Our results are in accordance

with those by Bower's and colleagues who have reported blunted aversive reactivity among PD patients that was attributed to amygdalar dysfunction as a result of suppression of the amygdala by the cortical regions (Bowers et al., 2006).

Since the sham lesioned animals did not exhibit any arousal or avoidance deficits as compared to the control animals in the behavioral tests, as well as, in the functional MRI experiment; we conclude that the observed deficits in the 6-OHDA administrated rats cannot be attributed to the stress of the surgery but to changes in dopamine levels.

To date, loss of aversion in humans PD patients has been reported in the early to middle stages of PD. However, the current study has provided additional insight into the fact that these deficits might indeed be present in the pre-motor stages as well. Since the human reports are based on exposure to facial expressions of disgust or photographs of mutilation and contamination, future studies need to address potential olfactory aversion in humans with PD. We believe that such studies may provide an additional non-motor marker for testing pre-motor stage PD.

Conclusion

Taken together, our results show that the rat model of pre-motor stage of PD exhibits lower arousal to aversive odor as compared to controls and fails to demonstrate avoidance of the aversive odor. These results might be comparable to reports in human PD patients in early stages of the disease exhibiting decreased arousal and blunted startle reactivity in response to aversive stimuli. Further, our functional MRI results support

the hypothesis that the observed behavioral deficits are not a result of deficits in olfactory recognition but are most likely caused by deficits in response generation by the amygdala.

Chapter 6. Cognitive deficits in PD

Rational

Co-morbid cognitive deficits are reported in PD patient population with a prevalence rate of approximately 40% at stage 1 to 86% at stage 4 (Growdon et al., 1990). Reports confirm estimates of cognitive decline in upwards of 14% per year of these patients(Galvin, 2006). The early deficits appear to mainly consist of cognitive functions that are associated with the frontal lobe(Gotham et al., 1988) and frontal-striatal pathways(Alexander et al., 1986; Monchi et al., 2007), which are pathways sub-serving attentional set-shifting, working memory and executive function (Adler, 2005; Cools et al., 2001; Downes et al., 1989; Sharpe, 1990; Sharpe, 1992). Hawkes and colleagues have hypothesized that the cognitive deficits may exist as early as in Braak stage 2 of PD (Hawkes et al., 2010). The goal of this study was to test the possibility of pre-motor executive function deficits in PD.

Sodium butyrate as a possible treatment for PD

This study explored the potential of sodium butyrate (NaBu), a drug from the histone deacetylase inhibitor (HDACi) family of drugs, as a therapeutic agent to mitigate the pre-motor cognitive deficits in PD. Even though dopamine plays an important role in multiple neuronal networks involved in cognition (Nagano-Saito et al., 2008; Winter et al., 2009), dopaminergic therapeutic agents, proven to relieve the motor symptoms of PD, are not always effective at alleviating the co-morbid emotional and cognitive symptoms (Downes et al., 1989; Gotham et al., 1988; Jubault et al., 2009). Drugs from the HDACi family have been shown to be useful in

multiple psychiatric and neuro-degenerative disorders (Sadri-Vakili and Cha, 2006; Schroeder et al., 2007; Tsankova et al., 2006) and have neuroprotective effects in an in-vitro model system, as well as, in in-vivo studies (Ferrante et al., 2003; Gardian et al., 2005; Gray and Dangond, 2006; Hockly et al., 2003; Ryu et al., 2003; Wu et al., 2008). Emerging evidence of reversal in contextual memory deficits in a mouse model of Alzheimer's disease (Kilgore et al., 2009) and improvement in learning and long-term memory in toxin-induced, as well as, genetic mouse models of cognitive deficits (Fontan-Lozano et al., 2008) point to a potential role of HDACis in neurocognition. Indeed, since this class of drugs is well-tolerated by humans and rodents, there may be a strong translational validity (Hoshino and Matsubara, ; Liu et al., 2006).

Methods

Animals

Adult male Long Evans rats (300-350g, N = 32) were obtained from Harlan Sprague–Dawley Laboratories (Indianapolis, IN). The animals were group-housed (2 per cage) in Plexiglas cages and maintained in ambient temperature (22–24°C) on a 12/12 h light/dark cycle. They were provided with food and water ad libitum. All procedures were approved and monitored by the University of Massachusetts Medical School Institutional Animal Care and Use Committee. Rats were randomly divided into controls, sham lesion, 6-OHDA lesion (3WKPD) or 6-OHDA lesion with NaBu treatment (3WKPD+NaBu) groups as described in Table 4. Surgical procedures were similar to those described in Chapter 4. All the groups were tested three weeks post lesion.

Study	Group	Number of rats per group
ED/ID test	Control	8
	Sham	8
	3WKPD	8
	3WKPD + NaBu	8

Table 4: Rat assignment per different groups in executive function test.

Extra dimensional/Intra dimensional set shifting test

Executive functioning was tested using the rat analog of the Wisconsin

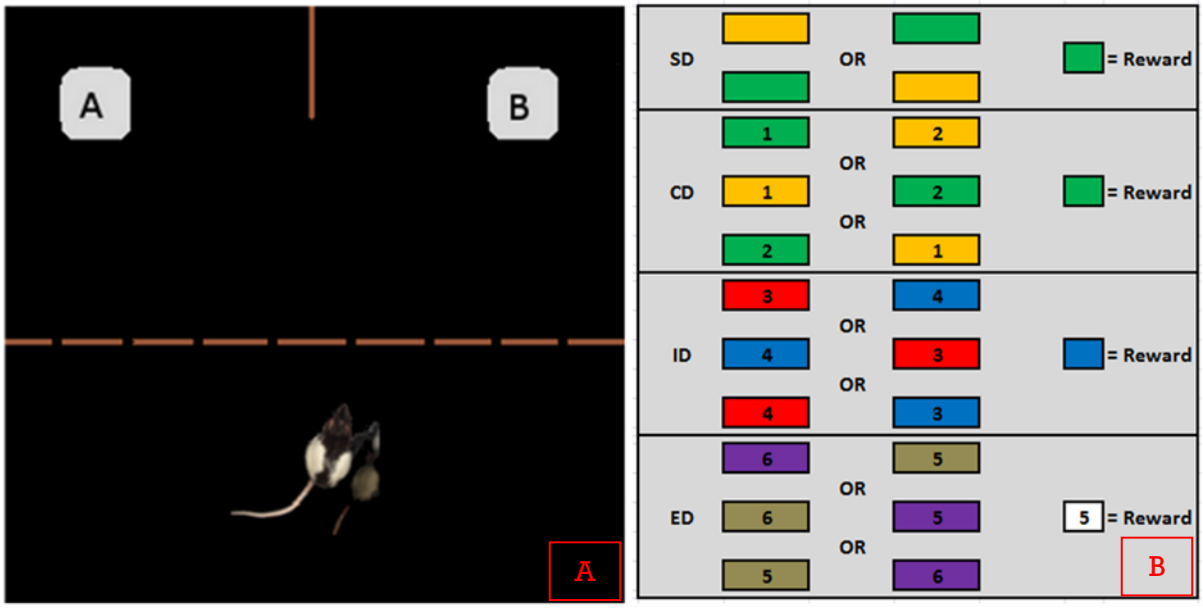

Figure 48: (A) ED/ID test setup. Dotted line represents temporary divider separating test area from the initial holding area. Areas A and B, separated by a partial divider (solid brown line), contained paper plates filled with bedding material. One of the plates contained the food reward that the rat could retrieve by digging into the bedding material. The rat had to dig into the correct plate to successfully complete a trial and retrieve the reward. (B) ED/ID shift behavioral paradigm. The colors represent the different colored lights (one dimension) and the numbers represent the different scents (second dimension)

Card sorting test called the Extra-Dimensional / Intra-Dimensional set shifting test (ED/ID test)(Birrell and Brown, 2000). The test apparatus (Figure 48A) consisted of a custom-built black Plexiglas arena (90cm x 90cm). A removable divider separated test area from the initial holding area at the other end. Test area was divided into two additional sections (Areas A and B) using a black partial divider. These areas were identified with a spotlight over a paper plate filled with bedding. Throughout the

test, stimuli from two dimensions (lights/odors) were used. The light dimension included pairs of lights (orange versus blue, purple versus yellow or green versus red), while the odor dimension consisted of pairs of different aromatic oils (100ul) mixed with a plate of bedding (vanilla versus lemon, peppermint versus thyme or rosemary versus cinnamon).

The test day was set at 3 weeks post second lesion. To prepare for this test, four days before the test day, rats were individually housed and maintained on a restricted diet (15 grams of pellets/day). They were habituated to the Plexiglas arena and trained in the home cages to find reward (pieces of rat chow) hidden in paper plates filled with bedding. Similar paper plates filled with bedding with or without the reward were presented to the rat during testing.

On the test day each rat randomly started with either the light or the odor dimension as the initially relevant dimension (IRD) and the other dimension initially irrelevant dimension (IID). Tests included simple discrimination (SD), compound discrimination (CD), intra-dimensional shifting (ID), and extra-dimensional set shifting (ED). Figure 48B describes the set of stimuli for different tasks. The tasks were always performed in the order of SD, CD, ID and then ED. This is critical because the performance in the subsequent task was dependent upon the completion of the preceding task. The rat started each trial in the holding area. As a trial began, the temporary divider separating the test area and the holding area was removed and the rat was allowed to explore the arena freely. During SD, rats had to discriminate between only one set of stimuli from the chosen dimension, IRD. The reward was associated with

one of the stimuli from the IRD. During SD, the IID was absent. For CD, reward was associated with the same stimulus as in SD, while a second set of stimuli from IID were introduced. IID stimuli needed to be ignored by the rat in order to complete the task successfully. ID was similar to CD but with a complete new set of stimuli from the IRD, as well as, the IID. Finally, during ED a whole new set of stimuli from both, the IRD and the IID, were introduced, but this time the reward was associated with one of the stimuli from the IID. Each time the rat completed a trial successfully by digging into the plate associated with the reward stimulus, he was allowed to continue digging until he retrieved the reward. If he first dug into the plate associated with the non-reward stimulus, he was picked up and returned back to the holding area with that trial marked as a failed trial; and a whole new trial then started. Each of the four tasks was marked as completed when the rat successfully completed six consecutive trials during that task.

Treatment

The 3WKPD+NaBu group received daily intra-peritoneal injections of NaBu treatment (250 mg/kg/ml in 0.9%saline; Sigma Aldrich, St. Louis, MO) starting at 2 week post surgery for 5 days during the dark phase of the light/dark cycle. The NaBu solution was prepared fresh at the start of the treatment. Treatment ended 2 days prior to the test day in order to minimize stress.

Data analysis

The total number of trials to successful completion of each task was noted. Repeated measures ANOVA with bonferroni correction for multiple

comparisons was used to analyze the group and task effects using SPSS (IBM Corp., Somers, NY). The groups were further compared with each other within individual tasks using univariate ANOVA with bonferroni correction. For each group, the effect of task difficulty was analyzed using repeated measures ANOVA on individual group results. Finally, to analyze the effects of NaBu treatment on attention after 6-OHDA lesions, 3WKPD group was compared with 3WKDP+NaBu group in the SD and ID tasks using repeated measured ANOVA.

Results

Repeated measures ANOVA revealed a significant main effect of task ($F_{(9,81)}$=31.729, p<0.001), as well as, a significant main effect of group

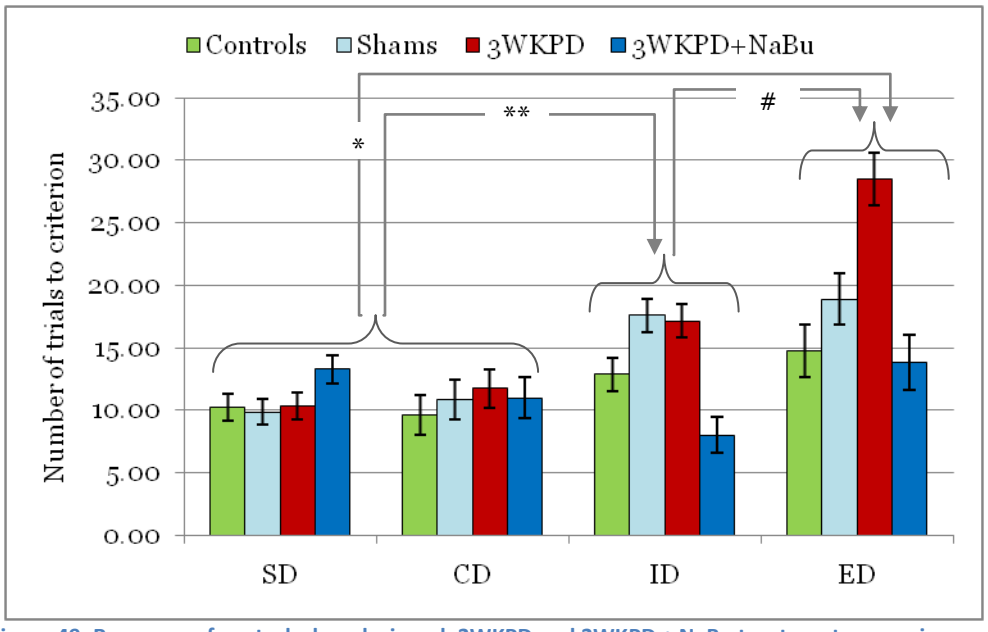

Figure 49: Response of control, sham lesioned, 3WKPD and 3WKPD + NaBu treatment groups in simple discrimination (SD), compound discrimination (CD), intra-dimensional shift (ID) and extra-dimensional set shifting (ED) tasks. There was a significant main effect of task ($F_{(3,81)}$=31.73,p<0.001), as well as, a significant main effect of group ($F_{(3,27)}$=5.786,p<0.004), qualified by significant interaction ($F_{(9,81)}$=7.651,p<0.001). There was no significant difference between the number of trials needed to complete SD and CD tasks. However, there was an overall increase in the number of trials needed to complete ID and ED tasks. (*p<0.001, **p<0.01, #p<0.001)

($F_{(3,27)}$=5.786, p<0.004) qualified by significant group x task interaction ($F_{(9,81)}$=7.651, p<0.001) as shown in Figure 49. Overall, there was no significant difference between the number of trials needed to complete SD and CD tasks ($t_{(27)}$=0.13, p=1.0). However, there was an increase in the number of trials needed to complete ID compared to SD ($t_{(27)}$ = 3.51, p<0.01) and CD ($t_{(27)}$=4.08, p<0.003) tasks. The ED task requireded an even higher number of trials to get to completion as compared to SD ($t_{(27)}$=6.79, pp<0.001), CD ($t_{(27)}$=9.71, p<0.001) and even ID ($t_{(27)}$=4.63, p<0.001) task, indicating a progressive increase in difficulty level across the tasks.

The within task univariate analysis revealed that there was no significant effect of group during the SD ($F_{(3,27)}$=2.02, p=0.135) and the CD ($F_{(3,27)}$=0.319, p=0.811) tasks. There was a significant main effect of

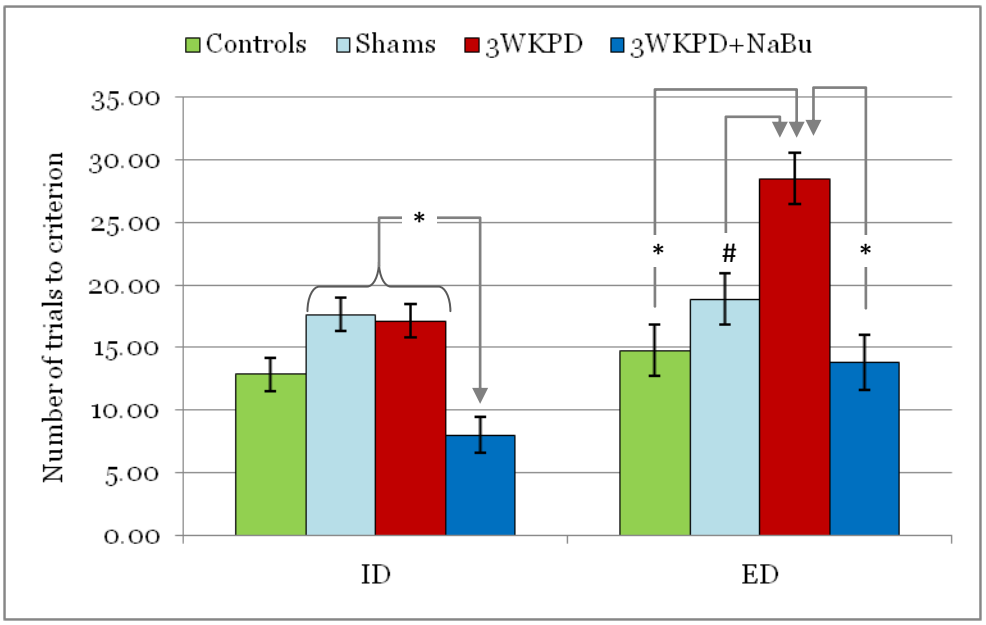

Figure 50: Univariate analysis of within task comparisons revealed a significant decrease in number of trials needed by the NaBu treatment group as compared to sham lesioned and 3WKPD groups. The 3WKPD groups needed significantly higher number of trials to complete the ED task as compared to all the other experimental groups. (*p<0.001, #p<0.02)

group ($F_{(3,27)}$=10.388, p<0.001) during the ID task (Figure 50). The post-hoc tests revealed that the NaBu treatment group needed significantly lesser number of trials as compared to the sham ($t_{(14)}$=4.93, p<0.001) and the 3WKPD ($t_{(14)}$=4.67, p<0.001) groups, implying a probable improvement in attentional set formation in the treatment group.

Significant main effect of group was observed in the ED ($F_{(3,27)}$=10.312, p<0.001) task as well. 3WKPD group needed significantly higher number of trials as compared to controls ($t_{(15)}$=4.72, p<0.001), sham lesioned ($t_{(15)}$=3.31, p<0.02), as well as, the 3WKPD+NaBu group ($t_{(14)}$=4.85,

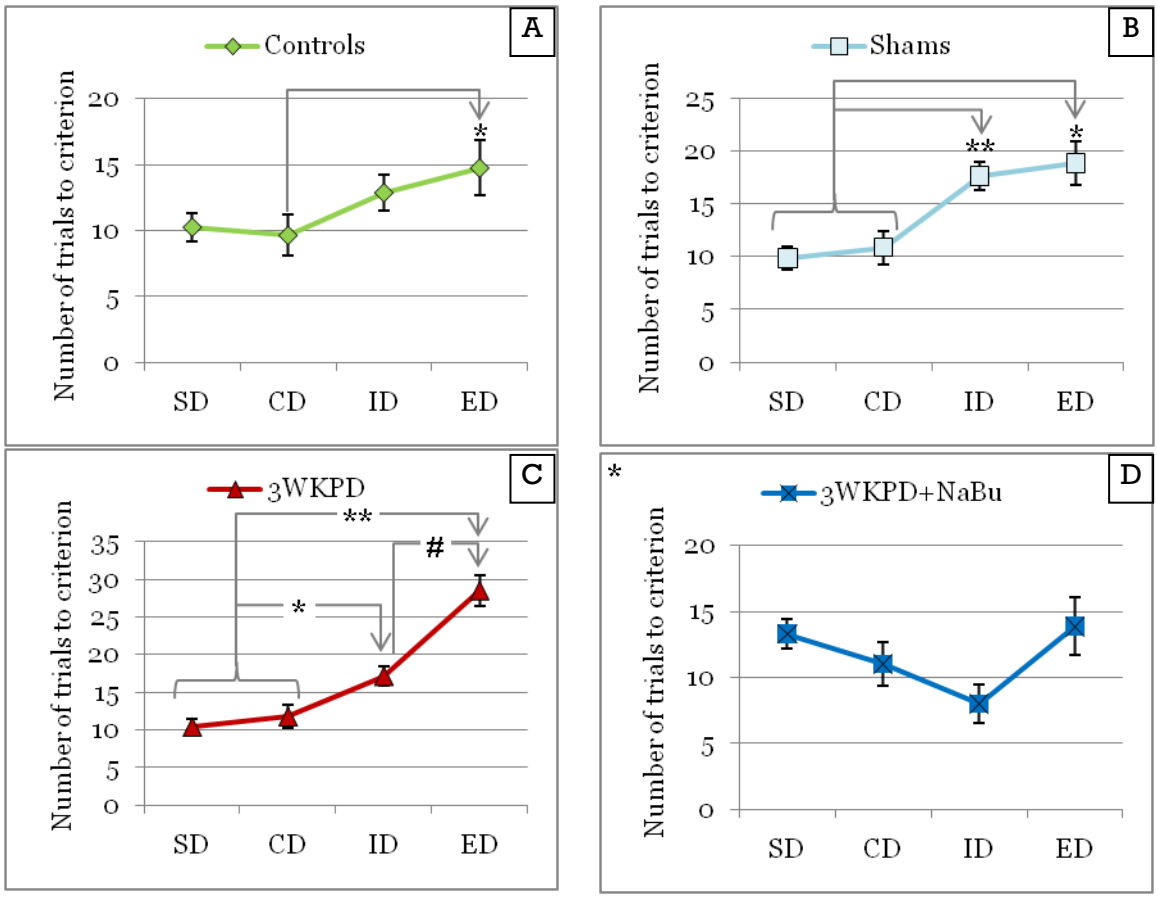

Figure 51: Controls (A) need significantly higher number of trials for ED task compared to CD task (*p<0.03). Sham rats (B) need significantly higher number of tasks to complete ID and ED tasks as compared to SD and CD tasks (*p<0.02, **p<0.007). The 3WKPD rats (C) needed higher number of trials to complete ED not just compared to SD (**p<0.002) and CD (** p<0.001), but also compared to ID task (#p<0.05). Similar to shams, 3WKPD rats had significantly higher number of trials in ID as compared to SD and CD tasks as well (*p<0.04). The NaBu treatment group (D), did not exhibit a significant main effect of task during the study.

$p<0.05$) as per the post-hoc tests (Figure 50).

The within group repeated measures ANOVA revealed that for the control group (Figure 51A), there was a significant effect of task on the number of trials needed to complete the four tasks ($F_{(3,21)}=4.11$, $p<0.02$) with a significant difference between the CD and ED tasks ($t_{(15)}=4.11$, $p<0.03$). The sham lesioned rats (Figure 51B) exhibited a main effect of task ($F_{(3,21)}=18.12$, $p<0.001$) with significantly higher number of trials to complete the ED task as compared to both the SD ($t_{(15)}=6.3$, $p<0.003$) and CD ($t_{(15)}=4.5$, $p<0.02$). The sham rats also needed significantly higher number of trials to complete the ID task as compared to the SD ($t_{(15)}=5.42$, $p<0.007$) and CD ($t_{(15)}=7.49$, $p<0.002$) implying a weaker attentional-set formation. Similar to the sham lesioned rats, the 3WKPD group (Figure 51C) also exhibited significant main effect of task ($F_{(3,21)}=34.26$, $p<0.001$) with significantly higher number of trials for the ID and ED tasks as compared to both the SD ($t_{(15)}=8.25$, $p<0.001$ with ID; $t_{(15)}=6.66$, $p<0.002$ with ED)and CD ($t_{(15)}=3.98$, $p<0.04$ with ID; $t_{(15)}=8.91$, $p<0.001$ with ED) tasks. In addition there was also a significant difference between the trials needed to complete the ID and the ED tasks ($t_{(15)}=3.76$, $p<0.05$) implying a weaker attentional-set formation as compared to controls, as well as, a set-shifting deficit.

On the other hand, the 3WKPD+NaBu group (Figure 51D) did not exhibit a task effect in completing the four tasks ($F_{(3,18)}=2.244$, $p=0.118$). This might be indicative of a stronger attentional set formation and better set-shifting abilities as a result of the treatment. Investigation of SD-CD-ID progression between 3WKPD and 3WKPD+NaBu groups using

repeated measures ANOVA revealed a significant task by group interaction ($F_{(2,26)}$=9.97, p<0.001) without any significant task or group effect.

Discussion

The four tasks in the ED/ID test are designed to test various aspects of executive function including attention, rule acquisition, cognitive flexibility, error correction and trouble shooting. The SD task tests the subjects' ability to accomplish reward association and learning. The CD task tests their ability to keep attention on the rule learnt in the SD task while ignoring the newly introduced irrelevant dimension stimuli. In the ID task, the subjects' ability to apply the rules from SD and CD to a new set of stimuli is assessed. During the SD, CD and ID tasks, the subjects develop an attentional-set with respect to the relevant dimension as a whole, and develop learned-irrelevance towards the second dimension (Ng et al., 2007). In the ED task, the subjects' need to revise the attentional-set, learnt relevance and irrelevance, based on alteration in the feedback they receive (Nagano-Saito et al., 2008; Ng et al., 2007). This exercise, tests the cognitive flexibility of the subjects. Humans, non-human primates, as well as, mammals such as sheep and rodents have all demonstrated successful completion of the four tasks (Fox et al., 2003; Morton and Avanzo, 2011; Owen et al., 1992). Because of the increasing levels of difficulty, higher number of trials are needed for the ID and ED tasks as compared to SD and CD tasks (Birrell and Brown, 2000; Fox et al., 2003; Robbins et al., 1996).

The overall performance of the rats during the four tasks in the current study aligned with the previous observations of progressively increasing difficulty levels while moving from SD to CD to ID to ED tasks. The control and the sham rats needed higher number of trials for completion of ID and ED tasks as compared to the first two tasks, though the difference was not significant for ID in controls. The 3WKPD rats also had similar performance, but needed significantly higher number of trials in the ED task as compared to ID task. Their performance in the first 3 tasks was comparable to the performance by the control and the sham groups, implying a similar reward association, rule-learning and attentional-set formation in the three groups. But the 3WKPD group was significantly weaker in the ED task, indicating a set-shifting specific deficit. These results are in accordance with previous observations in PD patients where set-shifting specific deficits have been reported (Cools et al., 2003; Owen et al., 1992; Schneider, 2006). The cognitive inflexibility, as depicted by deficit in the ED task, can be a result of two phenomena, deficits in revising the relevance of IRD, or enhanced learnt irrelevance towards IID, leading to the inability to attend to the dimension previously learnt as irrelevant. Owen's group has shown that the ED deficit in PD patients is more pronounced in the case of shifting attention to a dimension previously learnt as irrelevant, hence enhanced learnt irrelevance being the contributing factor to the deficit (Slabosz et al., 2006). In their study, they observed that the PD patients were indeed able to focus their attention away from the previously relevant dimension, therefore the preservation of the learnt relevance did not appear to be a contributing factor to the PD deficit. The tests in our study had the

complete-learnt irrelevance design in terms of the ED. Hence, our rats did exhibit deficits in revising learnt irrelevance based on negative feedback they received after incorrect trials. However, this study paradigm does not test for deficits in revision of IRD. Hence, additional testing with a completely novel dimension as the relevant dimension during the ED task would be able to delineate the exact cause of the observed ED deficit.

We hypothesize that the observed ED deficit in 3WKPD rats might be a result of an inability to learn new rules as a result of lowered dopamine levels disrupting PFC-striatal connectivity. This connectivity is hypothesized to be important for set shifting and is impacted in PD patients (Monchi et al., 2004). Dopamine depletion has been shown to cause disruption of PFC-striatal connectivity, as well as, ED deficit in healthy controls (Nagano-Saito et al., 2008). Indeed, lack of similar deficits in sham lesioned rats in this study supports dopamine depletion as a cause; thus, eliminating the potential impact of stress of the lesioning process as a probable cause for the ED deficit.

While shifting from CD to ID task, both the 3WKPD and sham lesioned groups needed significantly higher number of trials, as compared to their own performance in the CD task. A similar significance was missing in the control group. Even though the ID performance was not significantly different between the groups, the within group comparisons might be pointing towards a weaker attentional-set formation in the sham and the 3WKPD groups as a result of the surgical procedure, irrespective of the dopamine depletion. Cingulate cortex lesions have shown to result in ID

deficits in rats (Ng et al., 2007) without any ED deficits. As per our knowledge, our rats do not have cingulate cortex lesions. This is also supported by the fact that the deficits we observed are not in comparison with the controls as those observed by the Ng group. Additional research is needed to further analyze this observation of weakened attentional-set in our study.

The performance of the 3WKPD+NaBu group in the ED task had significant improvement over the performance of the 3WKPD group, and was comparable to the performance by the control group. Hence, NaBu appears to be effective in preventing the deleterious effects of 6-OHDA. In addition, the 3WKPD+NaBu rats, as they performed SD, CD and ID tasks, were able to focus increasing amount of attention on the IRD and completely ignore IID. NaBu treatment has been shown to enhance reward association (Schroeder et al., 2008). Hence, the NaBu treatment might have enhanced the reward association in our study, leading to improved attentional set. Additional experimentation is needed to confirm this hypothesis, but was outside the scope of this particular study. However, results of this study point towards HDACis as a promising treatment option for cognitive deficits in PD.

Conclusion

Stepwise striatal lesions with low doses of 6-OHDA in rats closely mimic the cognitive deficits observed in PD patients. The observed deficits are reported in post-clinical diagnosis stages in the patient population. Our results support the possibility of the presence of these deficits in pre-motor stages of PD as well. NaBu ameliorates the cognitive deficits

resulting from striatal dopamine depletion, by significantly improving the cognitive abilities of the treatment group. By improving attentional set formation, as well as, set shifting ability, the treatment of NaBu showed promising therapeutic potential to treat pre-motor stage PD. Further studies may offer more insight into the cognitive enhancing effects of this class of drugs.

Chapter 7. Resting State functional MRI

Rational

As described in Chapter 3 temporal correlations in low frequency fluctuations (<0.1Hz) in BOLD signals recorded in different brain regions can serve as a measure of functional connectivity between those regions.(Biswal et al., 1997) Resting state (RS) connectivity during resting or passive task states has been observed in humans, primates, and rats (Biswal and Kannurpatti, 2009; Greicius et al., 2008; Pawela et al., 2008; Zhang et al., 2010).

Thus, studying RS connectivity can further our understanding of how the brain functions by allowing us to map out complex neural circuits, referred to as intrinsic connectivity networks (Shehzad et al., 2009). Furthermore, the observed intrinsic networks have significant overlap with task-evoked activations (Biswal et al., 1995; Fox et al., 2007; Greicius et al., 2008) and structural connectivity(Greicius et al., 2009; Hagmann et al., 2008). RS connectivity, in turn, allows us to observe how the brain's functioning changes under different affected states. It has been shown to change with various disease stages like Alzheimer's Disease (AD) (Lustig et al., 2003; Rombouts and Scheltens, 2005), Depression(Anand et al., 2005), ADHD (Tian et al., 2006), Multiple Sclerosis(MS)(Lowe et al., 2008; Lowe et al., 2002) and even during normal aging (Andrews-Hanna et al., 2007). In this study, we analyzed the RS connectivity changes in our pre-motor rat model as compared to the age matched controls. We hypothesized that, 6-OHDA lesions would result in alterations in RS connectivity in the rat brain. We also

hypothesized that the RS observation might be able to delineate the beneficial effects of NaBu on brain networks that resulted in enhanced cognitive performance in the treatment group.

Methods

Animals

Three groups of rats, controls, 3WKPD, and 3WKPD rats with sodium butyrate treatment (3WKPD+NaBu) were used for this study. Table 5 described the number of rats in the different groups. The 3WKPD and 3WKPD+NaBu groups received 6-OHDA lesions of 10ug and 2ug each in 1ul of vehicle as described in Chapter 4. The 3WKPD+NaBu group received daily intra-peritoneal injections of NaBu treatment (250 mg/kg/ml in 0.9%saline; Sigma Aldrich, St. Louis, MO) for 5 days during the dark phase of the light/dark cycle, starting at 2 weeks post surgery. The NaBu solution was prepared fresh at the start of the treatment.

Study	Group	Number of rats per group
ED/ID test	Control	10
	3WKPD	13
	3WKPD + NaBu	9

Table 5: Assignment of rats to different groups in resting state connectivity study.

Imaging

Rats were anesthetized with isoflurane and restrained in the head holder and body tube set up. Isoflurane's effect wore off before the imaging session began. EMLA cream, a local anesthetic, was applied to relieve any pain associated with the head holder. Rats were acclimated to this setup for 9 days prior to the imaging session.

Gradient-Echo Echo Planar Imaging sequence with matrix size = 64×64 (3.2cm x 3.2cm), 1mm slice thickness, TR=1 s, TE = 30ms, flip angle = 60◦ was used to collect the resting state scans on 4.7T/40cm horizontal bore magnet (Oxford, UK) with 20 G/cm magnetic field gradients and Bruker Biospec console (Bruker, Germany) using a ^{1}H dual coil system (Insight NeuroImaging Systems, Worcester, MA). Five to seven scans of 200 repetitions each were collected per rat. The goal was to achieve at least five scans per rat with minimal motion. Each repetition was a 64x64x18 volume image of the brain.

Data analysis

Preprocessing of data

All resting state fMRI files were motion corrected using SPM8 (Functional Imaging Laboratory, London, UK) after discarding any scan with more than 0.5mm (1 pixel) motion. Areas outside the brain region were removed with hand drawn masks in MATLAB. All rats from all groups were aligned to one standard rat manually in MIVA. The alignment matrices were used to form aligned fMRI scans, which were fed into the MATLAB based GIFT toolbox for independent component analysis for 30 components. The 30 overall mean components generated by GIFT were thresholded at z-scores > 1.65 ($p<0.05$) and compared with the rat brain atlas to choose 6 components as seeds for seed based connectivity. (Figure 52) As compared to anatomical seed based ROIs, this method ensures a high correlation between the voxels selected within a seed.

Seed based connectivity analysis

Each run of the RS scans was spatially filtered using 4×4 Gaussian low-pass filter with the standard deviation of 0.5 (FWHM=1mm). All time courses were 0.0018–0.1 Hz band-pass filtered and the first 10 images were discarded to ensure an equilibrium state. This frequency range has been shown to contribute towards cortical connectivity in brain in humans (Biswal et al., 1995; Cordes et al., 2001), as well as, in rats (Williams et al., 2006). The cardiac and respiratory signals in humans are in the range of 0.6-1.1Hz and 0.1-0.5Hz, respectively (Cordes et al., 2001). In rats, the cardiac frequency is of the order of 4-5Hz and the respiratory frequency is of the range of ~1Hz (Majeed et al., 2009; Williams et al., 2006). The lower cutoff frequency removes any effects of magnet drift from the correlation calculations. The time courses for voxels within each of the seeds were averaged across the seeds to get averaged seed time courses (AST). Correlation coefficients between each of the ASTs and time courses for individual voxels were computed. The correlation values were averaged across each of the experimental groups in a pixel-by-pixel basis by removing any outlier pixel which had values 2 standard deviations away from the group to form the seed based connectivity maps. The seeds that were chosen included olfactory bulb, prefrontal cortex, motor cortex, cingulate cortex, CPu, and amygdala. CPu was chosen as a seed because it was our site of 6-OHDA lesions. Amygdala was chosen because of the observed aversion deficits seen in the 3WKPD group, and the known link between amygdala and emotional processing. The prefrontal cortex (PFC) and cingulate cortex were chosen based on their involvement in the cognitive processing. Motor cortex was chosen

because we had observed a trend towards development of subtle motor deficits in our 3WKPD rats.

For each seed, the correlation coefficient values for corresponding pixels were compared between groups using student's t-test with $p<0.005$ (corrected for false discovery rate of 0.05 for all the pixels that lie within the brain) and ttest maps were generated. The pixels that significantly changed between controls and 3WKPD groups were averaged to plot the connectivity values. The values for the same pixels were also averaged in the NaBu treatment group to see if NaBu was able to compensate for the changes in connectivity.

Significance levels for between group comparisons were calculated based on the number of voxels within the brain that were compared between the groups, by controlling for a false discovery rate of 0.05,

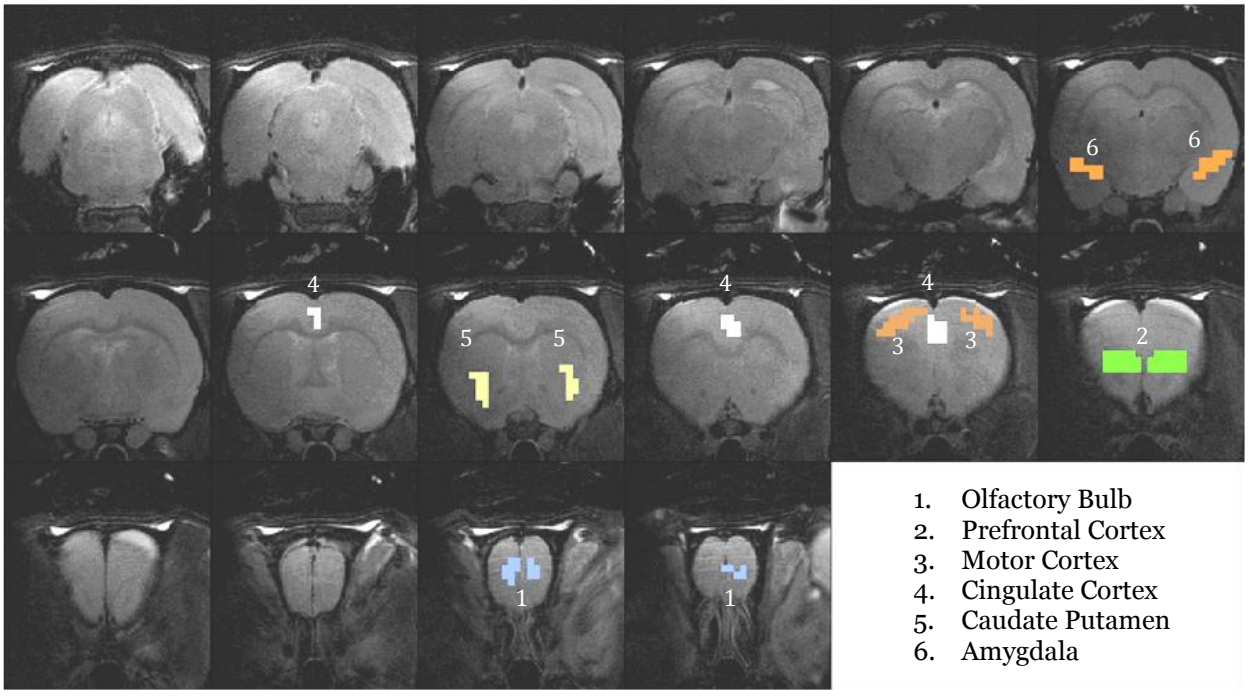

Figure 52: ROIs chosen for seed based connectivity

using Matlab. The significance levels used to compare the groups, based on seed regions were: Amygdala ($p< 0.0049$), CPu ($p< 0.0039$), motor cortex ($p < 0.0047$), PFC ($p < 0.0028$) cingulate cortex ($p < 0.0050$), and olfactory Bulb ($p < 0.0032$).

Results

Significant changes were observed in the RS connectivity of the various seeds tested during the analysis. Two seeds that exhibited major differences between the PD and the control groups were the motor cortex and the amygdala. The positive correlation between motor cortex (Figure 55, Figure 59C) and the majority of the brain had a significant increase in the PD rats as compared to controls. The amygdala in controls had significant negative correlation with PFCs, cingulate, motor and somatosensory cortices, as well as, CPu and thalamus. The amygdala in PD rats lost this negative correlation and had a weak positive correlation with those areas (Figure 58, Figure 60C).

However, the other seed regions had altered connectivity patterns as well. Following is the list of several of the altered connectivities. For example, the olfactory bulb seed (Figure 53,Figure 59A) in the 3WKPD rats had a drop in positive correlation with the thalamus. The OFB's correlation with the amygdala had changed from negative in controls to positive in PD rats. The OFB and lateral PFC (prefrontal cortex) also had significant increase in correlation between them in the PD rats compared to the controls. Along with the increase in the connectivity with the OFB, the PFC in PD rats (Figure 54, Figure 59B) had a drop in positive correlation with the Thalamus compared to controls. The negative

correlation between PFC and amygdala, as observed in controls, was also changed to positive correlation in PD. The cingulate cortex in PD rats had significantly lower positive correlation with the hippocampus and the thalamus, while its correlation with lateral PFC and hypothalamus increased as compared to controls (Figure 56, Figure 60A). The negative correlation between amygdala and cingulate cortex had also changed to positive correlation in PD rats. The CPu (Caudate Putamen) correlation with the PFC, cingulate cortex, and hypothalamus was higher in the PD rats compared to the controls (Figure 57, Figure 60B).

The NaBu treatment was successful in restoring some of the correlation changes observed in PD rats back to their control levels. Of particular notice were the motor and somatosensory cortices. However, any loss in the negative correlation in PD, as seen with the Amygdala and olfactory bulb, was not corrected by NaBu.

Discussion

Seed based RS connectivity, is thought to be a measure of functional connectivity of that seed region with the rest of the brain. However, the echo-planner imaging technique, used to collect the RS fMRI scans during this study, can suffer from image distortions (Buxton, 2002; McRobbie et al., 2003). Thus, an anatomical atlas based seed can, to some extent, have effects of surrounding regions in its final connectivity map. We based our seeds on localized voxels with high z-score ICA components within various regions of interests (ROIs) (Roy et al., 2009). Even though, the seeds only covered a part of the ROI that they belonged to, the final connectivity map had a good representation of the entire ROI. This

indicated that, this technique might indeed be a better technique of seed selection than pure anatomical map based seeds.

The control rats in this study exhibited specific connectivity patterns based on seeds similar to those reported previously by our lab (Zhang et al., 2010). Observations in the 3WKPD rats supported our hypothesis that, the 6-OHDA lesions would alter the RS connectivity.

One of the prominent changes observed in this study is the increased overall connectivity of the motor cortex. Connectivity studies in human PD patients have shown increased connectivity of the supplementary motor cortices (Gatev et al., 2006; Wu et al., 2010). Similarly, we also observed an increase in CPu connectivity with prefrontal cortices, cingulate cortex, and hypothalamus in the 3WKPD rats compared to the controls. These are in accordance with the observations by Kwak et al., who observed a significant increase in striatal connectivity with medial, inferior and orbital frontal gyruses, as well as, anterior cingulate cortex in unmedicated early-stage PD patients as compared to age matched controls (Kwak et al., 2010). The same study also reported a reduction in this hyper-connectivity with L-DOPA treatment known to increase dopamine levels in brain. Basal ganglia activity is modulated by dopamine, and reduction in dopamine levels result in oscillatory firing of neurons in the basal ganglia–thalamocortical circuitry, leading to increased synchronization between those regions (Gatev et al., 2006). Gatev has also hypothesized that the tremors observed in PD might be linked to this increase in basal ganglia oscillations and neuronal synchrony (Gatev et al., 2006). This is interesting because, even though

our 3WKPD rats did not exhibit any significant motor deficits, they exhibited a trend towards development of shuffling gait as observed in PD patients, and the rats at 4 week post 6-OHDA lesions, indeed exhibited gait similar to PD. Hence, our observations of increased CPu and motor cortex connectivity might be indicative of eminent onset of motor deficits.

Another major difference observed between the control and the PD group, was the loss of negative correlation between the amygdala and CPu, motor cortex, PFC, cingulate cortex and olfactory bulb in the PD group. Significant negative correlation has been reported between the baso-lateral amygdala and prefrontal cortex in healthy subjects (Roy et al., 2009). These regions are thought to be important in response expression and in facilitation of attention to salient stimuli (Roy et al., 2009). Negative correlations involving the amygdala have been shown to be disrupted, and even reversed, in addiction and are thought to be linked with loss of impulse control (Xie et al., 2011). We had hypothesized changes in cortico-amygdala connectivity due to dopamine depletion, as a probable cause for the aversion changes observed in Chapter 5. The results of this study suggest that, changes in cortico-amygdala connectivity might indeed be the causality of aversion deficits.

NaBu treatment was able to improve some of the lost positive correlations with respect to motor and sensory motor cortices. However, in was ineffective in mending the changes in negative correlations. Hence, a more extensive seed based or partial correlation analysis of the

data with a higher number of regions of interest might be able to delineate the pathway of NaBu treatment effect.

Conclusion

We observed significant changes in the brain network as a result of dopamine lesions. The observations of loss of negative correlations of amygdala and increased basal-ganglia striatal connectivity are accordance with the observations in addicts and various disease stated including PD. More extensive analysis is needed to predict how NaBu is effective in mitigating cognitive deficits.

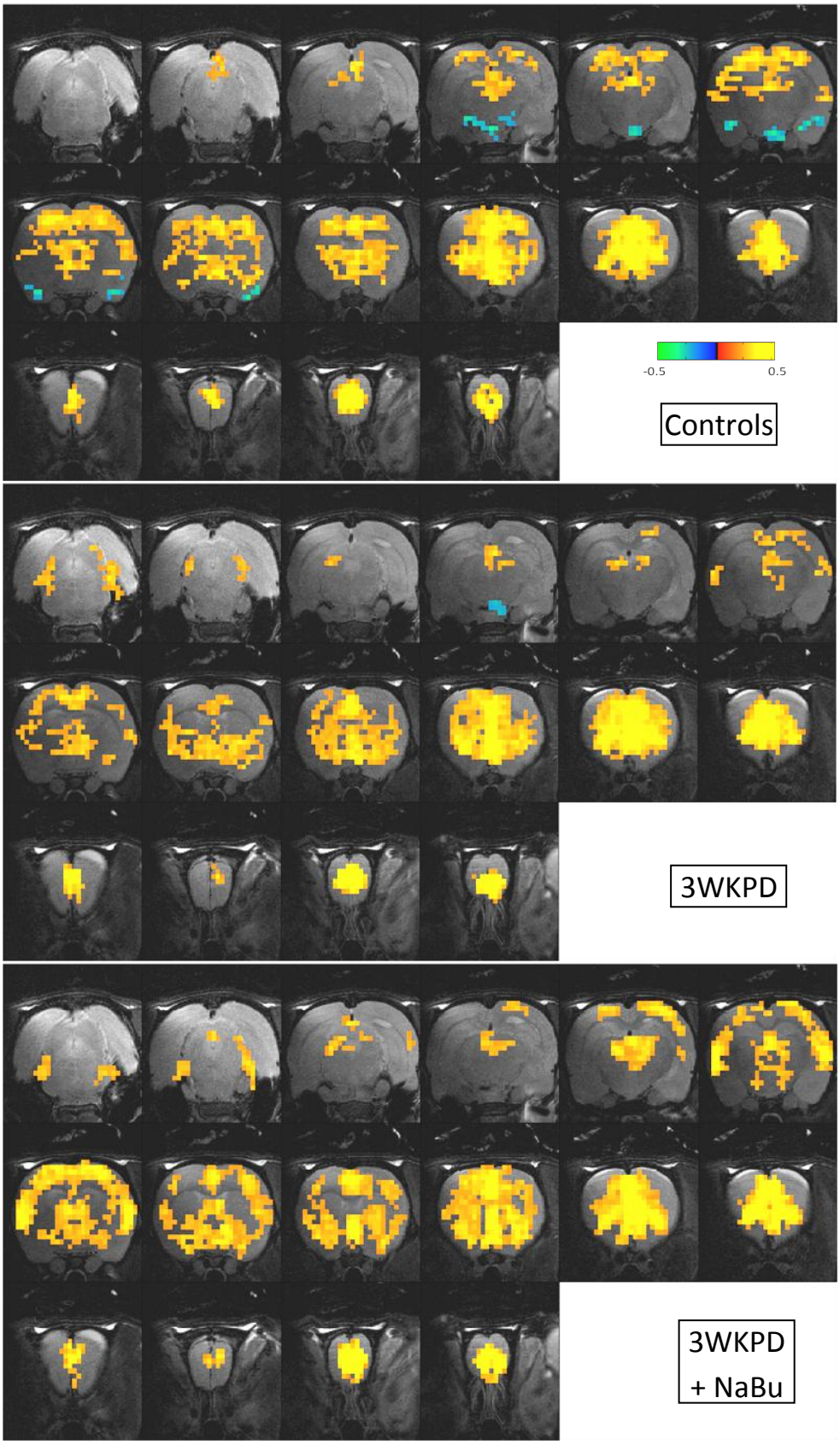

Figure 53: Olfactory Bulb connectivity

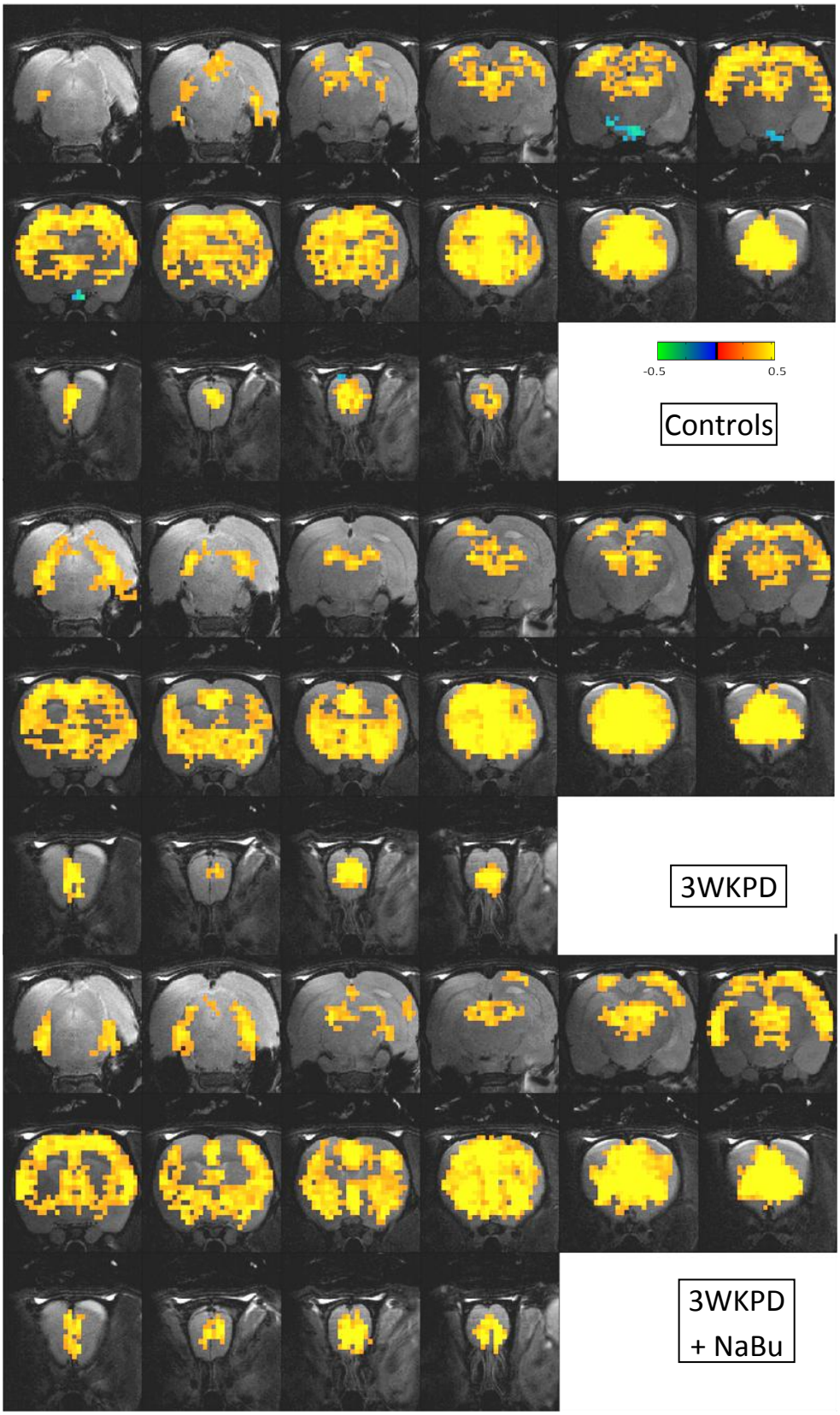

Figure 54: Prefrontal Cortex connectivity

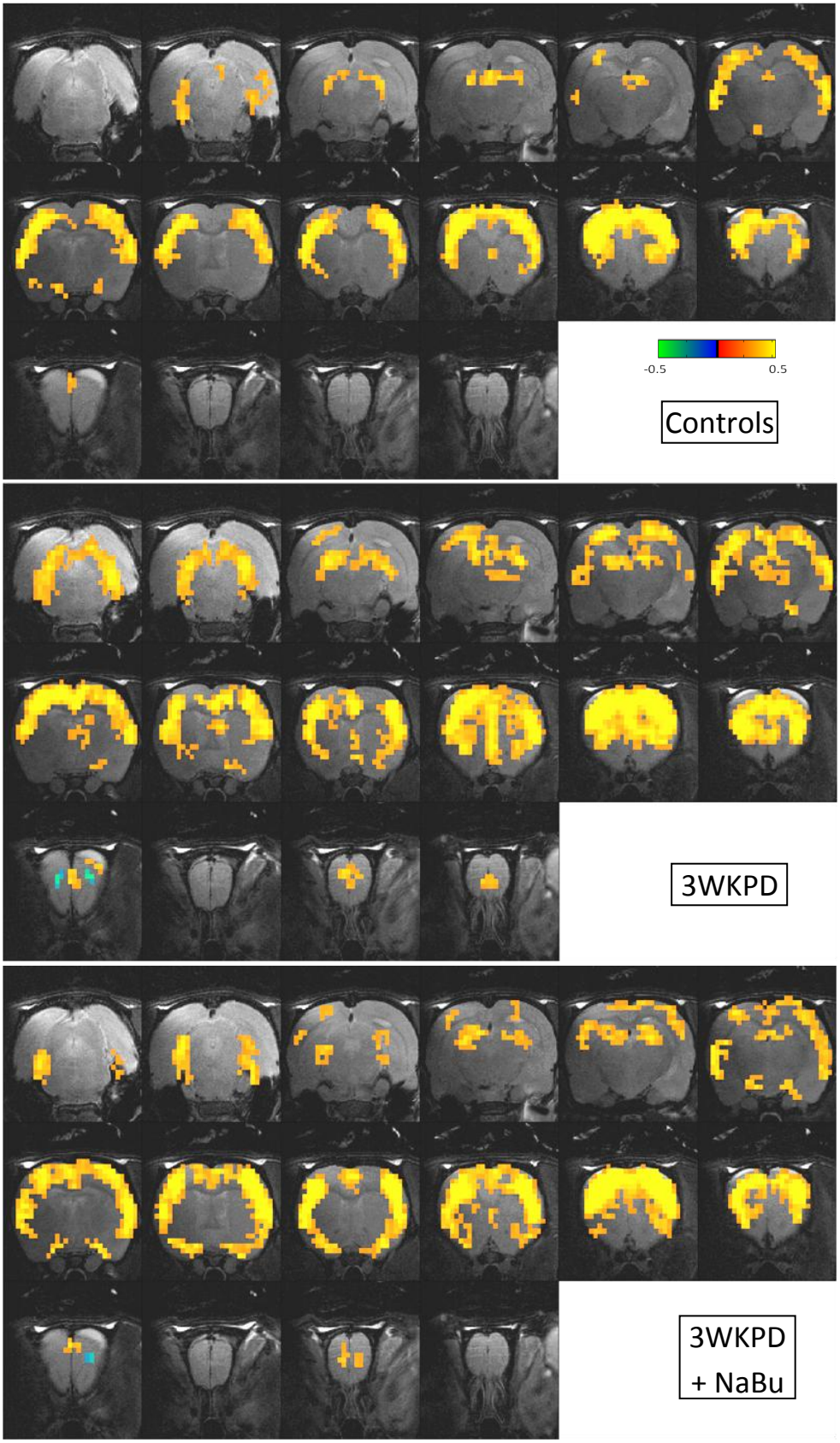

Figure 55: Motor Cortex connectivity

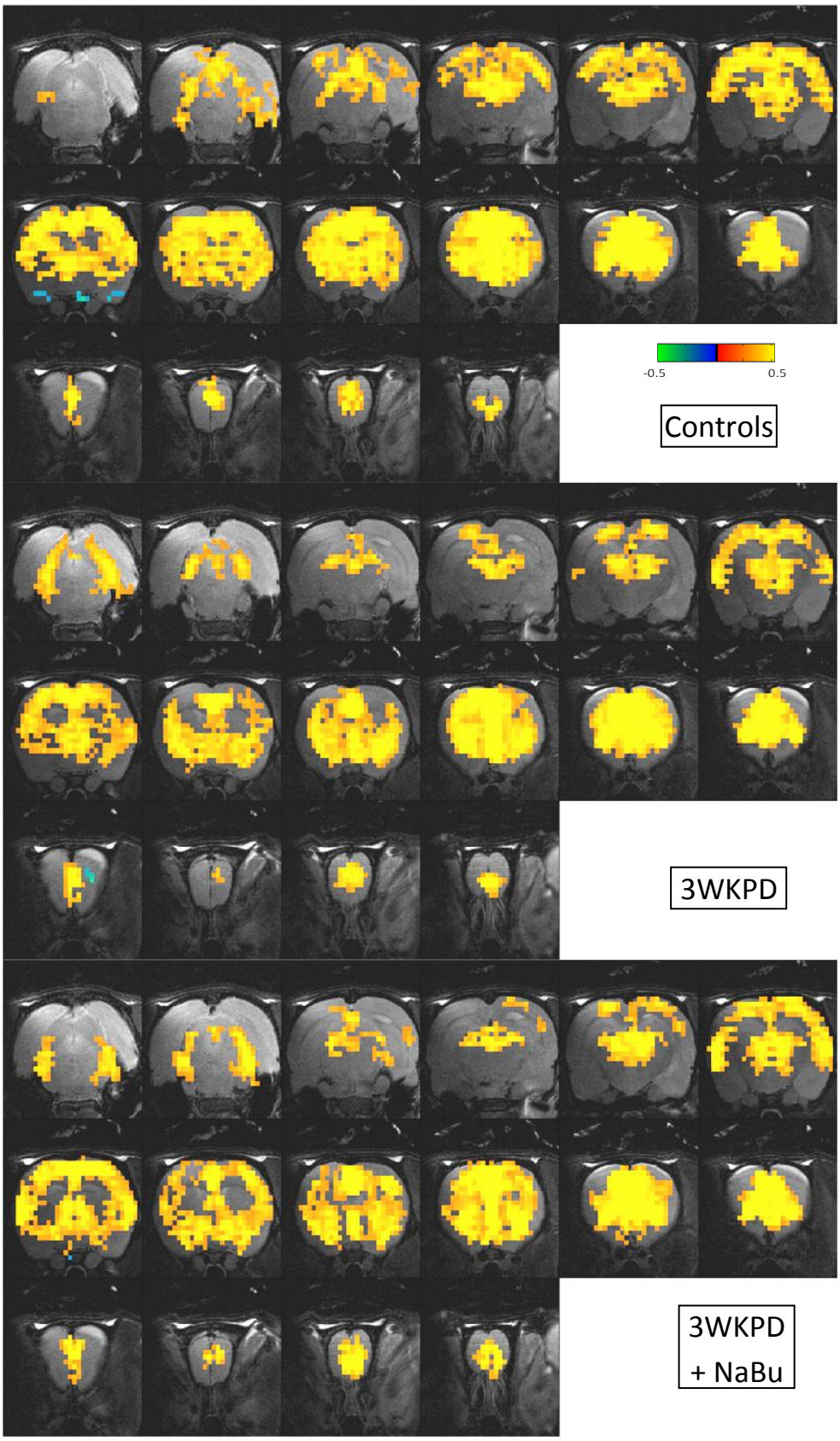

Figure 56: Cingulate Cortex connectivity

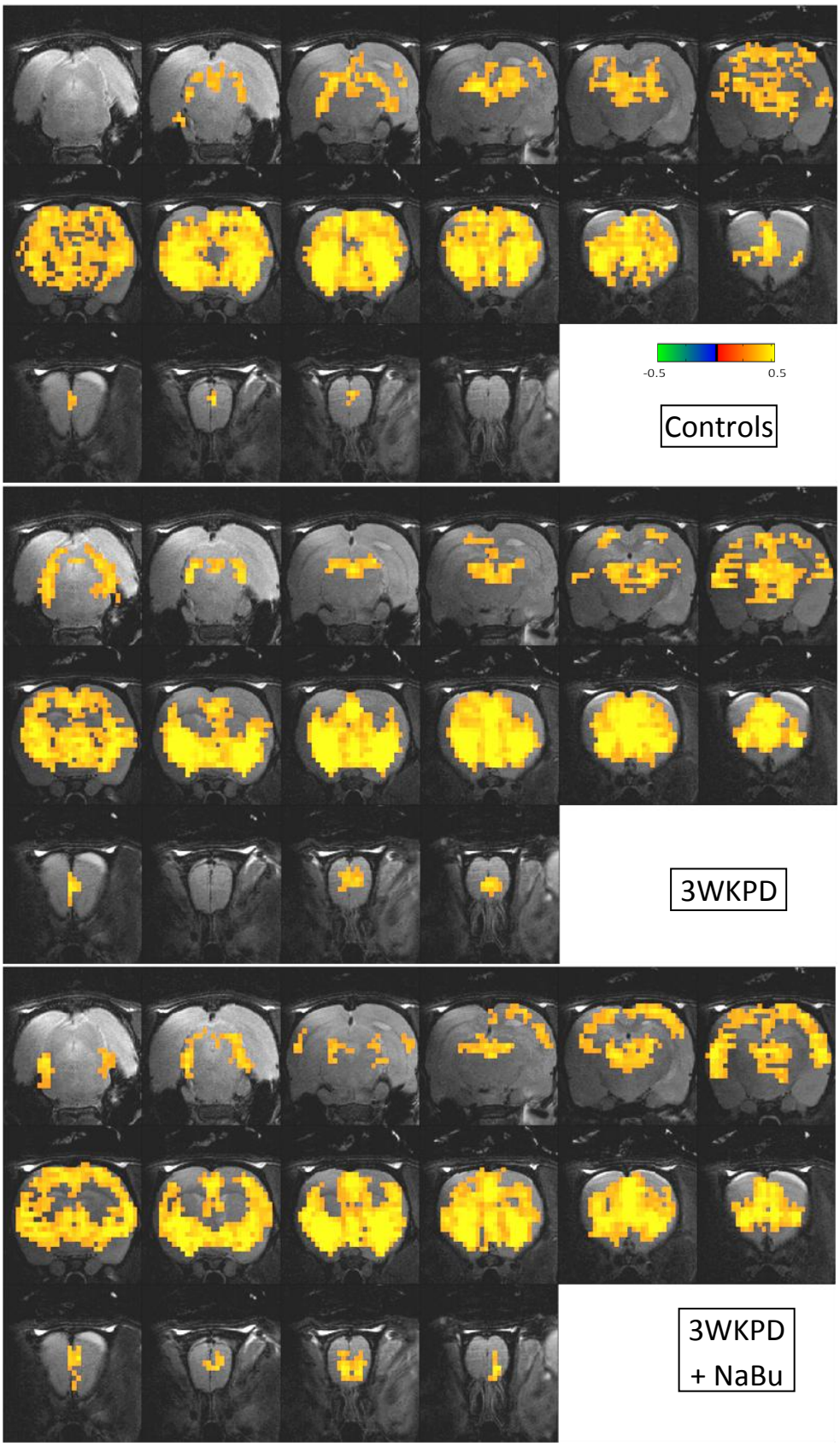

Figure 57: Caudate Putamen connectivity

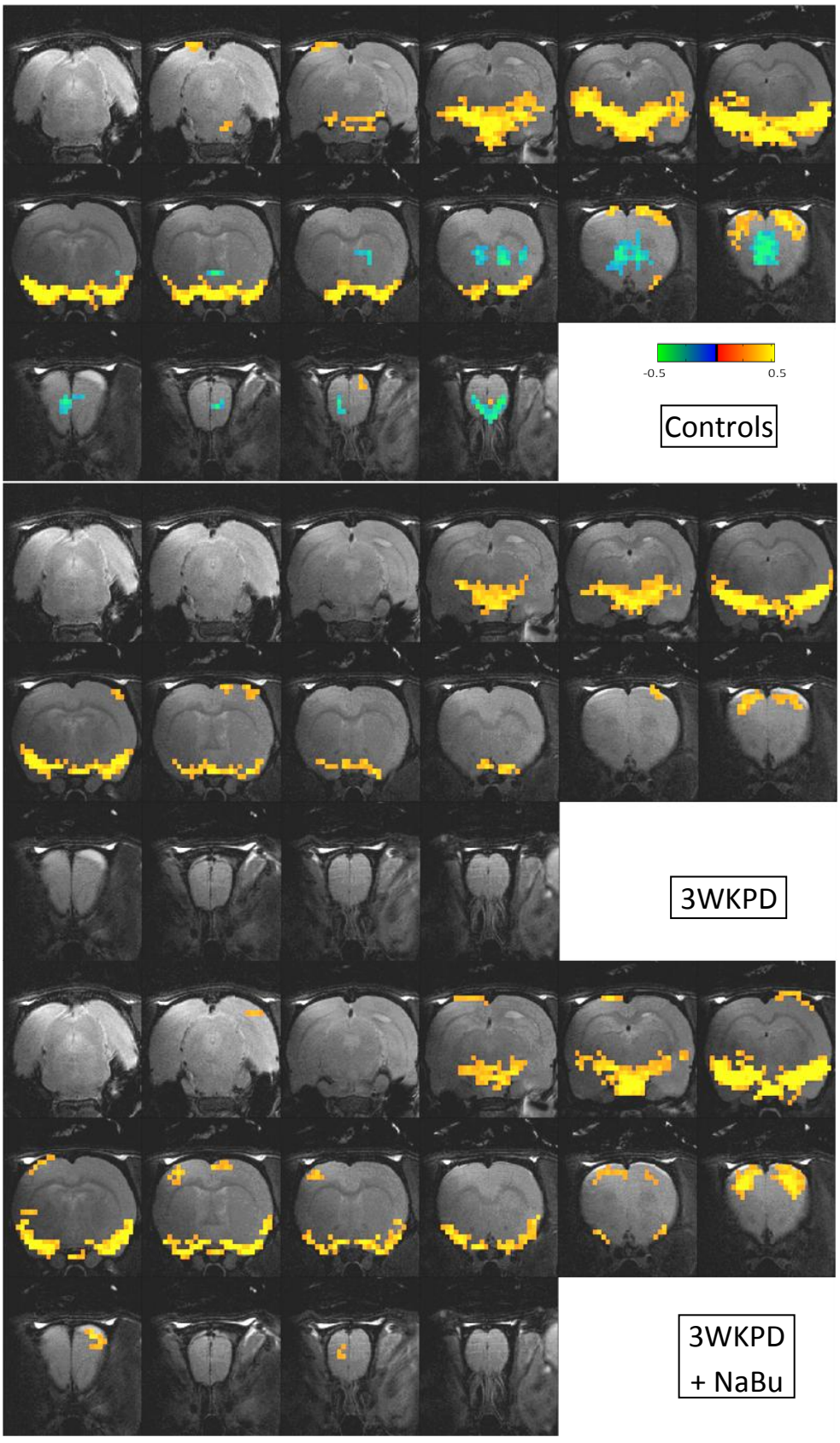

Figure 58: Amygdala connectivity

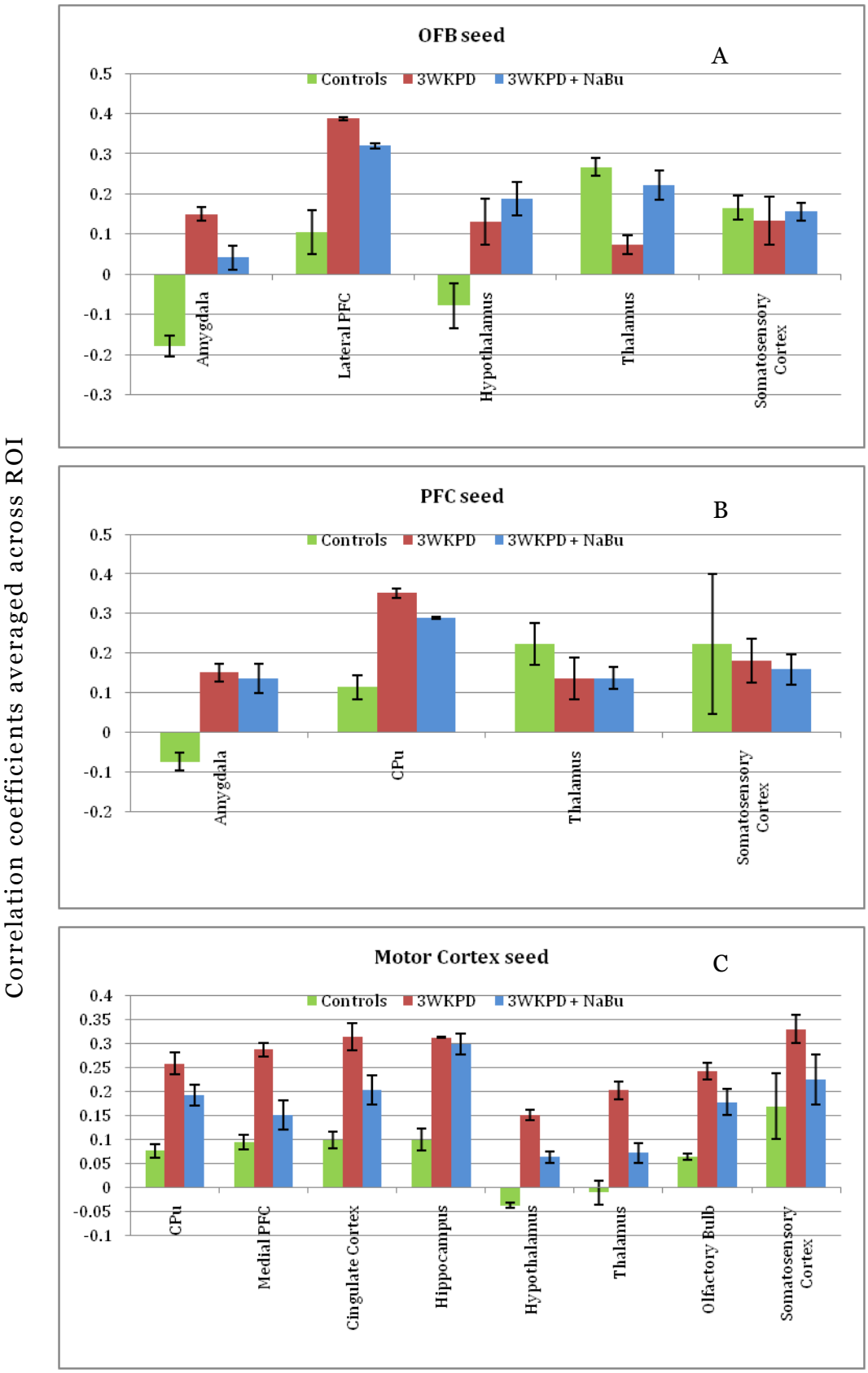

Figure 59: Between group resting state correlation comparisons

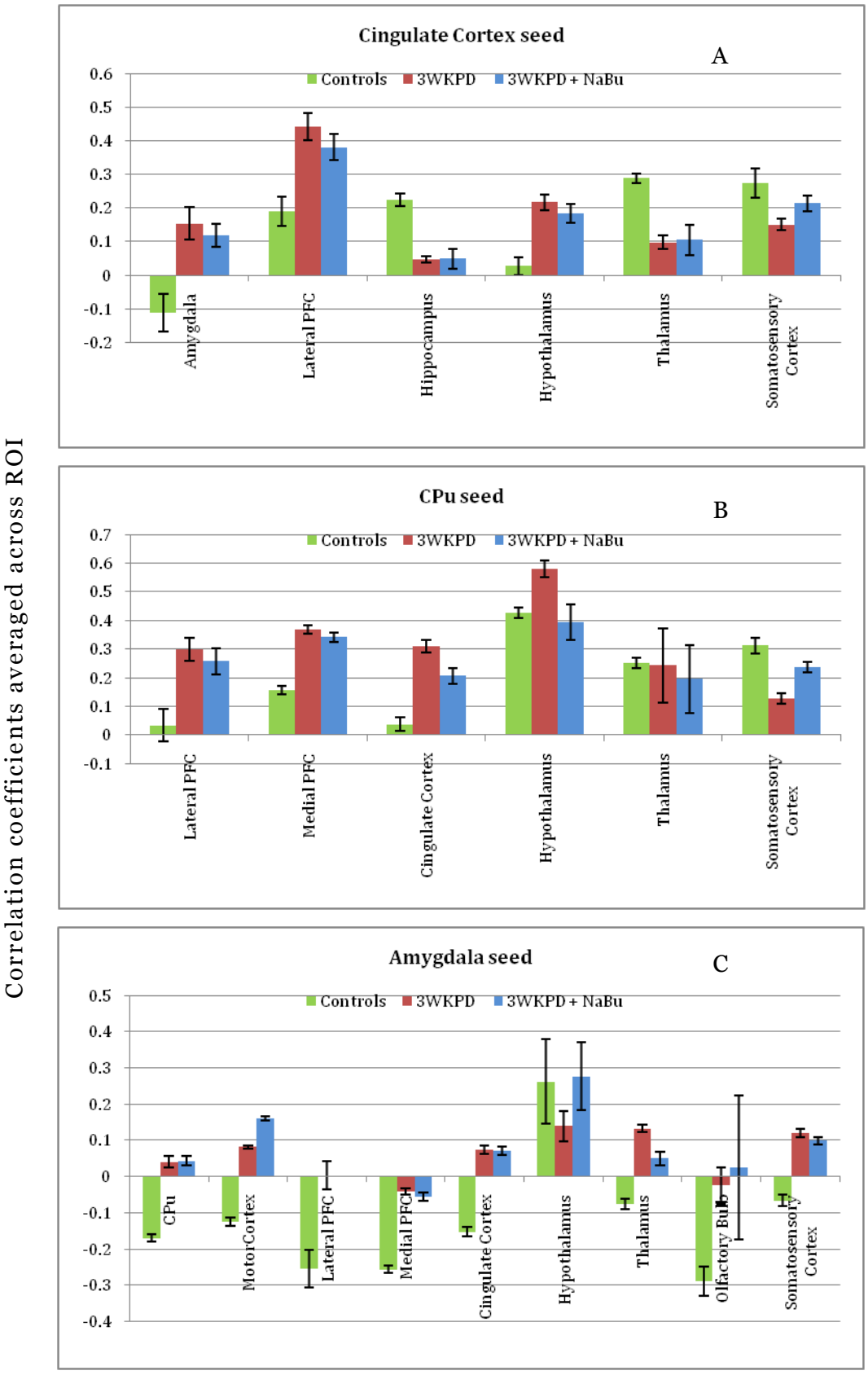

Figure 60: Between group resting state correlation comparisons

Chapter 8. Comprehensive summary

Parkinson's disease (PD) is a chronic, progressive, neurodegenerative disorder, with no known exact causes and no known cure. Predominantly thought of as a motor disorder of the elderly, PD has also been known to have young and juvenile onsets starting by as early as 20 years of age. With 1 million patients and $10.8 billion annual cost in the US alone, PD is the second most common neurodegenerative disorder (Chen, 2010; Parkinson'sDiseaseFoundation, Accessed 2011). Most of the PD cases are thought to be idiopathic, but a combination of genetic mutations and exposure to environmental toxins are implicated in increasing an individual's risk factor to this disease. Ever since it was first identified by Dr. James Parkinson's in the 1817 as 'shaking palsy', PD is still clinically diagnosed based on presence of motor symptoms. PD has a significant impact on quality of life of the patients, as well as, the caregivers and family members.

PD is predominantly thought of as a movement disorder. However, a variety of co-morbid non-motor symptoms are also reported in the PD patients including but not limited to depression, memory and executive function deficits, changes in sense of smell, deficits in recognition of various emotions and sleep disturbances. At the time of diagnosis, the PD pathology has shown to have irreversibly damaged the substantia nigra neurons by as much as 50% and reduced the striatal dopamine by as much as 80%. In fact, the predicted pre-diagnosis phase is thought to date back 5-20 years (Gaig and Tolosa, 2009; Hawkes et al., 2010). In the years prior to the onset of motor symptoms and clinical diagnosis, patients

report a gamut of subtle non-motor deficits, which if quantified correctly, might provide us with the markers for early detection. However, the problem is that these early signs are only apparent when the clinical diagnosis is made.

There were two overall goals of this study. First goal was to develop a rat model of PD that would successfully mimic the pre-clinical (or pre-motor) stages of PD along with delayed onset of motor deficits. The second goal was to characterize this model with behavioral and imaging experiment in order to develop pre-clinical markers for early detection of PD. Such a model would also facilitate the development and testing of potential treatment strategies for the non-motor PD symptoms.

Less than 20% of the PD cases are known to be linked to genetic mutations; and environmental toxins are thought to play a major role in the PD pathology (Caudle and Zhang, 2009; Tanner, 2010). Therefore, the primary focus of this research was on environmental approaches to PD symptoms and the neuropathology, as manifested in animal models exposed to the neurotoxin 6-hydroxy dopamine (6-OHDA). This neurotoxin is a dopamine analog, sharing some structural similarities with dopamine. It is easily taken up by dopamine transporters and known to cause oxidative stress, mitochondrial damage and neuro-inflamation (Na et al., 2010; Schober, 2004). These effects are very similar to the PD etiology in that similar observation have been made in postmortem studies in PD patients (Gaig and Tolosa, 2009). When injected into the striatum, 6-OHDA causes local reduction of dopamine content in the striatum and retrograde degeneration of dopamine cells in the SN

(Blandini et al., 2007; Fleming et al., 2005; Yuan et al., 2005). These lesions are progressive in nature and result in lower levels of dopamine cell loss over a period of several weeks post the insult (Sauer and Oertel, 1994). This facilitates the testing of potentially neuroprotective treatments in a time dependent manner, which is especially relevant to clinical treatment regimens (Lindholm et al., 2007). Double and bilateral lesions of the striatum with 6-OHDA have shown to produce long lasting dopamine loss without compensatory effects weeks after the infusion(Ben et al., 1999). Our 6-OHDA lesioning protocol included 2-step bilateral lesions of the striatum, where the rats received 10ug of 6-OHDA in 1ul of vehicle on day 1 and received 2ug of 6-OHDA on day 3. The dopamine loss in CPu and dopamine cell depletion in SN of the 6-OHDA lesioned rats, at 3 weeks post lesion, was determined to be 27% and 23%, respectively. This depletion was lower than the reports of 80% striatal loss of dopamine and 50% dopamine cell loss in the SN in PD patients at the time of onset of motor symptoms. The 6-OHDA lesioned rats, at 3 weeks post lesion time-point, neither exhibited any motor deficits in spontaneous locomotion, nor did they have any balance deficits in the elevated beam walk test as compared to controls. The 3WKPD rats, also did not exhibit any changes in gait, during the extensive gait analysis using DigiGait system. However, PD-like gait was observed at 4 weeks post 6-OHDA lesions, and a trend towards development of similar deficits was noted at week 3.

Among the reported non-motor deficits in PD, we tested our rat model for changes in aversion and changes in executive function. The aversion behavior studies showed that, there was significantly lower arousal to the

aversive BA odor in the 3WKPD group, compared to the sham and control groups. Sham lesioned and control rats also exhibited equivalent avoidance of the aversive butyric acid smell as exhibited by lower time spent in the area with the BA odor in the avoidance behavior test. However, the 3WKPD rats did not exhibit a similar avoidance. Increased time spent with the aversive odor by the 3WKPD group implied a diminished avoidance compared to the sham group. These results are in agreement with observations noted in early stages of human PD, where PD patients exposed to aversive pictures exhibit blunted reactivity and report less arousal as compared to controls, despite recognizing the negative/aversive nature of those pictures (Bowers et al., 2006; Sprengelmeyer et al., 2003).

One of the possible explanations of lower grooming and lower avoidance was that, the PD rats failed to smell the aversive odor as olfactory deficits are common in pre-motor PD. However, the lack of difference in the exploratory behavior between the groups in the arousal and avoidance behavior tests, along with equivalent BOLD activation of the olfactory system in the fMRI study, did not support that premise. Furthermore, it is important to note that hyposmia in the pre-motor phase of the PD in human studies has been reported as a selective deficit, which depends on the odor and concentration being tested, and not a uniform loss of olfaction across all the scents (Berendse and Ponsen, 2009; Ponsen et al., 2004).

Another possible consideration to address the behavioral deficits in aversive behavior in the PD rat model was the role of brain regions which

process aversive stimuli including Insular cortex, Nucleus Accumbens and Amygdala complex. Involvement of Insular cortex has been reported during aversion processing in human (Jabbi et al., 2008; Small et al., 2003; Sprengelmeyer et al., 1998), as well as, in rat studies (Desgranges et al., 2009). NAcc neurons are believed to be involved in attaching valance to a stimulus by either selective activation or inhibition of neurons (Carlezon and Thomas, 2009; Roitman et al., 2005; Schoenbaum and Setlow, 2003). We performed BOLD fMRI experiments on our rats in awake state during exposures to the same aversive smell. Our results did not indicate any differences in the insular cortex activation between groups, which might have been a contributing factor to the observed deficits in the behavioral responses. This result is in accordance with the disease stage-dependent hypoperfusion of insular cortex observed in human PD patients where there is no significant difference between the controls and early PD patients. (Kikuchi et al., 2001) We also observed equivalent positive BOLD activation in NAcc in controls, shams and 3WKPD rats, without any significant group effect in neuronal activation. However, the amygdala region, which is known to process emotions and generate the response cascade to stressful/aversive stimuli, had an overall lower positive BOLD activation in PD. When selective nuclei in the amygdala, medial (MNA), basal (BNA), lateral (LNA) and central (CNA) nuclei, were examined individually, significantly lower BOLD activation was observed in the BNA, LNA and CNA of PD rats compared to both sham lesioned and control rats. The amygdala complex comprises of a multi-level system that orchestrates both sensory input and output. In regards to olfaction, the MNA is thought to receive inputs from accessory

olfactory bulb (Davern and Head, 2011); inhibition of baso-lateral amygdala has been shown to result in impairment of conditioned olfactory aversion (Desgranges et al., 2008); and CNA thought to mediate behavioral response to aversive stimuli (Finn et al., 2003). Given the results of our studies, we speculate that the MNA, which serves as the input to the amygdala complex, was functional in the PD rats while the BNA, LNA and CNA, which orchestrate the response, were negatively impacted. Hence, it appeared that the behavioral deficit, exhibited by PD rats in our study, might have been a result of a deficit in appropriate response generation due to a possible cortico-amygdalar dysfunction, and not due to an inability to process the aversive stimulus. Our results are in accordance with those by Bower's and colleagues who have also reported blunted aversive reactivity among PD patients that was attributed to amygdalar dysfunction as a result of suppression of the amygdala by the cortical regions (Bowers et al., 2006). Since the sham lesioned animals did not exhibit any arousal or avoidance deficits as compared to the control animals in the behavioral tests, as well as, in the functional MRI experiment; we conclude that the observed deficits in the 6-OHDA administrated rats were not a result of the stress of the surgery but of actual dopamine depletion.

Executive functioning was tested in our rat model using a rat analog of the Wisconsin card sorting test used to test attentional set shifting in humans. The test in rats is called the ED/ID test, and comprises of four tasks designed to test various aspects of executive function including attention, rule acquisition, cognitive flexibility, error correction and trouble shooting. The overall performance of the rats during the four

tasks involved in the ED/ID test was similar to the previous observations of progressively increasing difficulty levels while moving from SD to CD to ID to ED tasks. The control and the sham rats required a higher number of trials for completion of ID and ED tasks as compared to the first two tasks, though the difference was not significant for ID in controls. The 3WKPD rats also had similar performance, but needed significantly more trials in the ED task as compared to ID task. Their performance in the first 3 tasks was comparable to the performance by the control and the sham groups, implying a similar reward association, rule-learning and attentional-set formation in the three groups. But the 3WKPD group was significantly less efficient in the ED task, indicating a set-shifting specific deficit. These results were in accordance with previous observations in PD patients where set-shifting specific deficits have been reported (Cools et al., 2003; Owen et al., 1992; Schneider, 2006). The cognitive inflexibility, as depicted by a deficit in the ED task, can be the result of two phenomena, deficits in revising the relevance of 'initially relevant dimension', and/or enhanced learnt irrelevance towards 'initially irrelevant dimension', leading to an inability to attend to the dimension previously learnt as irrelevant. Our study had the complete-learnt irrelevance design in terms of the ED. Hence, our rats did exhibit deficits in revising learnt irrelevance based on negative feedback they received after incorrect trials. Our results were in agreement with those by Owen's group reporting more pronounced ED deficit in PD patients in the case of shifting attention to a dimension previously learnt as irrelevant, hence enhanced learnt irrelevance being the contributing factor to the deficit (Slabosz et al., 2006). The observed ED deficit in

3WKPD rats, might be a result of an inability to learn new rules due to lowered dopamine levels disrupting PFC-striatal connectivity. This connectivity is hypothesized to be important for set shifting and is impacted in PD patients (Monchi et al., 2004). Dopamine depletion has been shown to cause disruption of PFC-striatal connectivity, as well as, ED deficits in healthy controls (Nagano-Saito et al., 2008). Indeed, lack of similar deficits in sham lesioned rats, support the hypothesis of dopamine depletion as a probable cause; thus, eliminating the potential impact of stress of the lesioning process as a probable cause for the ED deficit.

While shifting from CD to ID task, both the 3WKPD and sham lesioned groups needed significantly higher number of trials, as compared to their own performance in the CD task. A similar significance was missing in the control group. Even though the ID performance was not significantly different between the groups, the within group comparisons suggest a weaker attentional-set formation in the sham and the 3WKPD groups due to the surgical procedure and irrespective of the dopamine depletion. Cingulate cortex lesions have shown to result in ID deficits in rats (Ng et al., 2007) without any ED deficits. To our knowledge, our rats did not have cingulate cortex lesions. This was also supported by the fact that, the deficits we observed were not in comparison with the controls, as those observed by the Ng group, but were in comparison to the groups' own performances in the previous tasks. Additional research is needed to further analyze this observation of diminished attentional-set in our study.

The performance of the 3WKPD+NaBu group in the ED task had significant improvement over the performance of the 3WKPD group, and was comparable to the performance by the control group. Hence, NaBu appeared to be effective in alleviating the deleterious effects of 6-OHDA. In addition, the 3WKPD+NaBu rats, as they performed SD, CD and ID tasks, were able to focus increasing amount of attention on the IRD and completely ignore IID. Hence, the NaBu treatment might have additional cognitive enhancing effects over 3WKPD group, as reflected by significant group by task interaction. Additional experimentation is needed to confirm this hypothesis, but was outside the scope of this thesis. However, results of this study pointed towards HDACis as a promising treatment option for cognitive deficits in PD.

Seed based RS connectivity, was performed in our rats with seeds based on localized voxels with high z-score ICA components within various regions of interests (ROIs) (Roy et al., 2009). Even though, the seeds only covered a part of the ROI that they belonged to, the final connectivity map had a good representation of the entire ROI. We contend that, this technique might indeed be a better technique of seed selection than pure anatomical map based seeds. The control rats in this study exhibited specific connectivity patterns based on seeds similar to those reported previously by our lab (Zhang et al., 2010). We also observed significant RS connectivity alterations in the 3WKPD group.

One of the prominent changes observed in this study was the increased overall connectivity of the motor cortex, which was in accordance with the increased motor cortex connectivity observations in human PD

patients (Gatev et al., 2006; Wu et al., 2010). Similarly, we also observed an increase in CPu connectivity with prefrontal cortices, cingulate cortex, and hypothalamus in the 3WKPD rats compared to the controls. Kwak and group report a significant increase in striatal connectivity with medial, inferior and orbital frontal gyruses, as well as, anterior cingulate cortex in unmedicated early-stage PD patients as compared to age matched controls (Kwak et al., 2010). Hence, our results parallel observations in human PD. The same study by Kwak group, also reported a reduction in this hyper-connectivity with L-DOPA treatment. L-dopa is known to increase dopamine levels in brain. Basal ganglia activity is modulated by dopamine, and reduction in dopamine levels result in oscillatory firing of neurons in the basal ganglia – thalamocortical circuitry, leading to increased synchronization between those regions (Gatev et al., 2006). Gatev has also hypothesized that the tremors observed in PD might be linked to this increase in basal ganglia oscillations and neuronal synchrony (Gatev et al., 2006). This is interesting because, even though our 3WKPD rats did not exhibit any significant motor deficits, they exhibited a trend towards development of shuffling gait as observed in PD patients, and the rats at 4 week post 6-OHDA lesions, indeed exhibited gait similar to PD. Hence, our observations of increased CPu and Motor cortex connectivity might be indicative of oncoming onset of motor deficits.

Another major difference observed between the control and the PD group, was the loss of negative correlation between the amygdala and CPu, motor cortex, PFC, cingulate cortex and olfactory bulb in the PD group. Significant negative correlation has been reported between the

baso-lateral amygdala and prefrontal cortex in healthy subjects (Roy et al., 2009). These regions are thought to be important in response generation and in facilitation of attention to salient stimuli (Roy et al., 2009). Negative correlations involving the amygdala have been shown to be disrupted, and even reversed, in addiction and are thought to be linked with loss of impulse control (Xie et al., 2011). We had hypothesized changes in cortico-amygdala connectivity due to dopamine depletion, as a probable cause for the aversion changes observed in Chapter 5. The results of this study suggest that, changes in cortico-amygdala connectivity might indeed sub-serve the aversion deficits.

Based on the extended PD stages proposed by Braak group (Hawkes et al., 2010), PD patients at the late Braak stage 2 or at beginning of Braak stage 3, do not have any significant motor symptoms, but thought to have the SN pathology and striatal dopamine depletion. In addition, amygdalar pathology is also thought to start at these stages. Hence, we contend that this model might in fact be mimicking the symptomology of early Braak stage 3 or late Braak stage 2 PD, and the cognitive and aversion deficits observed, might indeed be present in these stages.

We have also shown that NaBu treatment was effective in treating extra-dimensional set shifting cognitive deficits. NaBu was also able to improve upon some of the lost positive correlations with respect to motor and sensory motor cortices which might underlie the motor deficits in PD. Given that the drugs from HDACi family of drugs are well-tolerated by humans (Hoshino and Matsubara, 2010; Liu et al., 2006), this treatment shows high translational validity.

Our RS connectivity study failed to delineate how NaBu was able to improve cognitive deficits. A more extensive seed based or partial correlation analysis of the data with a higher number of regions of interest might be able to delineate the pathway of NaBu treatment effect.

Global impact

Pre-clinical markers, if developed, can lead to the early diagnosis of PD in individuals predisposed to this disease due to genealogy or proximity to toxic environments. Early detection can enable us to devise strategies to prevent further damage.

- Findings of this research suggest that our model of pre-motor stage PD is a very high face validity rat model of late Braak stage 2 or early Braak stage 3 PD. These are the pre-motor stages of PD and hence, can be used for further research into non-motor symptoms of PD.
- PD patients, with as much as 80% dopamine depletion in the striatum, are still not clinically diagnosed because they do not exhibit any motor symptoms. However, we have shown that a combination of reduced aversion, extra-dimensional set shifting deficit, increased RS motor cortex and striatal connectivity and lack of negative RS connectivity of the amygdala could be a present in patients with as little as 30% striatal dopamine depletion. Hence, these could be viable biomarkers for early detection of PD.
- Sodium butyrate treatment, tested in the cognitive deficit study, was able to ameliorate the extra-dimensional set shifting deficit observed in this model. This treatment also improved the attentional set

formation. Our results, along with the prior reports of anti-depressant and neuroprotective effects of this drug, point towards a possible treatment strategy for the non-motor deficits of PD, which are not always treated by the current PD medication.

Chapter 9. Future direction

We have successfully demonstrated that our model exhibits some of the non-motor symptoms of Parkinson's disease. Although significant steps have been made with this study, more work needs to be done to reach the final goal of early detection of Parkinson's disease and treating its non-motor symptoms. Outlined below are possible studies that have been identified that will help us move closer to the above mentioned goal.

1. We performed all the studies at three weeks post 6-OHDA infusions, given that it was the pre-motor time-point. Our observations of dopamine depletion, aversive and cognitive deficits, as well as, RS connectivity changes, were all performed at this time-point. Immunohistochemistry studies at 2 week and 4 week time points would give an insight into the progression of these lesions.

2. Addition of brain regions such as olfactory bulb, PFC and medial forebrain bundle would add to the knowledge of spread of the 6-OHDA lesions.

3. Adding similar time-points in the aversion, cognitive and RS connectivity studies, would allow observation of manifestation and progression of the behavioral deficits and co-morbid connectivity changes in the brain.

4. Our aversion study focused on unconditioned olfactory aversion changes. Future studies with aversion in other sensory modalities, such as taste aversion, would help in generalization of this deficit. Also, testing conditioned aversion, might give added insight into the pathology.

5. The cognitive inflexibility, as depicted by deficit in the ED task, can be a result of two phenomena, deficits in revising the relevance of IRD, and enhanced learnt irrelevance towards IID, leading to inability to attend to dimension previously learnt as irrelevant. Our ED/ID study design onely tested for learnt-irrelevance. Hence, additional testing with a completely novel dimension as the relevant dimension during the ED task would be able to delineate the exact cause of the observed ED deficit.

6. Some of the preliminary work we have done is indicative of additional emotional changes in apathy and depression. Depression was tested using forced swim test, where the 3WKPD rats exhibited increased immobility, indicative of depression. Apathy was tested using novel object recognition test and sucrose preference test. Though there was no significant difference between the sucrose consumption by the test groups, we observed significantly lower exploration of the novel object by the 3WKPD group as compared to the control group. This observation points towards possible increased apathy in the 3WKPD rats. We had also tested olfaction, where behavior of the 3WKPD rats points towards selective olfactory deficits. All of these tests would add to the face validity of this model.

7. The RS connectivity changes, observed in our rat model of PD, have also been reported in early PD patients. The human reports also point out that the some of these connectivity changes are mitigated by L-DOPA treatment. Performing RS connectivity and the gait analysis studies with an additional L-DOPA treated group would be useful in determining the predictive validity of this model.

8. Sodium butyrate treatment was not just useful in alleviating the ED deficits observed in our 3WKPD rats, but it also improved the attentional set formation in the treatment group. But the RS connectivity study was unable to delineate the pathway of NaBu treatment effect. Hence, additional behavioral studies testing attention and RS analysis with more seed regions are needed to test the exact effect of NaBu. Adding a NaBu treatment group to immunohistochemistry study will help in determination of whether the treatment was effective in preventing the deleterious effects of 6-OHDA. NaBu has also been proven effective in treating depression and has been thought to have neuro-protective effects. It presents a promising treatment strategy for PD. Additional testing in other deficits would help determine this possibility.

9. We have used functional MRI to look at changes in functional responses of the brain. Adding Magnetic resonance spectroscopy to the list of studies will help detection of changes in brain metabolite as a function of neuronal viability.

References

Abbott RD, Ross GW, White LR, Tanner CM, Masaki KH, Nelson JS, et al. Excessive daytime sleepiness and subsequent development of Parkinson disease. Neurology. 2005; 65: 1442-6.

Abou-Sleiman PM, Muqit MM, Wood NW. Expanding insights of mitochondrial dysfunction in Parkinson's disease. Nat Rev Neurosci. 2006; 7: 207-19.

Abramoff MD, Magelhaes PJ, Ram SJ. Image Processing with ImageJ. Biophotonics International 2004; 11: 36-42.

Adler CH. Nonmotor complications in Parkinson's disease. Mov Disord. 2005; 20: S23-9.

Alexander GE, DeLong MR, Strick PL. Parallel organization of functionally segregated circuits linking basal ganglia and cortex. Annu Rev Neurosci. 1986; 9: 357-81.

Alvarez-Erviti L, Rodriguez-Oroz MC, Cooper JM, Caballero C, Ferrer I, Obeso JA, et al. Chaperone-Mediated Autophagy Markers in Parkinson Disease Brains. Arch Neurol 2010; 67: 1464–1472.

Anand A, Li Y, Wang Y, Wu J, Gao S, Bukhari L, et al. Activity and connectivity of brain mood regulating circuit in depression: a functional magnetic resonance study. Biol Psychiatry. 2005; 57: 1079-88.

Andrews-Hanna JR, Snyder AZ, Vincent JL, Lustig C, Head D, Raichle ME, et al. Disruption of large-scale brain systems in advanced aging. Neuron. 2007; 56: 924-35.

Arabia G, Grossardt BR, Geda YE, Carlin JM, Bower JH, Ahlskog JE, et al. Increased risk of depressive and anxiety disorders in relatives of patients with Parkinson disease. Arch Gen Psychiatry. 2007; 64: 1385-92.

Ariatti A, Benuzzi F, Nichelli P. Recognition of emotions from visual and prosodic cues in Parkinson's disease. Neurol Sci. 2008; 29: 219-27. Epub 2008 Sep 20.

Ascherio A, Chen H, Weisskopf MG, O'Reilly E, McCullough ML, Calle EE, et al. Pesticide exposure and risk for Parkinson's disease. Ann Neurol. 2006; 60: 197-203.

Bandettini PA, Wong EC, Hinks RS, Tikofsky RS, Hyde JS. Time course EPI of human brain function during task activation. Magn Reson Med. 1992; 25: 390-7.

Barbeau A. L-dopa in Parkinsonism. Br Med J. 1969; 2: 202.

Bargmann V, Michel L, Telegdi VL. Precession of the polarization of particles moving in a homogeneous electromagnetic field. Physical Review Letters 1959; 2: 435-436.

Beall PT, Amtey SR, Kasturi SR. NMR data handbook for biomedical applications. 1984.

Bekris LM, Mata IF, Zabetian CP. The genetics of Parkinson disease. Journal of geriatric psychiatry and neurology 2010; 23: 228.

Belliveau JW, Kennedy DN, Jr., McKinstry RC, Buchbinder BR, Weisskoff RM, Cohen MS, et al. Functional mapping of the human visual cortex by magnetic resonance imaging. Science. 1991; 254: 716-9.

Ben V, Blin O, Bruguerolle B. Time-dependent striatal dopamine depletion after injection of 6-hydroxydopamine in the rat. Comparison of single bilateral and double bilateral lesions. J Pharm Pharmacol. 1999; 51: 1405-8.

Berendse HW, Ponsen MM. Diagnosing premotor Parkinson's disease using a two-step approach combining olfactory testing and DAT SPECT imaging. Parkinsonism Relat Disord. 2009; 15: S26-30.

Bhatt MH, Elias MA, Mankodi AK. Acute and reversible parkinsonism due to organophosphate pesticide intoxication. Neurology 1999; 52: 1467.

Birrell JM, Brown VJ. Medial frontal cortex mediates perceptual attentional set shifting in the rat. J Neurosci. 2000; 20: 4320-4.

Biswal B, Yetkin FZ, Haughton VM, Hyde JS. Functional connectivity in the motor cortex of resting human brain using echo-planar MRI. Magn Reson Med. 1995; 34: 537-41.

Biswal BB, Kannurpatti SS. Resting-state functional connectivity in animal models: modulations by exsanguination. Methods Mol Biol. 2009; 489: 255-74.

Biswal BB, Van Kylen J, Hyde JS. Simultaneous assessment of flow and BOLD signals in resting-state functional connectivity maps. NMR Biomed. 1997; 10: 165-70.

Blandini F, Levandis G, Bazzini E, Nappi G, Armentero MT. Time-course of nigrostriatal damage, basal ganglia metabolic changes and behavioural alterations following intrastriatal injection of 6-hydroxydopamine in the rat: new clues from an old model. Eur J Neurosci. 2007; 25: 397-405.

Bove J, Prou D, Perier C, Przedborski S. Toxin-induced models of Parkinson's disease. NeuroRx. 2005; 2: 484-94.

Bowers D, Miller K, Mikos A, Kirsch-Darrow L, Springer U, Fernandez H, et al. Startling facts about emotion in Parkinson's disease: blunted reactivity to aversive stimuli. Brain. 2006; 129: 3356-65. Epub 2006 Nov 8.

Braak H, Braak E. Pathoanatomy of Parkinson's disease. J Neurol. 2000; 247: II3-10.

Braak H, Braak E, Yilmazer D, de Vos RAI, Jansen ENH, Bohl J, et al. Amygdala pathology in Parkinson's disease. Acta neuropathologica 1994; 88: 493-500.

Braak H, Del Tredici K, Rub U, de Vos RA, Jansen Steur EN, Braak E. Staging of brain pathology related to sporadic Parkinson's disease. Neurobiol Aging. 2003; 24: 197-211.

Burn DJ, Mark MH, Playford ED, Maraganore DM, Zimmerman TR, Jr., Duvoisin RC, et al. Parkinson's disease in twins studied with 18F-dopa and positron emission tomography. Neurology. 1992; 42: 1894-900.

Buxton RB. Introduction to functional magnetic resonance imaging: principles and techniques: Cambridge Univ Pr, 2002.

Carlezon WA, Jr., Thomas MJ. Biological substrates of reward and aversion: a nucleus accumbens activity hypothesis. Neuropharmacology. 2009; 56: 122-32. Epub 2008 Jul 15.

Caudle WM, Zhang J. Glutamate, excitotoxicity, and programmed cell death in Parkinson disease. Exp Neurol. 2009; 220: 230-3. Epub 2009 Oct 6.

Chen JJ. Parkinson's disease: health-related quality of life, economic cost, and implications of early treatment. Am J Manag Care 2010; 16: S87-S93.

Cho JW, Jeon BS, Jeong D, Choi YJ, Lee JY, Lee HS, et al. Association between parkinsonism and participation in agriculture in Korea. J Clin Neurol. 2008; 4: 23-8. Epub 2008 Mar 20.

Chuang C-S, Su H-L, Cheng F-C, Hsu S-h, Chuang C-F, Liu C-S. Quantitative evaluation of motor function before and after engraftment of dopaminergic neurons in a rat model of Parkinson's disease. Journal of Biomedical Science 2010; 17: 9.

Clark US, Neargarder S, Cronin-Golomb A. Specific impairments in the recognition of emotional facial expressions in Parkinson's disease. Neuropsychologia. 2008; 46: 2300-9. Epub 2008 Mar 30.

Cools R, Barker RA, Sahakian BJ, Robbins TW. Mechanisms of cognitive set flexibility in Parkinson's disease. Brain. 2001; 124: 2503-12.

Cools R, Barker RA, Sahakian BJ, Robbins TW. L-Dopa medication remediates cognitive inflexibility, but increases impulsivity in patients with Parkinson's disease. Neuropsychologia. 2003; 41: 1431-41.

Cordes D, Haughton VM, Arfanakis K, Carew JD, Turski PA, Moritz CH, et al. Frequencies contributing to functional connectivity in the cerebral cortex in" resting-state" data. American Journal of Neuroradiology 2001; 22: 1326.

Cotzias GC. L-Dopa for Parkinsonism. N Engl J Med. 1968; 278: 630.

Davern PJ, Head GA. Role of the medial amygdala in mediating responses to aversive stimuli leading to hypertension. Clin Exp Pharmacol Physiol 2011; 38: 136-43.

De Martino B, Camerer CF, Adolphs R. Amygdala damage eliminates monetary loss aversion. Proc 2010; 107: 3788-92.

Denmark A, Tien D, Wong K, Chung A, Cachat J, Goodspeed J, et al. The effects of chronic social defeat stress on mouse self-grooming behavior and its patterning. Behav 2010; 208: 553-9.

Desgranges B, Levy F, Ferreira G. Anisomycin infusion in amygdala impairs consolidation of odor aversion memory. Brain Res. 2008; 1236: 166-75. Epub 2008 Aug 12.

Desgranges B, Sevelinges Y, Bonnefond M, Levy F, Ravel N, Ferreira G. Critical role of insular cortex in taste but not odour aversion memory. Eur J Neurosci. 2009; 29: 1654-62.

Deumens R, Blokland A, Prickaerts J. Modeling Parkinson's disease in rats: an evaluation of 6-OHDA lesions of the nigrostriatal pathway. Exp Neurol. 2002; 175: 303-17.

Di Monte DA, Lavasani M, Manning-Bog AB. Environmental factors in Parkinson's disease. Neurotoxicology. 2002; 23: 487-502.

Downes JJ, Roberts AC, Sahakian BJ, Evenden JL, Morris RG, Robbins TW. Impaired extra-dimensional shift performance in medicated and unmedicated Parkinson's disease: evidence for a specific attentional dysfunction. Neuropsychologia. 1989; 27: 1329-43.

Endres T, Fendt M. Aversion- vs fear-inducing properties of 2,4,5-trimethyl-3-thiazoline, a component of fox odor, in comparison with those of butyric acid. J Exp Biol. 2009; 212: 2324-7.

Ernst RR. Ernst, Richard R.: The Success Story of Fourier Transformation in NMR. 2007.

Fearnley JM, Lees AJ. Ageing and Parkinson's disease: substantia nigra regional selectivity. Brain. 1991; 114: 2283-301.

Fendt M, Endres T. 2,3,5-Trimethyl-3-thiazoline (TMT), a component of fox odor - just repugnant or really fear-inducing? Neurosci Biobehav Rev. 2008; 32: 1259-66. Epub 2008 May 15.

Ferrante RJ, Kubilus JK, Lee J, Ryu H, Beesen A, Zucker B, et al. Histone deacetylase inhibition by sodium butyrate chemotherapy ameliorates the neurodegenerative phenotype in Huntington's disease mice. J Neurosci. 2003; 23: 9418-27.

Finn DP, Chapman V, Jhaveri MD, Samanta S, Manders T, Bowden J, et al. The role of the central nucleus of the amygdala in nociception and aversion. Neuroreport. 2003; 14: 981-4.

Fleming SM, Delville Y, Schallert T. An intermittent, controlled-rate, slow progressive degeneration model of Parkinson's disease: antiparkinson effects of Sinemet and protective effects of methylphenidate. Behav Brain Res. 2005; 156: 201-13.

Fleming SM, Salcedo J, Fernagut PO, Rockenstein E, Masliah E, Levine MS, et al. Early and progressive sensorimotor anomalies in mice overexpressing wild-type human alpha-synuclein. J Neurosci. 2004; 24: 9434-40.

Fontan-Lozano A, Romero-Granados R, Troncoso J, Munera A, Delgado-Garcia JM, Carrion AM. Histone deacetylase inhibitors improve

learning consolidation in young and in KA-induced-neurodegeneration and SAMP-8-mutant mice. Mol Cell Neurosci. 2008; 39: 193-201. Epub 2008 Jun 25.

Fox MD, Snyder AZ, Vincent JL, Raichle ME. Intrinsic fluctuations within cortical systems account for intertrial variability in human behavior. Neuron. 2007; 56: 171-84.

Fox MT, Barense MD, Baxter MG. Perceptual attentional set-shifting is impaired in rats with neurotoxic lesions of posterior parietal cortex. J Neurosci. 2003; 23: 676-81.

Fox PT, Raichle ME, Mintun MA, Dence C. Nonoxidative glucose consumption during focal physiologic neural activity. Science. 1988; 241: 462-4.

Gaig C, Tolosa E. When does Parkinson's disease begin? Mov Disord. 2009; 24: S656-64.

Galvin JE. Cognitive change in Parkinson disease. Alzheimer Dis Assoc Disord. 2006; 20: 302-10.

Gardian G, Browne SE, Choi DK, Klivenyi P, Gregorio J, Kubilus JK, et al. Neuroprotective effects of phenylbutyrate in the N171-82Q transgenic mouse model of Huntington's disease. J Biol Chem. 2005; 280: 556-63. Epub 2004 Oct 19.

Gatev P, Darbin O, Wichmann T. Oscillations in the basal ganglia under normal conditions and in movement disorders. Mov Disord. 2006; 21: 1566-77.

Gatto NM, Cockburn M, Bronstein J, Manthripragada AD, Ritz B. Well-water consumption and Parkinson's disease in rural California. Environ Health Perspect. 2009; 117: 1912-8. Epub 2009 Jul 31.

Ghods-Sharifi S, St Onge JR, Floresco SB. Fundamental contribution by the basolateral amygdala to different forms of decision making. J Neurosci. 2009; 29: 5251-9.

Gibb WR, Lees AJ. Anatomy, pigmentation, ventral and dorsal subpopulations of the substantia nigra, and differential cell death in Parkinson's disease. Journal of Neurology, Neurosurgery & Psychiatry 1991; 54: 388-396.

Gispen WH, Isaacson RL. ACTH-induced excessive grooming in the rat. Pharmacology & Therapeutics 1981; 12: 209-246.

Goldberg MS, Fleming SM, Palacino JJ, Cepeda C, Lam HA, Bhatnagar A, et al. Parkin-deficient mice exhibit nigrostriatal deficits but not loss of dopaminergic neurons. J Biol Chem. 2003; 278: 43628-35. Epub 2003 Aug 20.

Gotham AM, Brown RG, Marsden CD. 'Frontal' cognitive function in patients with Parkinson's disease 'on' and 'off' levodopa. Brain. 1988; 111: 299-321.

Gray SG, Dangond F. Rationale for the use of histone deacetylase inhibitors as a dual therapeutic modality in multiple sclerosis. Epigenetics. 2006; 1: 67-75. Epub 2006 Mar 5.

Graybiel AM, Hirsch EC, Agid Y. The nigrostriatal system in Parkinson's disease. Advances in neurology 1990; 53: 17.

Greicius MD, Kiviniemi V, Tervonen O, Vainionpaa V, Alahuhta S, Reiss AL, et al. Persistent default-mode network connectivity during light sedation. Hum Brain Mapp. 2008; 29: 839-47.

Greicius MD, Supekar K, Menon V, Dougherty RF. Resting-state functional connectivity reflects structural connectivity in the default mode network. Cereb Cortex. 2009; 19: 72-8. Epub 2008 Apr 9.

Growdon JH, Corkin S, Rosen TJ. Distinctive aspects of cognitive dysfunction in Parkinson's disease. Adv Neurol. 1990; 53: 365-76.

Guilarte TR. Manganese and Parkinson's disease: a critical review and new findings. Environ Health Perspect 2010; 118: 1071-80.

Gusnard DA, Raichle ME, Raichle ME. Searching for a baseline: functional imaging and the resting human brain. Nat Rev Neurosci. 2001; 2: 685-94.

Haacke EM, Brown RW, Thompson MR, Venkatesan R. Magnetic resonance imaging: physical principles and sequence design: Wiley New York:, 1999.

Hagmann P, Cammoun L, Gigandet X, Meuli R, Honey CJ, Wedeen VJ, et al. Mapping the structural core of human cerebral cortex. PLoS Biol. 2008; 6: e159.

Hahn EL. Spin echoes. Physical Review 1950; 80: 580.

Halliday GM, Li YW, Blumbergs PC, Joh TH, Cotton RGH, Howe PRC, et al. Neuropathology of immunohistochemically identified brainstem neurons in Parkinson's disease. Annals of neurology 1990; 27: 373-385.

Hanrott K, Gudmunsen L, O'Neill MJ, Wonnacott S. 6-hydroxydopamine-induced apoptosis is mediated via extracellular auto-oxidation and caspase 3-dependent activation of protein kinase Cdelta. J Biol Chem. 2006; 281: 5373-82. Epub 2005 Dec 16.

Hauser RA. Early pharmacologic treatment in Parkinson's disease. Am J Manag Care 2010; 16: S100-7.

Hawkes CH. The prodromal phase of sporadic Parkinson's disease: does it exist and if so how long is it? Mov Disord. 2008; 23: 1799-807.

Hawkes CH, Del Tredici K, Braak H. A timeline for Parkinson's disease. Parkinsonism Relat Disord 2009; 16: 79-84.

Hawkes CH, Del Tredici K, Braak H. A timeline for Parkinson's disease. Parkinsonism Relat Disord 2010; 16: 79-84.

Hawkes CH, Shephard BC, Daniel SE. Olfactory dysfunction in Parkinson's disease. J Neurol Neurosurg Psychiatry. 1997; 62: 436-46.

Hayes CJ, Stevenson RJ, Coltheart M. Disgust and Huntington's disease. Neuropsychologia. 2007; 45: 1135-51. Epub 2006 Nov 28.

Heining M, Young AW, Ioannou G, Andrew CM, Brammer MJ, Gray JA, et al. Disgusting smells activate human anterior insula and ventral striatum. Ann N Y Acad Sci. 2003; 1000: 380-4.

Henderson RG. Nuclear magnetic resonance imaging: a review. J R Soc Med. 1983; 76: 206-12.

Hindle J. A history of Parkinson's disease. Parkinson's Disease in the Older Patient 2008: 1.

Hinshaw WS, Lent AH. An introduction to NMR imaging: From the Bloch equation to the imaging equation. Proceedings of the IEEE 1983; 71: 338-350.

Hockly E, Richon VM, Woodman B, Smith DL, Zhou X, Rosa E, et al. Suberoylanilide hydroxamic acid, a histone deacetylase inhibitor, ameliorates motor deficits in a mouse model of Huntington's disease. Proc Natl Acad Sci U S A. 2003; 100: 2041-6. Epub 2003 Feb 7.

Hoehn MM, Yahr MD. Parkinsonism: onset, progression and mortality. Neurology. 1967; 17: 427-42.

Hoge RD, Atkinson J, Gill B, Crelier GR, Marrett S, Pike GB. Linear coupling between cerebral blood flow and oxygen consumption in activated human cortex. Proceedings of the National Academy of Sciences of the United States of America 1999a; 96: 9403.

Hoge RD, Atkinson J, Gill B, Crelier GR, Marrett S, Pike GB. Investigation of BOLD signal dependence on cerebral blood flow and oxygen consumption: the deoxyhemoglobin dilution model. Magnetic resonance in medicine 1999b; 42: 849-863.

Homberg JR, van den Akker M, Raaso HS, Wardeh G, Binnekade R, Schoffelmeer AN, et al. Enhanced motivation to self-administer cocaine is predicted by self-grooming behaviour and relates to dopamine release in the rat medial prefrontal cortex and amygdala. Eur J Neurosci. 2002; 15: 1542-50.

Hoshino I, Matsubara H. Recent advances in histone deacetylase targeted cancer therapy. Surg 2010; 40: 809-15. Epub 2010 Aug 26.

Hughes AJ, Daniel SE, Kilford L, Lees AJ. Accuracy of clinical diagnosis of idiopathic Parkinson's disease: a clinico-pathological study of 100 cases. Journal of Neurology, Neurosurgery & Psychiatry 1992; 55: 181.

Jabbi M, Bastiaansen J, Keysers C. A common anterior insula representation of disgust observation, experience and imagination shows divergent functional connectivity pathways. PLoS One. 2008; 3: e2939.

Jackson JD, Fox RF. Classical electrodynamics. American Journal of Physics 1999; 67: 841.

Jager WA, Bethlem J. The distribution of Lewy bodies in the central and autonomic nervous systems in idiopathic paralysis agitans. Journal of Neurology, Neurosurgery & Psychiatry 1960; 23: 283.

James Jr AE, Partain CL, Holland GN, Gore JC, Rollo FD, Harms SE, et al. Nuclear magnetic resonance imaging: the current state. American Journal of Roentgenology 1982; 138: 201.

Jolles J, Rompa-Barendregt J, Gispen WH. ACTH-induced excessive grooming in the rat: The influence of environmental and motivational factors. Hormones and behavior 1979; 12: 60-72.

Jubault T, Monetta L, Strafella AP, Lafontaine AL, Monchi O. L-dopa medication in Parkinson's disease restores activity in the motor cortico-striatal loop but does not modify the cognitive network. PLoS One. 2009; 4: e6154.

Kakita A, Takahashi H, Homma Y, Ikuta F. Lewy bodies in the cerebellar dentate nucleus of a patient with Parkinson's disease. Pathology international 1994; 44: 878-880.

Kalueff AV, Tuohimaa P. The grooming analysis algorithm discriminates between different levels of anxiety in rats: potential utility for neurobehavioural stress research. Journal of neuroscience methods 2005; 143: 169-177.

Kametani H. Analysis of Age related Changes in Stress induced Grooming in the Rat. Annals of the New York Academy of Sciences 1988; 525: 101-113.

Kan Y, Kawamura M, Hasegawa Y, Mochizuki S, Nakamura K. Recognition of emotion from facial, prosodic and written verbal stimuli in Parkinson's disease. Cortex. 2002; 38: 623-30.

Kidd PM. Parkinson's disease as multifactorial oxidative neurodegeneration: implications for integrative management. Alternative Medicine Review 2000; 5: 502-529.

Kikuchi A, Takeda A, Kimpara T, Nakagawa M, Kawashima R, Sugiura M, et al. Hypoperfusion in the supplementary motor area, dorsolateral prefrontal cortex and insular cortex in Parkinson's disease. J Neurol Sci. 2001; 193: 29-36.

Kilgore M, Miller CA, Fass DM, Hennig KM, Haggarty SJ, Sweatt JD, et al. Inhibitors of class 1 histone deacetylases reverse contextual memory deficits in a mouse model of Alzheimer's disease. Neuropsychopharmacology 2009; 35: 870-80.

Kim RH, Smith PD, Aleyasin H, Hayley S, Mount MP, Pownall S, et al. Hypersensitivity of DJ-1-deficient mice to 1-methyl-4-phenyl-1,2,3,6-tetrahydropyrindine (MPTP) and oxidative stress. Proc Natl Acad Sci U S A. 2005; 102: 5215-20. Epub 2005 Mar 22.

King JA, Garelick TS, Brevard ME, Chen W, Messenger TL, Duong TQ, et al. Procedure for minimizing stress for fMRI studies in conscious rats. J Neurosci Methods. 2005; 148: 154-60. Epub 2005 Jun 16.

Kish SJ, Shannak K, Hornykiewicz O. Uneven pattern of dopamine loss in the striatum of patients with idiopathic Parkinson's disease. New England Journal of Medicine 1988; 318: 876-880.

Kumar A, Welti D, Ernst RR. NMR Fourier zeugmatography. Journal of Magnetic Resonance (1969) 1975; 18: 69-83.

Kwak Y, Peltier S, Bohnen NI, Muller ML, Dayalu P, Seidler RD. Altered resting state cortico-striatal connectivity in mild to moderate stage Parkinson's disease. Front 2010; 4: 143.

Kwong KK, Belliveau JW, Chesler DA, Goldberg IE, Weisskoff RM, Poncelet BP, et al. Dynamic magnetic resonance imaging of human brain activity during primary sensory stimulation. Proc Natl Acad Sci U S A. 1992; 89: 5675-9.

Langston JW. The parkinson's complex: Parkinsonism is just the tip of the iceberg. Annals of Neurology 2006; 59: 591–596.

Langston JW, Palfreman J. The case of the frozen addicts: Pantheon Books, 1995.

Lauterbur PC. Image Formation by Induced Local Interactions: Examples Employing Nuclear Magnetic Resonance. Nature 1973; 242: 190-191.

Lin X, Parisiadou L, Gu XL, Wang L, Shim H, Sun L, et al. Leucine-rich repeat kinase 2 regulates the progression of neuropathology induced by Parkinson's-disease-related mutant alpha-synuclein. Neuron. 2009; 64: 807-27.

Lindholm P, Voutilainen MH, Lauren J, Peranen J, Leppanen V-M, Andressoo J-O, et al. Novel neurotrophic factor CDNF protects and rescues midbrain dopamine neurons in vivo. Nature 2007; 448: 73-77.

Liu J, Nieminen AOK, Koenig JL. Calculation of T1, T2, and proton spin density images in nuclear magnetic resonance imaging. Journal of Magnetic Resonance (1969) 1989; 85: 95-110.

Liu T, Kuljaca S, Tee A, Marshall GM. Histone deacetylase inhibitors: multifunctional anticancer agents. Cancer Treat Rev. 2006; 32: 157-65. Epub 2006 Mar 3.

Liu Y, Yang H. Environmental toxins and alpha-synuclein in Parkinson's disease. Mol Neurobiol. 2005; 31: 273-82.

Lotharius J, Brundin P. Pathogenesis of parkinson's disease: dopamine, vesicles and [alpha]-synuclein. Nat Rev Neurosci 2002; 3: 932-942.

Lowe MJ, Beall EB, Sakaie KE, Koenig KA, Stone L, Marrie RA, et al. Resting state sensorimotor functional connectivity in multiple sclerosis inversely correlates with transcallosal motor pathway transverse diffusivity. Hum Brain Mapp. 2008; 29: 818-27.

Lowe MJ, Phillips MD, Lurito JT, Mattson D, Dzemidzic M, Mathews VP. Multiple sclerosis: low-frequency temporal blood oxygen level-dependent fluctuations indicate reduced functional connectivity initial results. Radiology. 2002; 224: 184-92.

Ludwig R, Bodgdanov G, King J, Allard A, Ferris CF. A dual RF resonator system for high-field functional magnetic resonance imaging of small animals. J Neurosci Methods. 2004; 132: 125-35.

Lustig C, Snyder AZ, Bhakta M, O'Brien KC, McAvoy M, Raichle ME, et al. Functional deactivations: change with age and dementia of the Alzheimer type. Proc Natl Acad Sci U S A. 2003; 100: 14504-9. Epub 2003 Nov 7.

Majeed W, Magnuson M, Keilholz SD. Spatiotemporal dynamics of low frequency fluctuations in BOLD fMRI of the rat. J Magn Reson Imaging. 2009; 30: 384-93.

Mansfield P, Maudsley AA. Medical imaging by NMR. Br J Radiol. 1977; 50: 188-94.

Matzuk MM, Saper CB. Preservation of hypothalamic dopaminergic neurons in Parkinson's disease. Annals of neurology 1985; 18: 552-555.

McRobbie DW, Moore EA, Graves MJ. MRI from Picture to Proton: Cambridge Univ Pr, 2003.

Menon RS, Ogawa S, Kim SG, Ellermann JM, Merkle H, Tank DW, et al. Functional brain mapping using magnetic resonance imaging. Signal changes accompanying visual stimulation. Invest Radiol. 1992; 27: S47-53.

Mitchell IJ, Heims H, Neville EA, Rickards H. Huntington's disease patients show impaired perception of disgust in the gustatory and olfactory modalities. J Neuropsychiatry Clin Neurosci. 2005; 17: 119-21.

Monchi O, Petrides M, Doyon J, Postuma RB, Worsley K, Dagher A. Neural bases of set-shifting deficits in Parkinson's disease. J Neurosci. 2004; 24: 702-10.

Monchi O, Petrides M, Mejia-Constain B, Strafella AP. Cortical activity in Parkinson's disease during executive processing depends on striatal involvement. Brain. 2007; 130: 233-44. Epub 2006 Nov 21.

Montagne B, Kessels RP, Kammers MP, Kingma E, de Haan EH, Roos RA, et al. Perception of emotional facial expressions at different intensities in early-symptomatic Huntington's disease. Eur Neurol. 2006; 55: 151-4. Epub 2006 May 8.

Morton AJ, Avanzo L. Executive decision-making in the domestic sheep. PLoS 2011; 6: e15752.

Na SJ, Dilella AG, Lis EV, Jones K, Levine DM, Stone DJ, et al. Molecular Profiling of a 6-Hydroxydopamine Model of Parkinson's Disease. Neurochem Res 2010; 2010: 19.

Nagano-Saito A, Leyton M, Monchi O, Goldberg YK, He Y, Dagher A. Dopamine depletion impairs frontostriatal functional connectivity during a set-shifting task. J Neurosci. 2008; 28: 3697-706.

Nagatsu T, Levitt M, Udenfriend S. Tyrosine hydroxylase. Journal of Biological Chemistry 1964; 239: 2910.

Ng CW, Noblejas MI, Rodefer JS, Smith CB, Poremba A. Double dissociation of attentional resources: prefrontal versus cingulate cortices. J Neurosci. 2007; 27: 12123-31.

O'Brien JA, Ward A, Michels SL, Tzivelekis S, Brandt NJ. Economic burden associated with Parkinson disease. Drug Benefit Trends 2009; 21: 179-190.

Ogawa S, Lee TM, Kay AR, Tank DW. Brain magnetic resonance imaging with contrast dependent on blood oxygenation. Proc Natl Acad Sci U S A. 1990b; 87: 9868-72.

Ogawa S, Lee TM, Nayak AS, Glynn P. Oxygenation-sensitive contrast in magnetic resonance image of rodent brain at high magnetic fields. Magn Reson Med. 1990a; 14: 68-78.

Ohama E, Ikuta F. Parkinson's disease: distribution of Lewy bodies and monoamine neuron system. Acta neuropathologica 1976; 34: 311-319.

Oppenheim AV, Schafer RW, Buck JR. Discrete-time signal processing. 1999. 1999.

Orimo S, Amino T, Itoh Y, Takahashi A, Kojo T, Uchihara T, et al. Cardiac sympathetic denervation precedes neuronal loss in the sympathetic ganglia in Lewy body disease. Acta Neuropathologica 2005; 109: 583-588.

Owen AM, James M, Leigh PN, Summers BA, Marsden CD, Quinn NP, et al. Fronto-striatal cognitive deficits at different stages of Parkinson's disease. Brain. 1992; 115: 1727-51.

Oyanagi K, Wakabayashi K, Ohama E, Takeda S, Horikawa Y, Morita T, et al. Lewy bodies in the lower sacral parasympathetic neurons of a patient with Parkinson's disease. Acta neuropathologica 1990; 80: 558-559.

Pahwa R, Koller WC. Dopamine agonists in the treatment of Parkinson's disease. Cleve Clin J Med. 1995; 62: 212-7.

Parkinson'sDiseaseFoundation. Ten frequently asked questions about Parkinson's disease. www.pdf.org/Publications/factsheets/PDF Accessed 2011.

Parkinson J. An essay on the shaking palsy. (Republished in 2002). J Neuropsychiatry Clin Neurosci. 1817; 14: 223-36; discussion 222.

Paulmann S, Pell MD, Kotz SA. Comparative processing of emotional prosody and semantics following basal ganglia infarcts: ERP evidence of selective impairments for disgust and fear. Brain Res. 2009; 1295: 159-69. Epub 2009 Aug 4.

Pawela CP, Biswal BB, Cho YR, Kao DS, Li R, Jones SR, et al. Resting-state functional connectivity of the rat brain. Magn Reson Med. 2008; 59: 1021-9.

Perez FA, Palmiter RD. Parkin-deficient mice are not a robust model of parkinsonism. Proc Natl Acad Sci U S A. 2005; 102: 2174-9. Epub 2005 Jan 31.

Petrovitch H, Ross GW, Abbott RD, Sanderson WT, Sharp DS, Tanner CM, et al. Plantation work and risk of Parkinson disease in a

population-based longitudinal study. Arch Neurol. 2002; 59: 1787-92.

Ponsen MM, Stoffers D, Booij J, van Eck-Smit BL, Wolters E, Berendse HW. Idiopathic hyposmia as a preclinical sign of Parkinson's disease. Ann Neurol. 2004; 56: 173-81.

Ponsen MM, Stoffers D, Wolters E, Booij J, Berendse HW. Olfactory testing combined with dopamine transporter imaging as a method to detect prodromal Parkinson's disease. J Neurol Neurosurg Psychiatry 2009; 81: 396-9.

Prichard J, Rothman D, Novotny E, Petroff O, Kuwabara T, Avison M, et al. Lactate rise detected by 1H NMR in human visual cortex during physiologic stimulation. Proceedings of the National Academy of Sciences of the United States of America 1991; 88: 5829.

Pykett IL, Newhouse JH, Buonanno FS, Brady TJ, Goldman MR, Kistler JP, et al. Principles of nuclear magnetic resonance imaging. Radiology 1982; 143: 157.

Racette BA, Tabbal SD, Jennings D, Good L, Perlmutter JS, Evanoff B. Prevalence of parkinsonism and relationship to exposure in a large sample of Alabama welders. Neurology 2005; 64: 230-235.

Raichle ME, MacLeod AM, Snyder AZ, Powers WJ, Gusnard DA, Shulman GL. A default mode of brain function. Proc Natl Acad Sci U S A. 2001; 98: 676-82.

Rane P, King JA. Exploring aversion in an animal model of pre-motor stage PD. Neuroscience 2011.

Rascol O, Payoux P, Ory F, Ferreira JJ, Brefel-Courbon C, Montastruc J-L. Limitations of current Parkinson's disease therapy. Annals of Neurology 2003; 53: S3-S15.

Reilly S, Bornovalova MA. Conditioned taste aversion and amygdala lesions in the rat: a critical review. Neurosci Biobehav Rev. 2005; 29: 1067-88.

Reimer P, Parizel PM. Clinical MR imaging: a practical approach: Springer Verlag, 2006.

Robbins TW, Weinberger D, Taylor JG, Morris RG. Dissociating Executive Functions of the Prefrontal Cortex [and Discussion]. Philosophical Transactions: Biological Sciences 1996; 351: 1463-1471.

Rockenstein E, Mallory M, Hashimoto M, Song D, Shults CW, Lang I, et al. Differential neuropathological alterations in transgenic mice expressing alpha-synuclein from the platelet-derived growth factor and Thy-1 promoters. J Neurosci Res. 2002; 68: 568-78.

Rohlf JW, Collings PJ. Modern Physics from alpha to Z [sup°]. Physics Today 1994; 47: 62.

Roitman MF, Wheeler RA, Carelli RM. Nucleus Accumbens Neurons Are Innately Tuned for Rewarding and Aversive Taste Stimuli, Encode Their Predictors, and Are Linked to Motor Output. Neuron 2005; 45: 587-597.

Rombouts S, Scheltens P. Functional connectivity in elderly controls and AD patients using resting state fMRI: a pilot study. Curr Alzheimer Res. 2005; 2: 115-6.

Ross GW, Petrovitch H, Abbott RD, Tanner CM, Popper J, Masaki K, et al. Association of olfactory dysfunction with risk for future Parkinson's disease. Ann Neurol. 2008; 63: 167-73.

Roy AK, Shehzad Z, Margulies DS, Kelly AM, Uddin LQ, Gotimer K, et al. Functional connectivity of the human amygdala using resting state fMRI. Neuroimage. 2009; 45: 614-26. Epub 2008 Dec 9.

Royet JP, Plailly J, Delon-Martin C, Kareken DA, Segebarth C. fMRI of emotional responses to odors: influence of hedonic valence and judgment, handedness, and gender. Neuroimage. 2003; 20: 713-28.

Ryu H, Lee J, Olofsson BA, Mwidau A, Dedeoglu A, Escudero M, et al. Histone deacetylase inhibitors prevent oxidative neuronal death independent of expanded polyglutamine repeats via an Sp1-dependent pathway. Proc Natl Acad Sci U S A. 2003; 100: 4281-6. Epub 2003 Mar 14.

Sadri-Vakili G, Cha JH. Histone deacetylase inhibitors: a novel therapeutic approach to Huntington's disease (complex mechanism of neuronal death). Curr Alzheimer Res. 2006; 3: 403-8.

Sakai K, Gash DM. Effect of bilateral 6-OHDA lesions of the substantia nigra on locomotor activity in the rat. Brain Res. 1994; 633: 144-50.

Sappey-Marinier D, Calabrese G, Fein G, Hugg JW, Biggins C, Weiner MW. Effect of photic stimulation on human visual cortex lactate and phosphates using 1H and 31P magnetic resonance spectroscopy. Journal of Cerebral Blood Flow & Metabolism 1992; 12: 584-592.

Sauer H, Oertel WH. Progressive degeneration of nigrostriatal dopamine neurons following intrastriatal terminal lesions with 6-hydroxydopamine: A combined retrograde tracing and immunocytochemical study in the rat. Neuroscience. 1994; 59: 401-415.

Schapira AH. Etiology of Parkinson's disease. Neurology. 2006; 66: S10-23.

Schapira AH. Neurobiology and treatment of Parkinson's disease. Trends Pharmacol Sci. 2009; 30: 41-7. Epub 2008 Nov 29.

Schneider JS. Modeling Cognitive Deficits Associated with Parkinsonism in the Chronic-Low-Dose MPTP-Treated Monkey. In: Levine ED and Buccafusco JJ, editors. Animal Models of Cognitive Impairment: CRC Press, 2006.

Schober A. Classic toxin-induced animal models of Parkinson's disease: 6-OHDA and MPTP. Cell Tissue Res. 2004; 318: 215-24. Epub 2004 Jul 28.

Schoenbaum G, Setlow B. Lesions of nucleus accumbens disrupt learning about aversive outcomes. J Neurosci. 2003; 23: 9833-41.

Schroeder FA, Lin CL, Crusio WE, Akbarian S. Antidepressant-like effects of the histone deacetylase inhibitor, sodium butyrate, in the mouse. Biol Psychiatry. 2007; 62: 55-64. Epub 2006 Aug 30.

Schroeder FA, Penta KL, Matevossian A, Jones SR, Konradi C, Tapper AR, et al. Drug-induced activation of dopamine D(1) receptor signaling and inhibition of class I/II histone deacetylase induce chromatin remodeling in reward circuitry and modulate cocaine-related behaviors. Neuropsychopharmacology. 2008; 33: 2981-92. Epub 2008 Feb 20.

Seidler A, Hellenbrand W, Robra BP, Vieregge P, Nischan P, Joerg J, et al. Possible environmental, occupational, and other etiologic factors for Parkinson's disease. Neurology 1996; 46: 1275.

Sharpe MH. Patients with early Parkinson's disease are not impaired on spatial orientating of attention. Cortex. 1990; 26: 515-24.

Sharpe MH. Auditory attention in early Parkinson's disease: an impairment in focused attention. Neuropsychologia. 1992; 30: 101-6.

Shehzad Z, Kelly AM, Reiss PT, Gee DG, Gotimer K, Uddin LQ, et al. The resting brain: unconstrained yet reliable. Cereb Cortex. 2009; 19: 2209-29. Epub 2009 Feb 16.

Shiba M, Bower JH, M. MD, McDonnell SK, Peterson BJ, Ahlskog JE, et al. Anxiety disorders and depressive disorders preceding Parkinson's disease: A case-control study. Movement Disorders 2000; 15: 669–677.

Shmuel A, Leopold DA. Neuronal correlates of spontaneous fluctuations in fMRI signals in monkey visual cortex: Implications for functional connectivity at rest. Hum Brain Mapp. 2008; 29: 751-61.

Shulman GL, Corbetta M, Buckner RL, Fiez JA, Miezin FM, Raichle ME, et al. Common blood flow changes across visual tasks: I. Increases in subcortical structures and cerebellum but not in nonvisual cortex. Journal of Cognitive Neuroscience 1997; 9: 624-647.

Singh M. Toward proton MR spectroscopic imaging of stimulated brain function. Nuclear Science, IEEE Transactions on 1992; 39: 1161-1164.

Slabosz A, Lewis SJ, Smigasiewicz K, Szymura B, Barker RA, Owen AM. The role of learned irrelevance in attentional set-shifting impairments in Parkinson's disease. Neuropsychology. 2006; 20: 578-88.

Small DM, Gregory MD, Mak YE, Gitelman D, Mesulam MM, Parrish T. Dissociation of neural representation of intensity and affective valuation in human gustation. Neuron. 2003; 39: 701-11.

Smith WW, Pei Z, Jiang H, Moore DJ, Liang Y, West AB, et al. Leucine-rich repeat kinase 2 (LRRK2) interacts with parkin, and mutant LRRK2 induces neuronal degeneration. Proc Natl Acad Sci U S A. 2005; 102: 18676-81. Epub 2005 Dec 13.

Spillantini MG, Schmidt ML, Lee VM, Trojanowski JQ, Jakes R, Goedert M. Alpha-synuclein in Lewy bodies. Nature. 1997; 388: 839-40.

Sprengelmeyer R, Rausch M, Eysel UT, Przuntek H. Neural structures associated with recognition of facial expressions of basic emotions. Proc Biol Sci. 1998; 265: 1927-31.

Sprengelmeyer R, Young AW, Mahn K, Schroeder U, Woitalla D, Buttner T, et al. Facial expression recognition in people with medicated and unmedicated Parkinson's disease. Neuropsychologia. 2003; 41: 1047-57.

Squire LR. Fundamental neuroscience: Academic Pr, 2003.

Steece-Collier K, Maries E, Kordower JH. Etiology of Parkinson's disease: Genetics and environment revisited. Proceedings of the National Academy of Sciences of the United States of America 2002; 99: 13972-13974.

Suzuki A, Hoshino T, Shigemasu K, Kawamura M. Disgust-specific impairment of facial expression recognition in Parkinson's disease. Brain. 2006; 129: 707-17. Epub 2006 Jan 16.

Tang CC, Eidelberg D. Abnormal metabolic brain networks in Parkinson's disease:: from blackboard to bedside. Progress in Brain Research 2010: 160-176.

Tanner CM. Advances in environmental epidemiology. Mov 2010; 25: S58-62.

Terzioglu M, Galter D. Parkinson's disease: genetic versus toxin-induced rodent models. Febs J. 2008; 275: 1384-91. Epub 2008 Feb 12.

Tian L, Jiang T, Wang Y, Zang Y, He Y, Liang M, et al. Altered resting-state functional connectivity patterns of anterior cingulate cortex in adolescents with attention deficit hyperactivity disorder. Neurosci Lett. 2006; 400: 39-43. Epub 2006 Feb 28.

Tsankova NM, Berton O, Renthal W, Kumar A, Neve RL, Nestler EJ. Sustained hippocampal chromatin regulation in a mouse model of depression and antidepressant action. Nat Neurosci. 2006; 9: 519-25. Epub 2006 Feb 26.

Tuchsen F, Jensen AA. Agricultural work and the risk of Parkinson's disease in Denmark, 1981-1993. Scand J Work Environ Health. 2000; 26: 359-62.

Ungerstedt U. 6-Hydroxy-dopamine induced degeneration of central monoamine neurons. Eur J Pharmacol. 1968; 5: 107-10.

Vlajinac HD, Sipetic SB, Maksimovic JM, Marinkovic JM, Dzoljic ED, Ratkov IS, et al. Environmental factors and Parkinson's disease: a case-control study in Belgrade, Serbia. Int 2010; 120: 361-7.

von dem Hagen EA, Beaver JD, Ewbank MP, Keane J, Passamonti L, Lawrence AD, et al. Leaving a bad taste in your mouth but not in my insula. Soc Cogn Affect Neurosci. 2009; 4: 379-86. Epub 2009 Jun 8.

Wakabayashi K, Mori F, Takahashi H. Progression patterns of neuronal loss and Lewy body pathology in the substantia nigra in Parkinson's disease. Parkinsonism & Related Disorders 2006; 12: S92-S98.

Wakabayashi K, Takahashi H. The intermediolateral nucleus and Clarke's column in Parkinson's disease. Acta neuropathologica 1997; 94: 287-289.

Weintraub D, Comella CL, Horn S. Parkinson's disease—Part 1: pathophysiology, symptoms, burden, diagnosis, and assessment. Am J Manag Care 2008; 14: S40-S48.

Williams KA, Peltier S, LaConte S, Keilholz SD. MRI evidence of resting state connectivity in rodent brain. 14th Annual Meeting of ISMRM. Vol 14. Seattle, Washington, 2006: 2119.

Willis AW, Sterling C, Racette BA. Conjugal Parkinsonism and Parkinson disease: a case series with environmental risk factor analysis. Parkinsonism Relat Disord 2010; 16: 163-6.

Winter S, Dieckmann M, Schwabe K. Dopamine in the prefrontal cortex regulates rats behavioral flexibility to changing reward value. Behav Brain Res. 2009; 198: 206-13. Epub 2008 Nov 11.

Wright P, He G, Shapira NA, Goodman WK, Liu Y. Disgust and the insula: fMRI responses to pictures of mutilation and contamination. Neuroreport. 2004; 15: 2347-51.

Wright Willis A, Evanoff BA, Lian M, Criswell SR, Racette BA. Geographic and ethnic variation in Parkinson disease: a population-based study of US Medicare beneficiaries. Neuroepidemiology. 2010; 34: 143-51. Epub 2010 Jan 15.

Wu T, Long X, Wang L, Hallett M, Zang Y, Li K, et al. Functional connectivity of cortical motor areas in the resting state in Parkinson's disease. Hum Brain Mapp 2010; 2010: 25.

Wu X, Chen PS, Dallas S, Wilson B, Block ML, Wang CC, et al. Histone deacetylase inhibitors up-regulate astrocyte GDNF and BDNF gene transcription and protect dopaminergic neurons. Int J Neuropsychopharmacol. 2008; 11: 1123-34. Epub 2008 Jul 9.

Xie C, Li S-J, Shao Y, Fu L, Goveas J, Ye E, et al. Identification of hyperactive intrinsic amygdala network connectivity associated with impulsivity in abstinent heroin addicts. Behavioural Brain Research 2011; 216: 639-646.

Yuan H, Sarre S, Ebinger G, Michotte Y. Histological, behavioural and neurochemical evaluation of medial forebrain bundle and striatal 6-OHDA lesions as rat models of Parkinson's disease. J Neurosci Methods. 2005; 144: 35-45. Epub 2004 Dec 8.

Zhang N, Rane P, Huang W, Liang Z, Kennedy D, Frazier JA, et al. Mapping resting-state brain networks in conscious animals. J 2010; 189: 186-96. Epub 2010 Apr 9.